THE UNIVERSITY OF MICHIGAN

INDUSTRY PROGRAM OF THE COLLEGE OF ENGINEERING

THE INFLUENCE OF HIGH PRESSURE ON THE PROPERTIES OF HYDROGEN-OXYGEN DETONATION WAVES

Roy L. Gealer

A dissertation submitted in partial fulfillment
of the requirements for the degree of
Doctor of Philosophy in the
University of Michigan
1958

June, 1958

IP-295

Doctoral Committee:

Professor Stuart W. Churchill, Chairman
Associate Professor Thomas C. Adamson, Jr.
Professor Donald L. Katz
Associate Professor Richard B. Morrison
Associate Professor David V. Ragone

ACKNOWLEDGMENTS

The experimental and part of the computational phases of this work were sponsored by Project SQUID which is supported by the Office of Naval Research, Department of the Navy, under contract Nonr 1858 (25) NR-098-038. Reproduction in full or in part is permitted for any use of the United States Government. The support of Project SQUID is deeply appreciated.

I want to thank the doctoral committee for their advice relative to this work, and especially Dr. Richard B. Morrison who suggested the problem, obtained the support of the above mentioned Project SQUID, and contributed much advice and encouragement during the beginning stages of this work. I also wish to thank Dr. Alexander Weir, Jr. (now with the Ramo-Wooldridge Corporation) for his efforts as original doctoral committee chairman during the initial part of my doctoral work.

I appreciate the use of the space and facilities afforded me by the Aircraft Propulsion Laboratory, University of Michigan, where the investigation was carried out, and the support given me by many people connected with the laboratory.

Finally, I would like to thank my wife Norma Gealer who typed the entire first draft of this thesis, and the Industry Program of the University of Michigan who reproduced it in final form.

TABLE OF CONTENTS

	Page
ACKNOWLEDGMENT	iii
LIST OF TABLES	vi
LIST OF FIGURES	vii
NOMENCLATURE	ix
ABSTRACT	xii
I. INTRODUCTION	1
The Detonative Phenomena	1
History	2
Purpose of the Investigation	2
II. EXPERIMENTAL EQUIPMENT	5
Equipment Location	5
Description of System and Procedure	5
Experimental Procedure	5
The Detonation Tube	9
The Pressurizing Tube	10
Probes	15
Velocity Measuring Equipment	15
III. PREDICTION OF DETONATION VELOCITIES, PRESSURES, AND TEMPERATURES	25
The Hydrodynamic Equations	25
The Chemical Equilibrium Equations	28
Computer Programming	31
Computational Procedure	34
Interpolation Equations	35
Impact Pressures	37
IV. THE EFFECT OF ERRORS IN PRESSURE SENSITIVE PHYSICAL PROPERTIES ON DETONATION WAVE VELOCITIES	41
V. RESULTS	47
Experimental Effect of Initial Pressure on Detonation Velocity	47
Theoretical Results	51

TABLE OF CONTENTS CONT'D

	Page
Effect of Initial Pressure on Detonation Velocity Using Idealized Physical Properties.	51
Impact Pressures	54
Accidental Explosion	58
VI. DISCUSSION	63
VII. CONCLUSIONS	67
APPENDICES	
A. DEVELOPMENT OF THE HYDRODYNAMIC EQUATIONS	72
B. DEVELOPMENT OF THE CHEMICAL EQUILIBRIUM EQUATIONS	79
C. IBM-650 COMPUTER PROGRAM FOR SOLUTION OF CHEMICAL EQUILIBRIUM EQUATIONS	83
D. DEVELOPMENT OF EQUATIONS FOR DETERMINATION OF THE EFFECT OF ERRORS IN PHYSICAL PROPERTIES ON DETONATION VELOCITY	93
E. ORIGINAL AND CORRECTED EXPERIMENTAL DETONATION VELOCITIES	99
F. EQUILIBRIUM COMPOSITIONS IN HYDROGEN-OXYGEN MIXTURES	107
G. THEORETICAL DETONATION VELOCITIES, PRESSURES, AND TEMPERATURES	125
BIBLIOGRAPHY	129

LIST OF TABLES

Table		Page
I.	The Effect of Initial Pressure on Detonation Induction Distance	21
II.	The Effect of Property Errors on Detonation Velocity	42
III.	Experimental Percent Increase in Detonation Velocity for Increase in Initial Pressure from 14.4 to 1000 Psia	69
IV.	Original and Corrected Experimental Detonation Velocities	101
V.	Equilibrium Compositions in Hydrogen-Oxygen Mixtures.	109
VI.	Theoretical Detonation Velocities, Pressures, and Temperatures (Based on Idealized Properties)	126

LIST OF FIGURES

Figure		Page
1	Schematic Cross-Section of Test Cell and Pit.....	6
2	Schematic Flow Diagram of Experimental System.....	7
3	Assembly of Detonation Tube and Cap.....	11
4	Photograph of Detonation Tube and Cap.....	12
5	Assembly of Pressurizing Tube and Cap.....	13
6	Liquid Level Indicator for Pressurizing Tube.....	14
7	Photograph of Pressurizing Tube and Cap.....	16
8	Ionization Probe Assembly.....	17
9	Ignitor Assembly.....	18
10	Thermocouple Assembly.....	19
11	Assembly of Connector Between Detonation Tube and Heavy-Duty Valve.....	20
12	Timing Circuitry.....	22
13	Schematic of Standing Detonation Wave Reference System.....	25
14	Graphical Illustration of Computer Convergence Technique.....	31
15	Computer Program Flowsheet for Chemical Equilibrium Computations.....	32
16	Graphical Illustration of Temperature Interpolation Technique.....	36
17	Schematic of Moving Detonation and Reflected Wave Reference System.....	38
18	Graphical Illustration of Method of Correcting Points to Nominal Hydrogen Mole Fraction.....	48
19	Experimental Effect of Initial Composition on Detonation Velocity at Various Initial Pressures.....	49

LIST OF FIGURES CONT'D

Figure		Page
20	The Effect of Pressure on the Equilibrium Composition of a Stoichiometric Mixture of Hydrogen and Oxygen at 3000 and 5000°K	53
21	Comparison Between Theoretical and Corrected Experimental Effects of Initial Pressure on Detonation Velocity -- High Range	55
22	Comparison Between Theoretical and Corrected Experimental Effects of Initial Pressure on Detonation Velocity -- Low Range	56
23	Theoretical Ratios of Detonation and Impact Pressures to Initial Pressure as a Function of Initial Pressure	57
24	Photograph of Pressurizing Tube After Accidental Explosion	59
25	Photograph of Test Pit and Equipment After Accidental Explosion	60

NOMENCLATURE

A, B, C	Symbols given to quantities in order of magnitude analysis (See Appendix A).
a, b, c, d, e, g, h	Symbols given to quantities in chemical equilibrium equations (See Chapter III)
a_2	Sonic velocity in product gases, ft/sec.
c_P	Specific heat at constant pressure, cal/gm mol °K
D	Denominator in mole fraction error equations (See Appendix D).
F	Molar ratio of O_2 to H_2 in initial gas mixture.
f	Fugacity
$(H^\circ_{T_2} - H^\circ_0)_P$	Sensible enthalpy of product at T_2 above enthalpy at 0°K, cal/gm mol.
$(H^\circ_{T_1} - H^\circ_0)_R$	Sensible enthalpy of reactant at T_1 above enthalpy at 0°K, cal/gm mol.
$(H^\circ_f)_P$	Enthalpy of formation of product at 0°K, cal/gm mol.
h	Total enthalpy, cal/gm.
K_f	Fugacity chemical equilibrium constant.
K_P	Pressure chemical equilibrium constant.
K_ν	Ratio of fugacity coefficients.
M'	Mach number (moving wave reference system).
m	Molecular weight.
N	Property in error.
n	Number of moles.
$\mathcal{O}$	Order of magnitude operator.
P	Pressure, psia or atmospheres.
p	Partial pressure, psia or atmospheres.

R	Universal gas constant.
s	Slope on u_1 vs $(x_{H_2})_1$ plot.
T	Temperature, °K.
u_1	Particle velocity of gas in state 1 in standing wave reference system = detonation wave velocity, ft/sec.
u_2	Particle velocity of gas in state 2 in standing wave reference system = a_2, ft/sec.
u'_w	Detonation wave velocity in moving wave reference system, ft/sec.
u'_{rw}	Reflected wave velocity in moving wave reference system, ft/sec.
u'_1	Particle velocity of gas in state 1 in moving wave reference system, ft/sec.
u'_2	Particle velocity of gas in state 2 in moving wave reference system, ft/sec.
u'_3	Particle velocity of gas in state 3 (after wave reflection) in moving wave reference system, ft/sec.
w, x, y, z	Arbitrary variables in discussion of interpolation and error equations.
$x_{R,P}$	Mole fraction of a reactant or product.
$z_{1,2}$	Compressibility factor.

GREEK LETTERS

γ	Ratio of specific heat at constant pressure to specific heat at constant volume.
Δ	Difference operator.
δ	Tube diameter, inches.
∂	Partial differential operator.
ϵ	Error between calculated and assumed final temperatures.
ν	Fugacity coefficient.

Π	Interpolation factor.
ρ	Density
Σ	Summation operator.

SUBSCRIPTS

1	State 1 (Reactants).
2	State 2 (Products).
3	State 3 (After wave reflection).
ACT	Actual
AS	Assumed
CALC	Calculated
CORR	Corrected
H	Atomic hydrogen
H_2	Molecular hydrogen
H_2O	Water
n	General numerical index
NOM	Nominal
O	Atomic oxygen
O_2	Molecular oxygen
OH	Hydroxyl radical
P	Any product
R	Any reactant
rw	Reflected wave
T	Total
w	Incident wave

Note: The subscripts 1, 2, 3, and 4 have also been used in defined places as distinguishing indeces on K_p, K_f, K_v, ϵ, Π, T_2, γ_2, and m_2. Subscripts 1, 2, and 3 refer to the state unless otherwise defined.

I. INTRODUCTION

The Detonative Phenomena

Two types of gaseous combustion are normally encountered. In the first type, called deflagration, the rate of propagation is controlled by molecular transport phenomena, diffusion and/or thermal conductivity, and for this reason is ordinarily rather slow, (of the order of a few feet per second). If a deflagration is initiated in a tube, under the proper conditions and after a suitable induction distance, a shock wave traveling at supersonic velocity, and having sufficient strength to ignite the combustible mixture may develop ahead of the flame front. The region immediately behind the shock wave then becomes the zone of combustion. This supersonic wave followed by combustion is known as a detonation wave. The shock wave develops due to the piston action of the expanding products of combustion, which send out pressure pulses ahead of the flame front. Each sonic pulse must travel faster than the preceding one due to increased temperature and particle velocity of the unburned gases and thus they may eventually coalesce into a shock front of sufficient strength to ignite the mixture. A possible mechanism for the transition from deflagration to detonation has been proposed by Zeldovich[41].

Detonative combustion eventually becomes a stable situation whereby a shock wave initiates combustion, and the realization of the combustion contributes energy for the continued propagation of the shock wave.

History

A detailed history of the development of the theory of detonation waves will not be presented here since such references as (20) and (26) have, in describing the phenomena, included rather complete chronologies.

The history is highlighted by the discovery of the detonative phenomena by Berthelot and Vieille[3] and by Mallard and Le Chatelier[27] in 1881, the development of the correct pressure-volume relationships to be used for strong shock waves by Rankine[36] in 1870 and Hugoniot[19] in 1889, and the suggestion and utilization of the fact that the detonation wave moves at the speed of sound relative to the burned gases by Dixon[8] in 1893, Chapman[6] in 1899, and Jouguet[21] in 1905. This assumption has been justified in various ways by Jouguet[21], Becker[1], Scorah[37], and Brinkley and Kirkwood[5].

Numerical calculations, refinements of the hydrodynamic theory, and unique forms of the equations have been made by many investigators including references 7, 9, 10, 11, 22, 29, 30, 39.

Excellent agreement between velocities computed from the hydrodynamic theory and experimentally measured velocities has been found by Lewis and Friauf[25], Berets, Greene, and Kistiakowsky[2], Moyle and Churchill[31] and by many of the investigators listed immediately above.

Purpose of the Investigation

Until recently, the hydrodynamic theory has not been tested and detonation properties have not been determined throughout very wide ranges of initial temperature and pressure. Dixon[8] measured detonation velocities

in stoichiometric mixtures of H_2-O_2 at 10°C and 100°C over a pressure range from 200 to 1500 mm Hg. Moyle and Churchill[31] measured and calculated detonation velocities over a temperature range from 160 to 480°K, a pressure range from 0.5 to 2 atm, and a composition range from 0.25 to 0.78 mole fraction hydrogen in H_2-O_2 mixtures, for various tube diameters. Hoelzer and Stobaugh[15] measured detonation velocities in hydrogen-oxygen mixtures and ethane-oxygen mixtures over a pressure range from 1 to 10 atm for several compositions. The effect of temperature and pressure on detonation induction distances were measured by Laffitte[23] and Dumanois and Laffitte[24] respectively.

What should by the effect of increasing the initial pressure on the detonation velocity? As was stated in the description of the detonative phenomena, not only does the existence of the supersonic combustion depend upon the existence of the shock wave, but also the stable propagation of the shock wave depends upon the presence of the combustion following it. This is true in a quantitative sense, i.e., the velocity of the wave depends upon the energy released in the combustion. Thus, for a given mixture, anything done to increase the energy available for the propagation of the wave should increase the wave velocity. One way to accomplish this increased "available" energy would be to decrease the amount of dissociation (an endothermic process) in the products of combustion by increasing the final pressure. If the ratio of final to initial pressure does not change too much due to a change in the detonation velocity (this dependence will be seen further on in the text), the final pressure should be increased by increasing the initial pressure.

Therefore an increase in initial pressure can be expected to cause an increase in detonation velocity.

The main purpose of this work was to investigate the effect of initial pressure on the velocity of detonation of hydrogen-oxygen mixtures, and to investigate the reliability of the hydrodynamic theory of detonation over a wide range of initial pressures and compositions. Detonation wave impact pressures are computed for design purposes.

II. EXPERIMENTAL EQUIPMENT

Equipment Location

The apparatus was built at the University of Michigan Aircraft Propulsion Laboratory in a test cell isolated from the rest of the laboratory area by a one foot thick poured concrete wall (See Figure 1). The test cell contains a concrete lined pit at its center, 11 ft. deep, 6 ft. wide, and 6 ft. long. The equipment was contained in this pit. All operating controls were located in the laboratory area, beyond the protecting wall. Valves were operated by means of "push-pull" flexible controls and a lever system on the valves. Pressure gages, located near the pit bottom, were read by means of a mirror system and telescope and viewed through a bullet proof plate glass window in the protecting wall.

Description of System and Procedure

Experimental Procedure

A schematic diagram of the system is shown in Figure 2. The pressurizing tube was evacuated, flushed with hydrogen, evacuated, and then filled with hydrogen to the desired partial pressure. Oxygen was then admitted to the desired pressure and the gases were allowed to mix for a few hours. Oxygen was admitted last to take advantage of the gravitational mixing due to density difference. To ensure that the time allowed for mixing was sufficient, the detonation velocity of the first batch was measured after 2 and 5 hours of mixing. No difference in results was observed. After the gases were mixed, the detonation tube was evacuated, flushed with mixture, evacuated, and filled with mixture

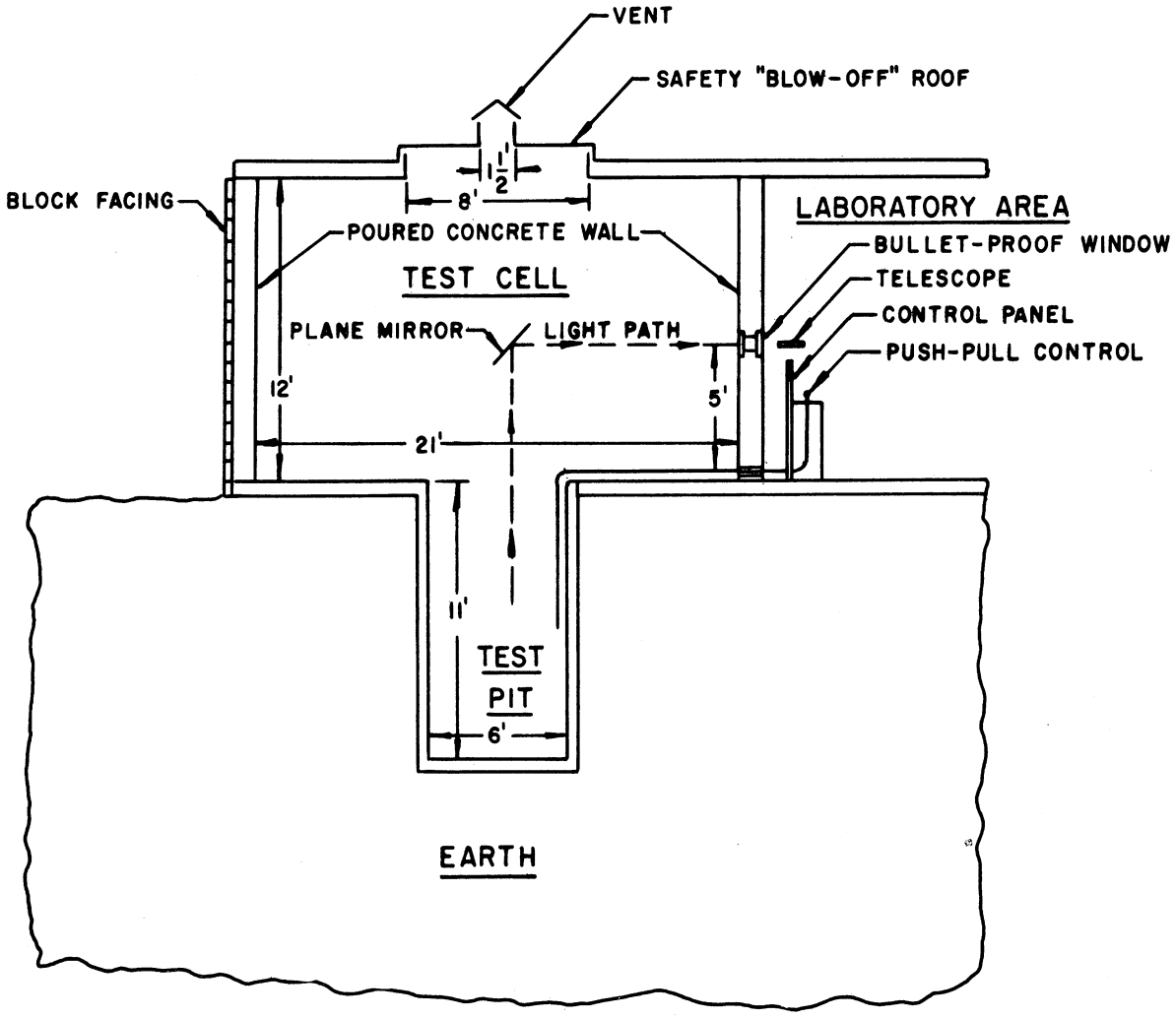

Figure 1. Schematic Cross-Section of Test Cell and Pit.

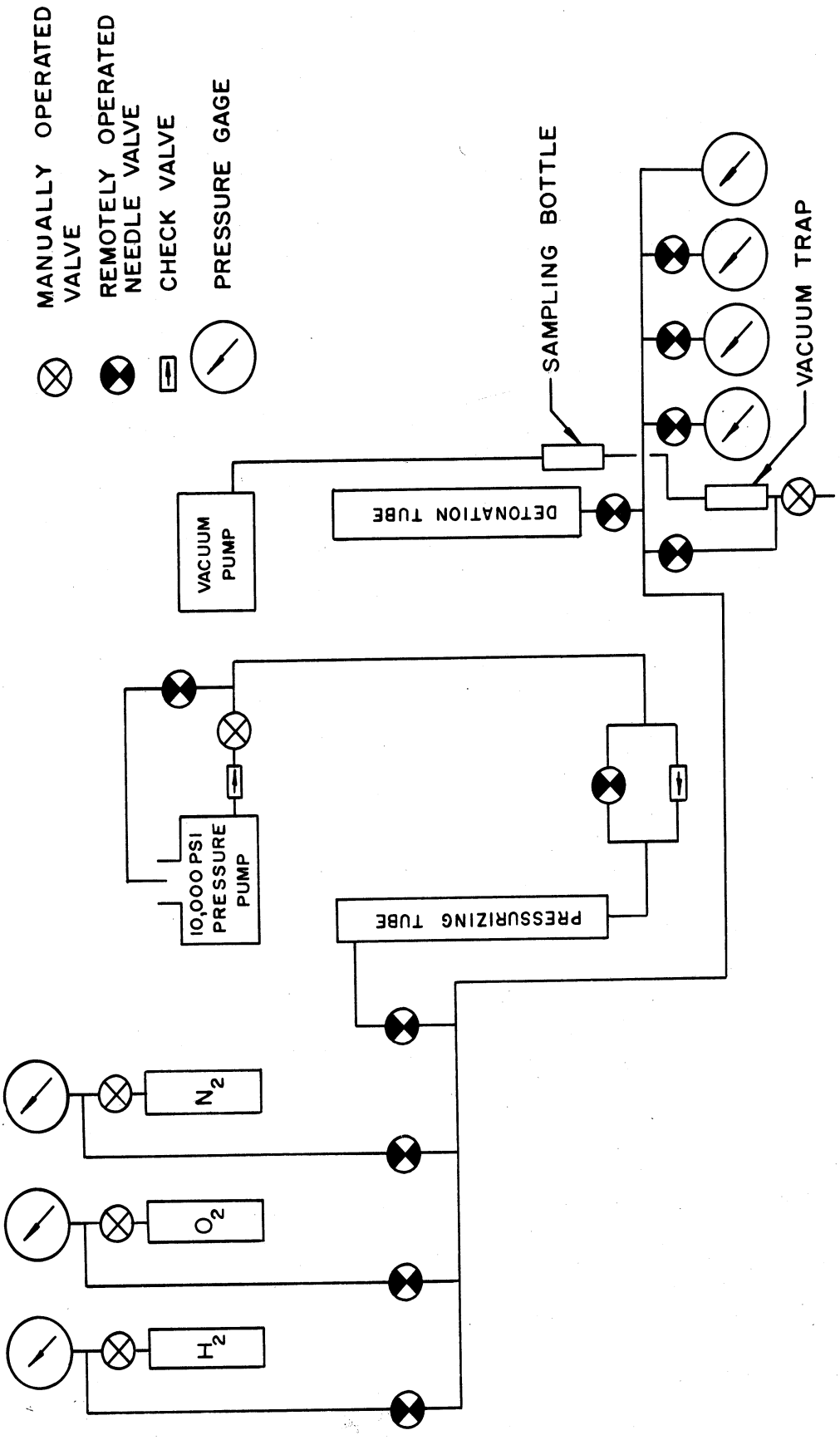

Figure 2. Schematic Flow Diagram of Experimental System.

to the desired pressure. If the desired pressure was less than the pressure in the pressurizing tube, hydraulic fluid* was forced up through the bottom of the pressurizing tube by means of a 10,000 lb/sq in. pressure tester, to compress the gas in the system to the desired pressure. The valves to the detonation tube and pressurizing tube were closed and the lines between the tubes evacuated to guard against igniting the gas in the pressurizing tube by shock through the valves. The gas in the detonation tube was ignited at the bottom by a hot wire and the detonation wave velocity determined by measuring the time required for the wave to pass between two ionization probes, spaced a known distance apart, at the top of the tube. The detonation was allowed to burst a brass diaphragm at the top of the tube whose bursting pressure was slightly above the initial pressire, in order to minimize the strength of the reflected shock wave.

This procedure was repeated until the gas in the pressurizing tube was nearly exhausted. A sample was then drawn from the pressurizing tube to be analyzed and the hydraulic fluid forced by nitrogen pressure out of the tube and back into the pump resevoir. The analysis was necessary, since the composition was only approximately known from the partial-pressure charging technique.

The analyses were made by absorbing the oxygen from a sample in a solution of alkaline pyrogallol and measuring the volumetric loss at constant pressure. Three analyses were made for each sample and the arithmetic average used as the correct one. The analyzing apparatus was periodically checked by analyzing a sample of air and was considered to

* Shell Irus Fluid 902, a fire-resistant hydraulic fluid containing 32-37% water in emulsion.

be operating correctly when it indicated 0.210 $\pm$ 0.002 as the mole fraction of oxygen in air.

The Detonation Tube

Since it was not known at the beginning of the experiment what the highest initial pressures would be, the detonation tube was designed with the assumption that the initial pressure would get as high as the pressure pump rating (10,000 lb/sq in.). With this initial pressure, a pressure rise across the detonation wave of 20 to 1, and a slight multiplication of pressure due to the reflected wave (even with a blow-off diaphram in the end of the tube), the maximum pressure in the tube could be expected to approach a quarter of a million psi. Thick walled tube theory predicts[34] that the maximum pressure an unstressed single tube will contain is the tensile strnegth of the material in lb/sq in. Since stainless steel was selected as the tube material, for corrosion and rust resistance, this would mean that a tube with infinite outside to inside diameter ratio could be expected to fail at less than 100,000 lb/sq in. However, Bridgman[4] found that for very thick walled tubes, this upper limit could be multiplied by 2 or 3. Also, since the maximum pressures would exist for very short times, the inertia of the mass of metal surrounding the bore of a very thick walled tube was depended upon to boost the upper pressure limit somewhat. The system was located as described previously in case the above mentioned assumptions were not valid. These ideas were considered in designing the detonation tube. As it happened, the tube was only required to hold some 70,000 lb/sq in.

The detonation tube (Figure 3) was fabricated from a length of stainless steel rod, 7 ft. long and 4 in. in diameter. A 1/2 in. hole was drilled lengthwise through its center, yielding a tube with an outside to inside diameter ratio of 8. Five receptacle taps were machined in the wall of the tube, one near one end for receiving the ignitor wire fitting, and four near the other end for receiving two ionization probes at various spacing, and a thermocouple.

The end near the ignitor receptacle was machined to receive a fitting to which was attached a 150,000 lb/sq in. rated valve for closing the detonation tube off from the rest of the system during high pressure ignition. The other end was machined to receive a cap whose purpose was to retain a blowoff diaphragm which was replaced after each detonation. A photograph of the detonation tube and cap is shown in Figure 4.

The Pressurizing Tube

The pressurizing tube (Figure 5) was fabricated from a length of 2 1/2 in. double extra heavy steel pipe, 8 ft. long, 2 7/8 in. in outside diameter, and 1 3/4 in. in inside diameter. One end was fitted to connect directly to the hydraulic fluid line. The other end was fitted with a cap similar in design to the one on the detonation tube for retaining a safety blow-off diaphragm. Several holes were tapped into the wall near each end. At the diaphragm end, one hole was made for the gas inlet-outlet line, and one for a thermocouple (so that too-rapid compression, with subsequent temperature rise, could be avoided). Three more holes at this end and three at the other end were made for

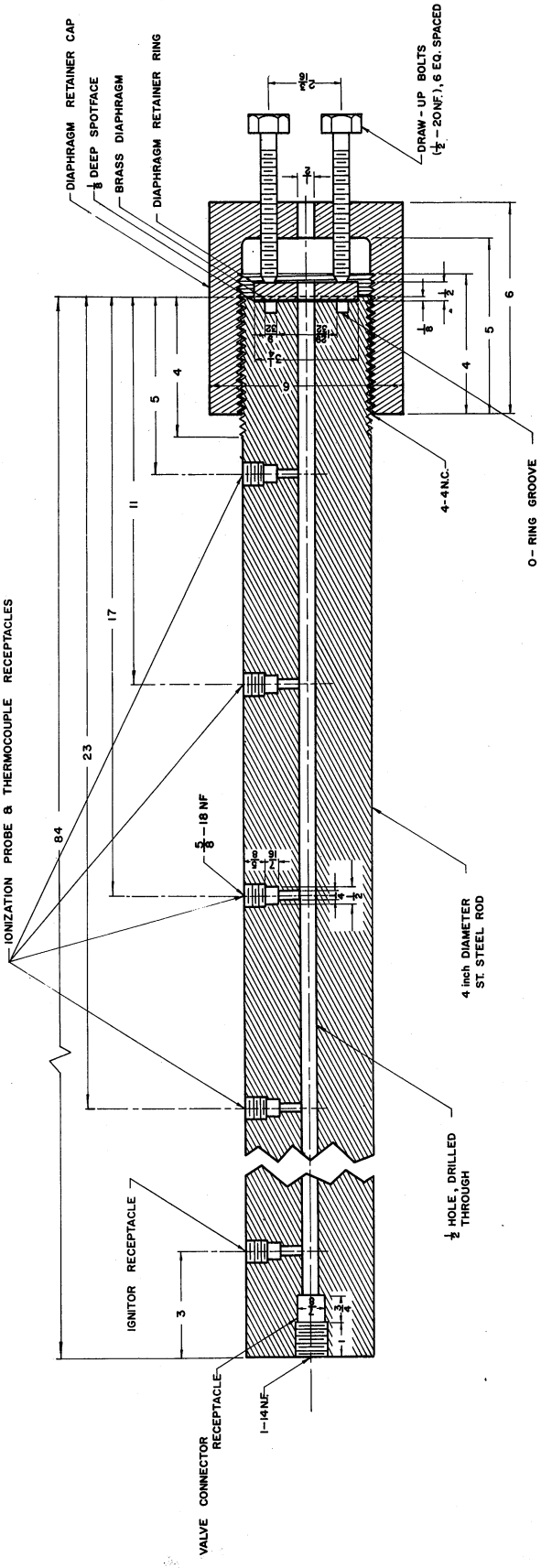

Figure 3. Assembly of Detonation Tube and Cap

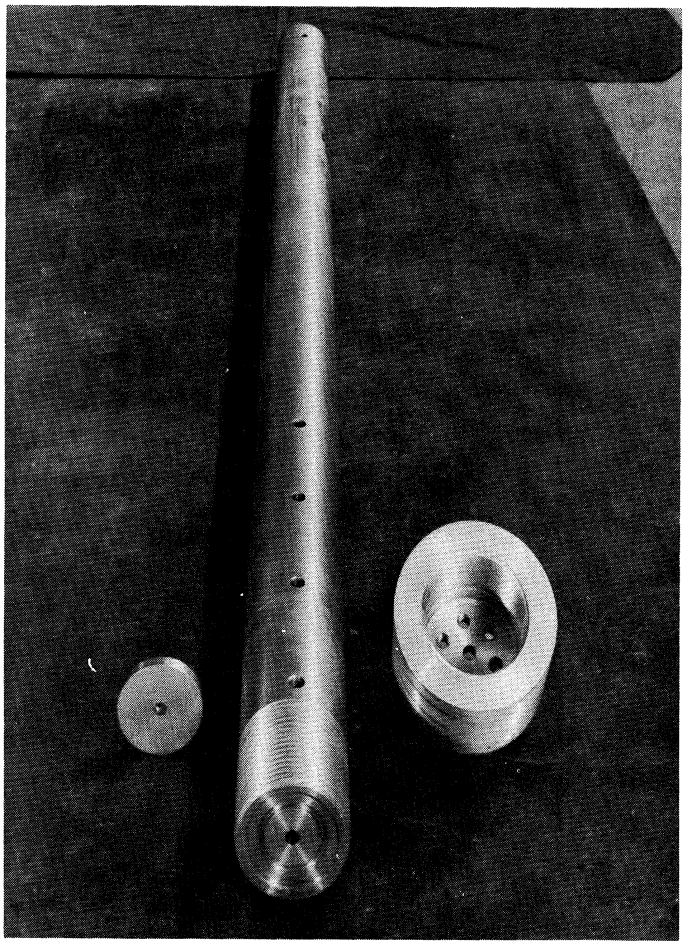

Figure 4. Photograph of Detonation Tube and Cap

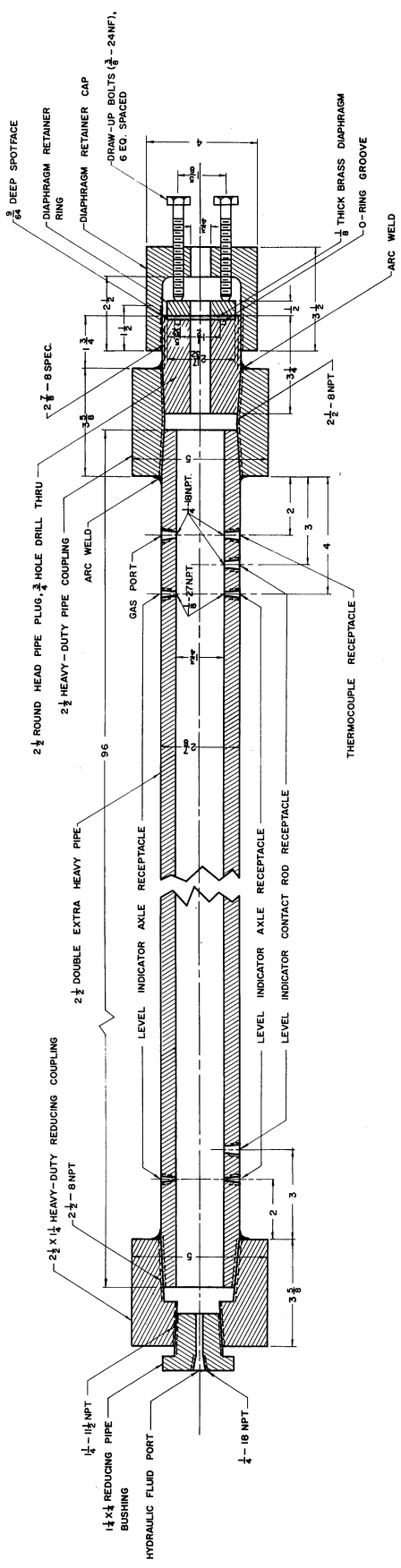

Figure 5. Assembly of Pressurizing Tube and Cap

mounting the fluid level indicators. In order to ensure that the hydraulic fluid did not get below the tube bottom, which might allow gas to leak out through the check valve, or above the gas outlet, in which case fluid would flood the system, special high pressure level indicators (Figure 6) were fabricated and mounted near the top (below the gas port) and near the bottom (above the hydraulic fluid port).

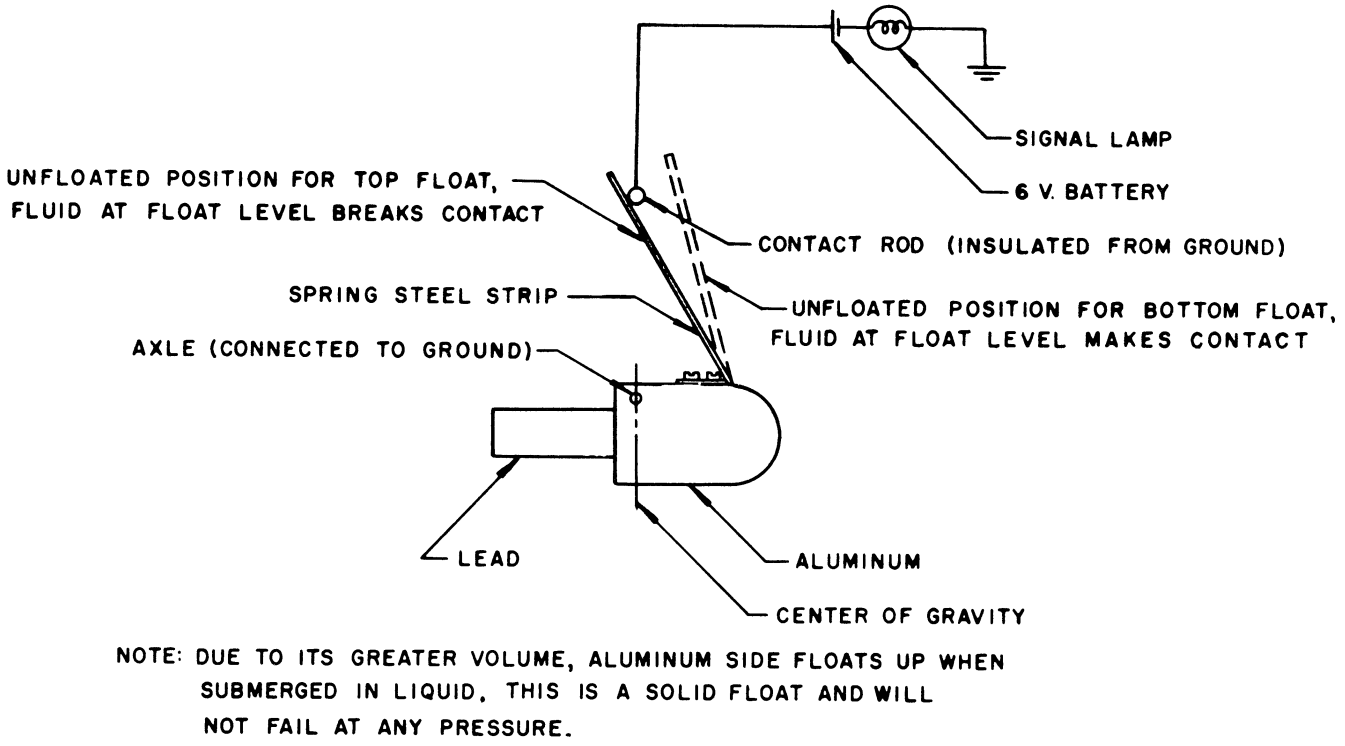

Figure 6. Liquid Level Indicator for Pressurizing Tube.

The indicators were arranged such that signal lights attached to them wer both lit when the fluid was between the two levels. If the fluid rose

above the upper level, or fell below the lower level, the indicated signal light would go out, and the situation could be remedied. A photograph of the pressurizing tube and cap is shown in Figure 7.

Probes

The ionization probes designed for high pressure application are shown in Figure 8. These probes were mounted in the detonation tube wall and pressure sealed by means of Bridgman[4] "unsupported area" packings. With this type of packing, an increase in pressure results automatically in an increase in sealing compression so that leakage cannot occur and failure occurs only when the pressure is high enough to cause the packing material to pinch off the tube. The same principle was used to seal the electrode within the probe, but the design is more complex here because the electrode must be insulated from the tube wall (ground) as well as sealed against leaks.

The ignitor and thermocouple (Figures 9 and 10) were similarly designed using the unsupported area packing and were mounted in the detonation tube wall in the same way. The connector between the detonation tube and heavy valve (Figure 11) was mounted in a similar fashion. The entire system, with the exception of low pressure gages, was pressure checked to 10,000 lb/sq in. abs and all probes and connectors were determined to be sealed against leaks at this pressure.

Velocity Measuring Equipment

The two ionization probes were mounted in the receptacles spaced furthest from each other at the diaphragm end of the detonation tube,

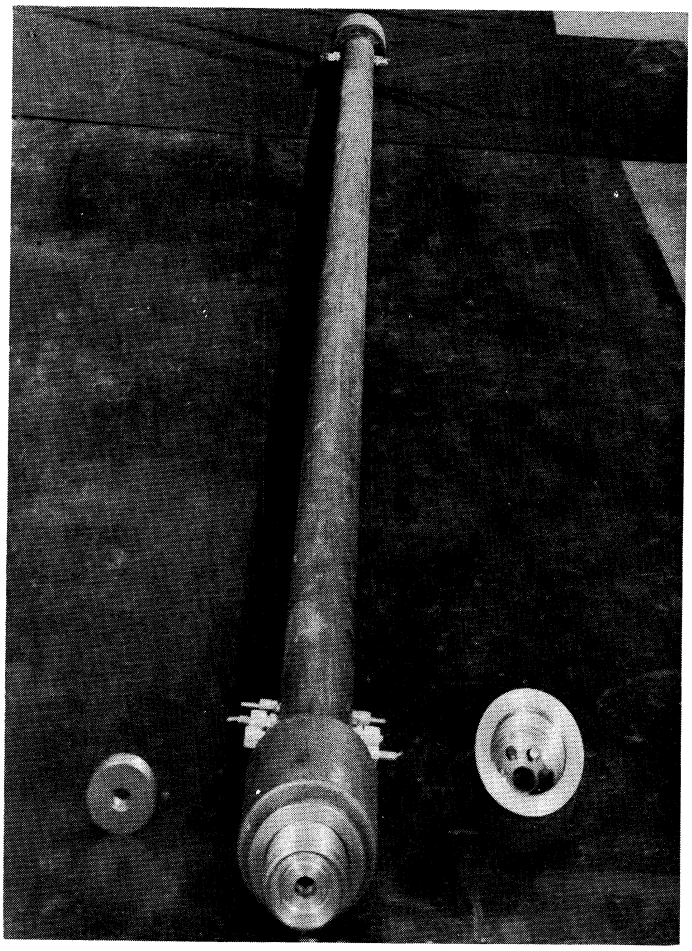

Figure 7. Photograph of Pressurizing Tube and Cap

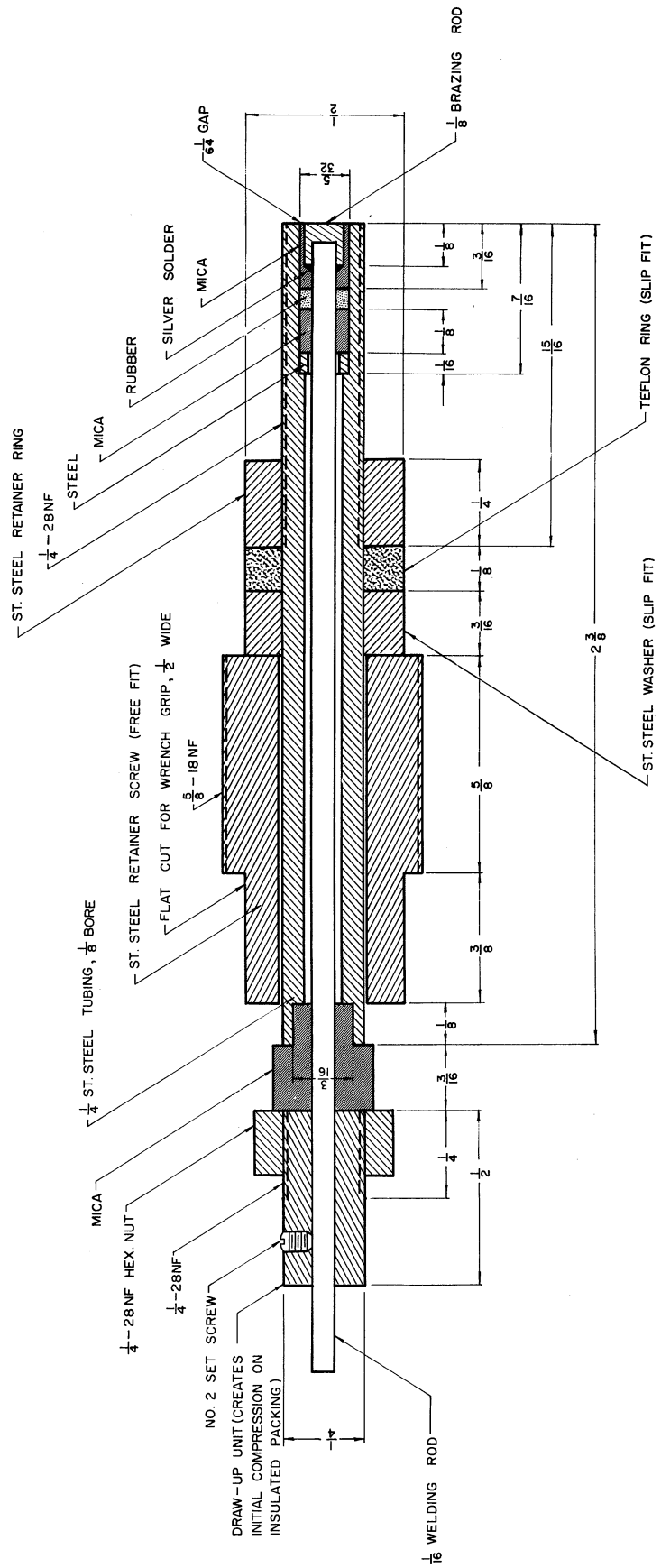

Figure 8. Ionization Probe Assembly

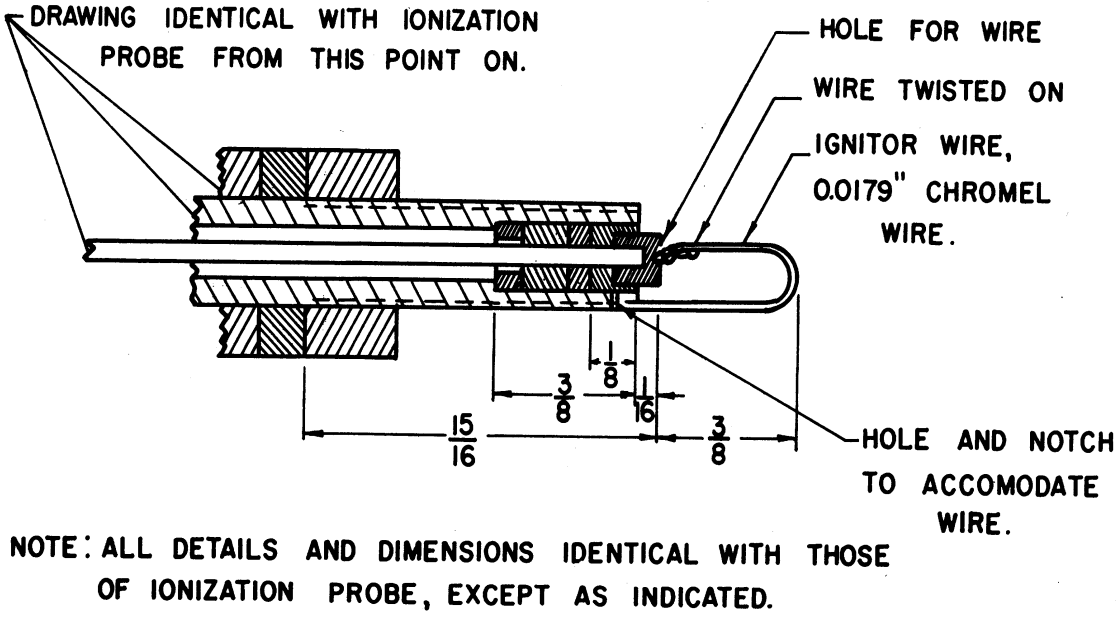

Figure 9. Ignitor Assembly

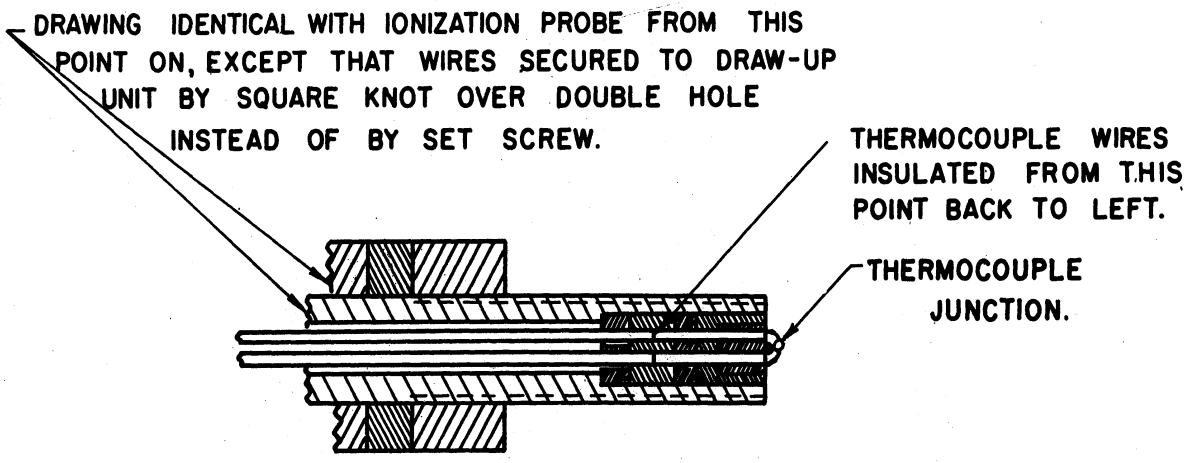

Figure 10. Thermocouple Assembly.

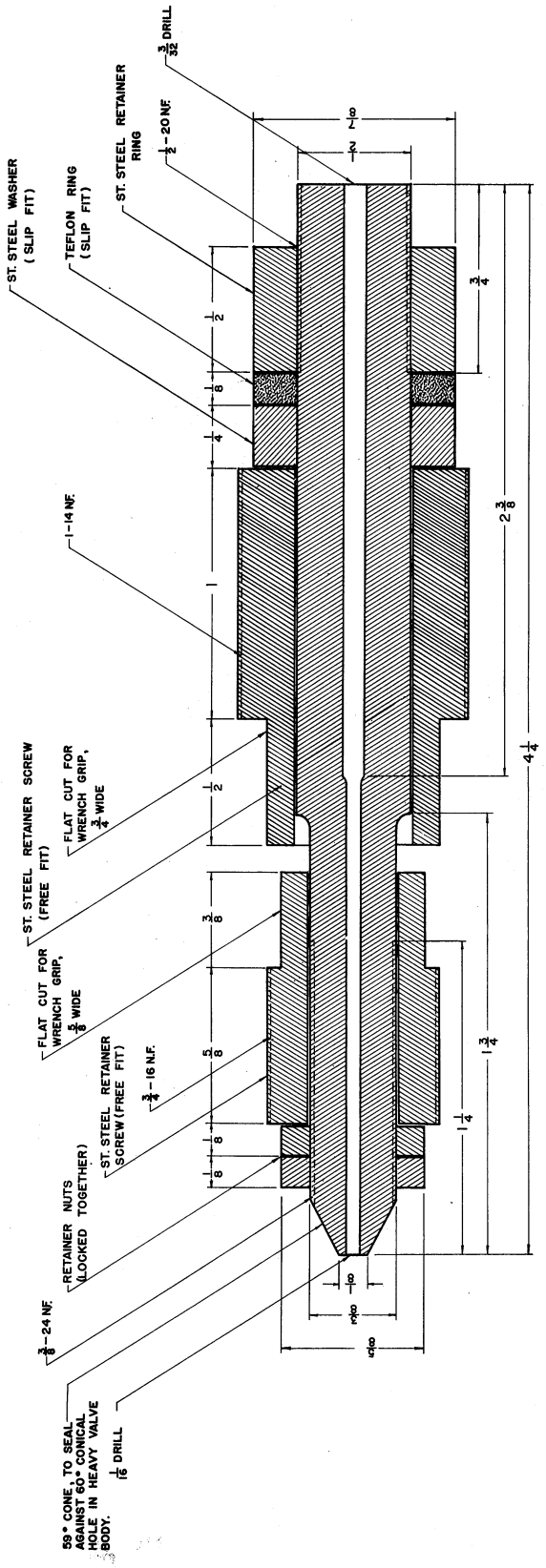

Figure 11. Assembly of Connector Between Detonation Tube and Heavy-Duty Valve

creating a distance of 18 in. between them. For a few runs, the probe nearest the ignitor was moved up to the next receptacle so that the spacing was 12 in. and the distance from the ignitor to the first probe was 6 in. greater. This was done to ensure that the detonation wave had developed fully by the time it reached the first probe. When no significant difference in detonation velocity was detected by doing this, it was assumed that the wave had developed before reaching the first probe, and the probe was moved back to its original position for maximum probe spacing. Further confidence that the wave had developed fully before reaching the first probe is gained from data given in Reference (12) which indicates that probably (although no data is given for this particular tube diameter) the wave develops in less than two feet from the point of ignition.

The detonation wave induction distance is also dependent upon initial pressure. Data by Dumanois and Laffitte[24] for a stoichiometric hydrogen-oxygen mixture in a 25 mm tube is reproduced below in Table I.

TABLE I.

THE EFFECT OF INITIAL PRESSURE ON DETONATION INDUCTION DISTANCE

Initial Pressure, atm	Induction Distance, cm
1	70
2	60
3	52
4	44
5	35
6	30
6.5	27

Since detonation is more easily set up in smaller than larger diameter tubes[26], no difficulty was expected with this system for stoichiometric mixtures, even at the lowest pressure (1 atm). However, difficulty was experienced in obtaining consistent data for the rich mixtures at the lower pressures. This is attributed to the possibility that under these conditions, the wave had not developed before reaching the first probe, which is reasonable in view of the fact that the induction distance for the stoichiometric mixture at 1 atm is approaching the distance allotted between the ignitor and the first probe (58 in.). This is discussed more fully in Chapter VI.

The detonation velocity was measured as follows (Figure 12): A positive potential was placed on the anodes of the thyratron tubes.

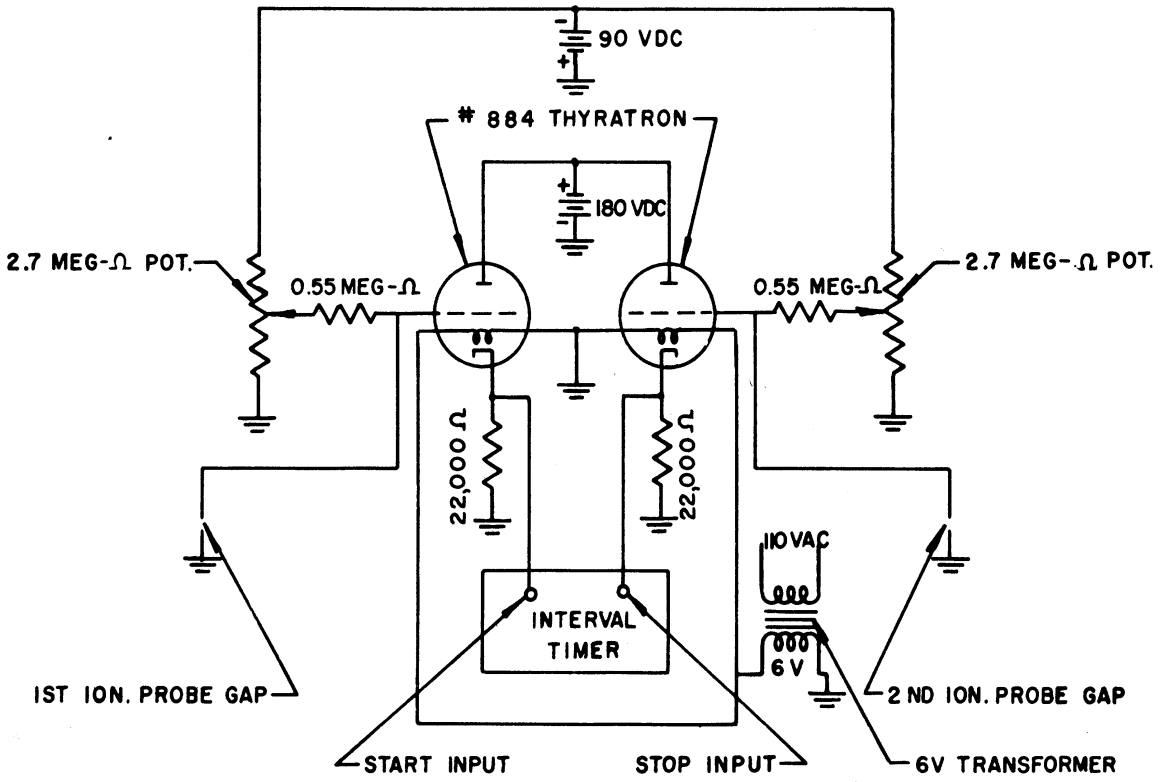

Figure 12. Timing Circuitry.

A negative potential just sufficient to prevent the tubes from firing was placed on the grids of the thyratrons. Each grid was also connected to the electrode of one of the ionization probes. The cathodes of the thyratrons were connected to the start and stop jacks respectively, of the interval timer. The detonation wave, passing over the first probe, ionized the gas near the probe gap allowing a current to flow across the gap. This caused the voltage on the grid of the first thyratron to be decreased enough to allow that thyratron to fire. The resultant current pulse caused the start circuit in the timer to be activated. The detonation wave passing over the second probe caused the second thyratron to fire activating the stop circuit in the timer. The timer now displayed a time interval which indicated the time necessary for the wave to pass between the probes. Dividing the probe spacing by this time yielded wave velocity directly. The timer used was a Hewlett-Packard Electronic Counter Model 524B with a Time Interval Unit Model 526B. This timer registers time intervals down to 0.1 microsecond with an accuracy of $\pm$ 0.1 microsecond. Intervals measured were of the order of 100 or 200 microseconds. The 100 kilocycle oscillator on the timer was standardized by beating the output against a frequency of the National Bureau of Standards radio station WWV, the crystal being adjusted until zero beat was obtained.

III. PREDICTION OF DETONATION VELOCITIES, PRESSURES, AND TEMPERATURES

The Hydrodynamic Equations

For the situation of a detonation wave moving along a tube, the tube wall is stationary, the wave has a velocity u_w', the unburned gases have a velocity $u_1' = 0$, and the products of combustion have a velocity u_2', all primed velocities being taken with respect to the tube wall. The mathematical analysis of the system is simplified considerably if a transformation of velocity co-ordinates is performed such that all velocities are taken with respect to the detonation wave. Consider the system shown in Figure 13. The vertical line represents

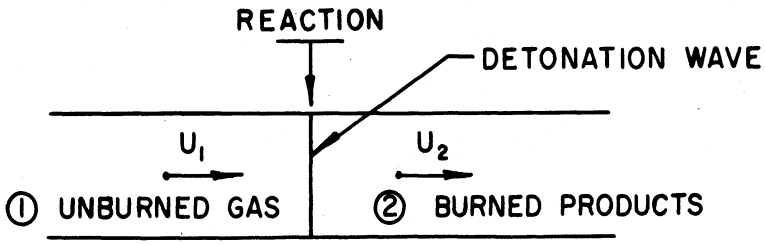

Figure 13. Schematic of Standing Detonation Wave Reference System.

a detonation wave or shock wave with heat addition (the "heat" being provided by the exothermic chemical reaction). In the standing wave co-ordinate system, the wave has zero velocity, the unburned gases enter the wave with velocity u_1, and the products of combustion leave the wave

with velocity u_2, unprimed velocities being taken with respect to the detonation wave. It is apparent that the two velocity co-ordinate systems are connected by the relationships: $u_1 = -u_w'$ (for $u_1' = 0$) and $u_2 = u_2' - u_w'$.

Lewis and Von Elbe[26] have reproduced arguments that the velocity of the detonation wave relative to the burned gases, is usually equal to the speed of sound in the burned gases in state 2. This condition is known as the Chapman-Jouguet condition. State 2 is then defined as that state wherein the products of combustion are in chemical equilibrium and moving at the local speed of sound relative to the detonation wave. The assumption of chemical equilibrium at the Chapman-Jouguet plane is usually made and velocities calculated on this basis are found to agree with experiment better than velocities calculated assuming complete reaction (22, 25, 42).

If it is assumed that molecular diffusion, viscous, and thermal conductivity terms are negligible[30], four equations may be written relating state 1 and state 2, without a consideration of the process by which the change took place:

$$\rho_1 u_1 = \rho_2 u_2 \qquad \text{(Conservation of mass)} \qquad (1)$$

$$P_1 + \rho_1 u_1^2 = P_2 + \rho_2 u_2^2 \qquad \text{(Conservation of momentum)} \qquad (2)$$

$$h_1 + \frac{u_1^2}{2} = h_2 + \frac{u_2^2}{2} \qquad \text{(Conservation of energy)} \qquad (3)$$

$$P = \frac{z\rho RT}{m} \qquad \text{(Equation of state)} \qquad (4)$$

These equations are developed from the viewpoint of one who is stationed on the wave watching gas in state 1 enter and gas in state 2 leave the wave. The situation is the same if the observer watches the wave move into the unburned gas. The gas in state 1 is then stationary,

the wave moves to the left with a velocity $u_w' = -u_1$, and the gas in state 2 moves to the left with a velocity $u_2' = u_2 - u_1$. If all velocities are taken relative to the wave, u_1 is then the detonation velocity and u_2 is the local speed of sound in state 2.

Equations (1), (2), (3), and (4), are manipulated (see Appendix A) to yield the following equations relating the two states. The form of these equations is designed for ease in handling this particular problem.

$$T_2 = \left(\frac{\Delta h}{R} + \frac{z_1 T_1}{m_1}\right) \frac{2 m_2 \gamma_2}{(1 + 2\gamma_2) Z_2} \tag{5}$$

$$u_1 = \sqrt{2R\left[\frac{z_2 T_2 (1 + \gamma_2)^2}{2 m_2 \gamma_2} - \frac{z_1 T_1}{m_1}\right]} \tag{6}$$

$$\frac{P_2}{P_1} = \left\{ \frac{2}{(z_1 T_1 / m_1)} \left[\frac{z_2 T_2 (1 + \gamma_2)^2}{2 m_2 \gamma_2}\right] - 1 \right\} \Big/ (1 + \gamma_2) \tag{7}$$

and by definition:

$$\Delta h = \frac{1}{m_2}\left[\sum_P x_P (H^\circ_{T_2} - H^\circ_0)_P + \sum_P x_P (\Delta H^\circ_f)_P\right] - \frac{1}{m_1} \sum_R x_R (H^\circ_{T_1} - H^\circ_0)_R \tag{8}$$

In order to determine u_1, T_2 must be determined, but T_2 depends directly upon Δh which in turn depends upon the chemical composition of the products of combustion. Since the composition of the products of combustion is a function of T_2 (the equilibrium constants vary with T_2), the procedure for computing u_1 is apparent. The temperature must be determined by a simultaneous solution between Equation (5) and the equations of chemical equilibrium. This temperature, along with m_2 and γ_2 which are known once the product composition is known, are used in Equation (6) to determine u_1. Since P_1 will finally be the main independent

variable in the presentation of results, it is not necessary to "aim for" a particular value of P_1, i.e., P_2 may be fixed in the equilibrium calculations and a lengthy successive approximation computation is eliminated. Then P_1 may be explicitly obtained from Equation (7). If it were necessary to obtain a solution for a particular P_1, then P_2 would have to be assumed and the temperature - composition calculations adjusted till the desired P_1 was obtained.

The Chemical Equilibrium Equations

In calculating the composition of the products of combustion, it is first necessary to determine what chemical products will be present. It is assumed that six chemical species are present: H_2, O_2, H_2O, H, O, and OH. The equilibrium constant for the decomposition of ozone is so large compared to the other constants that ozone is not considered as being present in the product gases. The chemical equilibrium equations relating the species are:

$$H_2O \rightleftarrows H_2 + 1/2\ O_2 \tag{9}$$

$$H_2O \rightleftarrows 1/2\ H_2 + OH \tag{10}$$

$$1/2\ H_2 \rightleftarrows H \tag{11}$$

$$1/2\ O_2 \rightleftarrows O \tag{12}$$

The fugacities of the six components are related by the equilibrium constants as follows:

$$K_{f1} = \frac{f_{H_2} f_{O_2}^{1/2}}{f_{H_2O}} \tag{13}$$

$$K_{f2} = \frac{f_{H_2}^{1/2} f_{OH}}{f_{H_2O}} \tag{14}$$

$$K_{f3} = \frac{f_H}{f_{H_2}^{1/2}} \tag{15}$$

$$K_{f4} = \frac{f_O}{f_{O_2}^{1/2}} \tag{16}$$

and since $f = \nu\ p$ and $p = x\ P$, then:

$$K_{f1} = \frac{\nu_{H_2}\nu_{O_2}^{1/2}}{\nu_{H_2O}} \cdot \frac{x_{H_2}x_{O_2}^{1/2}}{x_{H_2O}} P_2^{1/2} = K_{\nu 1}K_{P1} \tag{17}$$

$$K_{f2} = \frac{\nu_{H_2}^{1/2}\nu_{OH}}{\nu_{H_2O}} \cdot \frac{x_{H_2}^{1/2}x_{OH}}{x_{H_2O}} P_2^{1/2} = K_{\nu 2}K_{P2} \tag{18}$$

$$K_{f3} = \frac{\nu_H}{\nu_{H_2}^{1/2}} \cdot \frac{x_H}{x_{H_2}^{1/2}} P_2^{1/2} = K_{\nu 3}K_{P3} \tag{19}$$

$$K_{f4} = \frac{\nu_O}{\nu_{O_2}^{1/2}} \cdot \frac{x_O}{x_{O_2}^{1/2}} P_2^{1/2} = K_{\nu 4}K_{P4} \tag{20}$$

Mass balance equations may be written for H_2 and O_2:

$$2(n_{O_2})_1 = (2n_{O_2} + n_O + n_{H_2O} + n_{OH})_2 \tag{21}$$

$$2(n_{H_2})_1 = (2n_{H_2} + n_H + 2n_{H_2O} + n_{OH})_2 \tag{22}$$

Equations (17)-(22) are sufficient to determine the mole fraction of the six product components as functions of T_2, P_2 and initial composition. These six equations were manipulated (see Appendix B) to reduce them to two equations in two unknowns, with the other four unknowns appearing as

explicit functions of those two (the subscripts denoting state 2 have been dropped from the x's):

$$x_{H_2O} = \frac{1}{c}\left\{ - e \pm \sqrt{e^2 + 2c\,(1 - x_{H_2} - d)} \right\} \tag{23}$$

$$x_{H_2O} = \frac{1}{2c}\left\{ - h \pm \sqrt{h^2 + 4cF(2x_{H_2} + d)} \right\} \tag{24}$$

$$x_{O_2} = \frac{K_{P1}^2}{P_2}\left(\frac{x_{H_2O}}{x_{H_2}}\right)^2 \tag{25}$$

$$x_{OH} = \frac{K_{P2}}{\sqrt{P_2}}\left(\frac{x_{H_2O}}{x_{H_2}^{1/2}}\right) \tag{26}$$

$$x_H = \frac{K_{P3}}{\sqrt{P_2}}\, x_{H_2}^{1/2} \tag{27}$$

$$x_O = \frac{K_{P1}K_{P4}}{P_2}\left(\frac{x_{H_2O}}{x_{H_2}}\right) \tag{28}$$

where:

$$e = a + b + 1 \tag{29}$$

$$g = F(b + 2) \tag{30}$$

$$h = e - g \tag{31}$$

$$a = K_{P1}K_{P4}/P_2x_{H_2} \tag{32}$$

$$b = K_{P2}/\sqrt{P_2}\,\sqrt{x_{H_2}} \tag{33}$$

$$c = 2K_{P1}^2/P_2x_{H_2}^2 \tag{34}$$

$$d = K_{P3}\sqrt{x_{H_2}}\,/\sqrt{P_2} \tag{35}$$

In summary, the procedure is to determine the product compositions as a function of T_2, P_2 and initial composition by means of Equations (23) - (28); determine T_2 at a fixed P_2 and initial composition by

means of Equations (5) and (8); and determine u_1 and P_1 by means of Equations (6) and (7) respectively.

Computer Programming

The chemical equilibrium equations were solved with the use of an IBM-650 computer. The iteration method developed for these computations is illustrated graphically in Figure 14. The program flowsheet is shown in Figure 15.

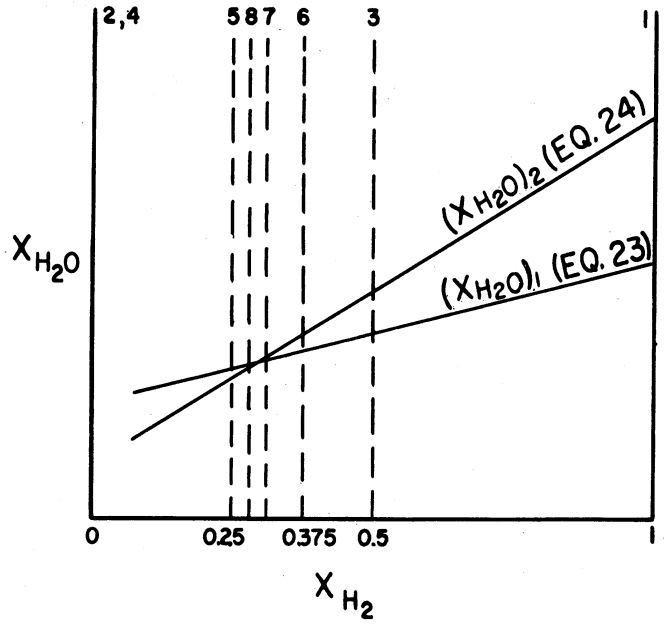

Figure 14. Graphical Illustration of Computer Convergence Technique.

It is clear that the solution is represented by the intersection of two curves representing solutions of Equations (23) and (24). The solution involves converging on this point by a "half-interval" method, i.e., by successively cutting in half the interval between two sets of solutions, given by a "right" and a "left" difference between $(x_{H_2O})_2$ and $(x_{H_2O})_1$,

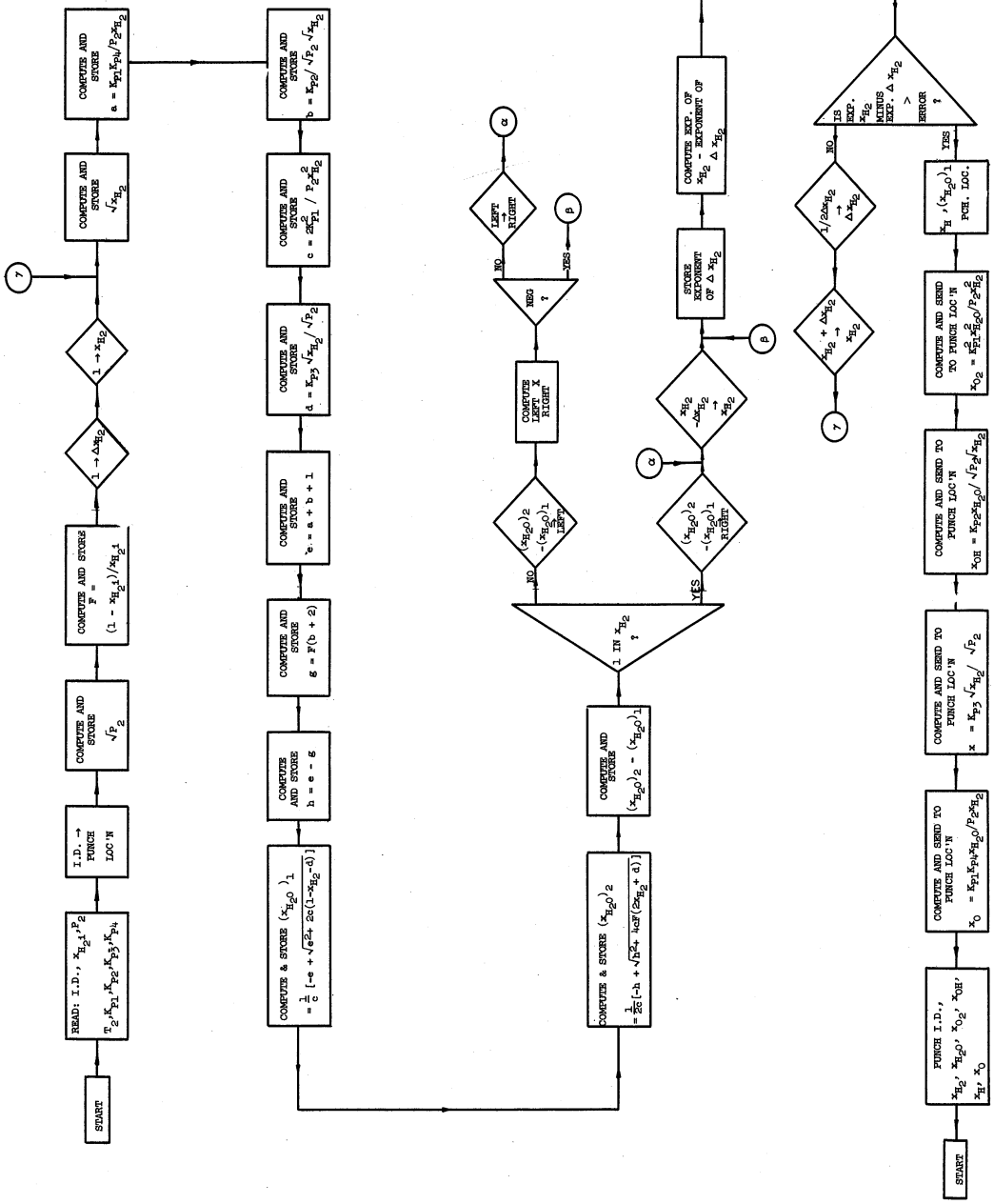

Figure 15. Computer Program Flowsheet for Chemical Equilibrium Computations

(see Figure 15). By the following testing method, it is assured that the true solution is always within the interval bounded by "left" and "right". If "left" and "right" differences between $(x_{H_2O})_2$ and $(x_{H_2O})_1$ are of the same sign, the intersection is not in the interval. If they are of opposite sign, it is in the interval. This sign is tested by taking the product of "left" and"right" differences. The next step in the program is decided on the basis of the sign of this product. The test for convergence is such that there will be a pre-determined number of accurate significant figures (in this case 5) in the result regardless of decimal point location. A floating decimal point program was used.

The input data were fed to the machine on data cards on which were punched an identification number, initial hydrogen concentration, P_2, T_2, K_{P1}, K_{P2}, K_{P3}, and K_{P4}. The output cards (one for each input card) had punched on them the identification number, and the mole fractions of the six product components. The coded program which operated on the data cards is shown in Appendix C. A description of the coding symbols and format is given in Reference (38) which describes the operation of the IBM-650 computer and an assembly program allowing the use of a coded alphabetic operational program (Symbolic Optimal Assembly Program II). The reader may follow the program logic by application of the flowsheet (Figure 15) to Figure 14. Successive steps (values of x_{H_2}) are indicated by the numbered vertical lines in Figure 14. Recycle loops are indicated by Greek letters on the flowsheet.

Computational Procedure

The equations and information necessary for the computation of detonation velocities as a function of initial pressure and mixture composition are: Equations (5), (6), (7), and (8); product equilibrium concentration data as a function of final pressure, final temperature, and initial composition; and enthalpy and specific heat data. The procedure which first suggests itself is to employ a successive approximation calculation. This would involve the following steps:

1. Fix initial composition and final pressure.
2. Assume final temperature (T_2).
3. Determine product composition from equilibrium data.
4. Determine Δh from Equation (8).
5. Calculate T_2 from Equation (5).
6. Adjust assumed T_2 based on step 5.
7. Go back to step 3 and repeat until calculated T_2 matches assumed T_2.
8. Calculate u_1 from Equation (6).
9. Calculate P_1 from Equation (7).

This procedure, on the surface, is straightforward and simple. However, each time T_2 is adjusted, temperature interpolations must be performed on the mole fractions, enthalpies, and specific heats of all six components, and these new values applied to calculating final molecular weight, final specific heat ratio, Δh, and T_2. Graphical interpolation is ruled out in most cases due to the range of variation of the values of the quantities, linear interpolation sacrifices too much accuracy, and a more refined mathematical interpolation would be too

time consuming. Therefore, the following procedure was developed:

1. Fix initial composition and final pressure.
2. Determine product composition from equilibrium data, Δh from Equation (8), and T_2 from Equation (5) for four assumed T_2's surrounding the expected T_2, for which tabulated data are available.
3. Establish the "error" between the four calculated T_2's and the corresponding assumed T_2's.
4. Employ a Lagrangian four point interpolation on these errors to zero error, to determine T_2. (See development of interpolation equations below.)
5. Use the same interpolation factors to calculate m_2 and γ_2 at the interpolated T_2.
6. Calculate u_1 from Equation (6).
7. Calculate P_1 from Equation (7).

With this method, tabulated data may be used throughout and essentially only a single interpolation is necessary for each point.

Interpolation Equations

In order to find y at a particular x where there is available a table of y_1, y_2, etc. corresponding to values of x_1, x_2, etc., one may apply the Lagrangian interpolation formula[40], which, for four points, is:

$$y = y_1\left[\frac{x-x_2}{x_1-x_2}\times\frac{x-x_3}{x_1-x_3}\times\frac{x-x_4}{x_1-x_4}\right] + y_2\left[\frac{x-x_1}{x_2-x_1}\times\frac{x-x_3}{x_2-x_3}\times\frac{x-x_4}{x_2-x_4}\right]$$

$$+ y_3\left[\frac{x-x_1}{x_3-x_1}\times\frac{x-x_2}{x_3-x_2}\times\frac{x-x_4}{x_3-x_4}\right] + y_4\left[\frac{x-x_1}{x_4-x_1}\times\frac{x-x_2}{x_4-x_2}\times\frac{x-x_3}{x_4-x_3}\right] \quad (36)$$

This may be applied to this case as follows:

Let $y = T_2$ (= final temperature) (37)

$x_n = (T_{2\ CALC})_n - (T_{2\ ASSUMED})_n = \epsilon_n$ (38)

$y_n = (T_{2\ ASSUMED})_n$ (39)

Then when $T_2 = T_2$, $\epsilon = 0$. This is illustrated graphically in Figure 16 below.

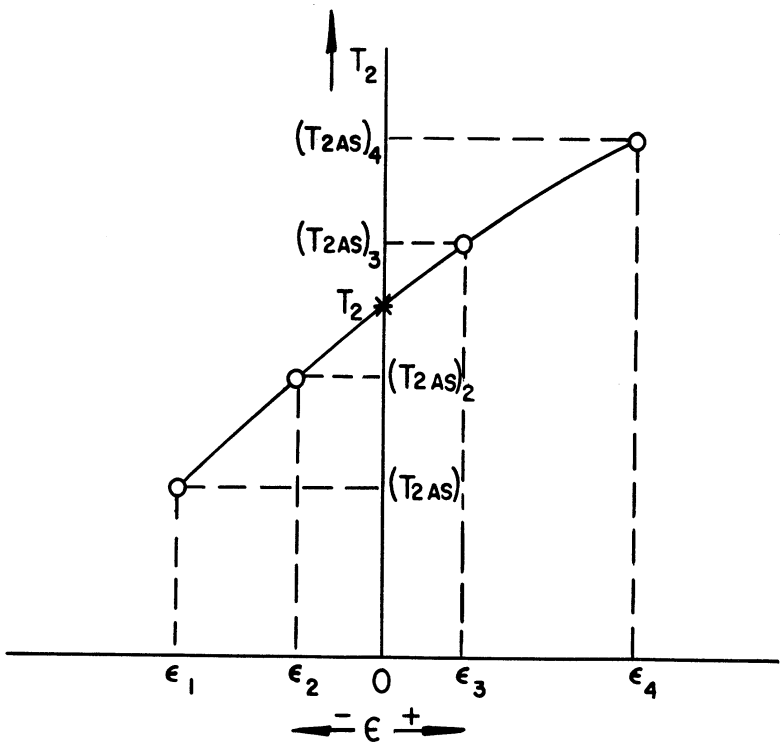

Figure 16. Graphical Illustration of Temperature Interpolation Technique.

Equation (36) then becomes:

$$T_2 = (T_{2\ AS})_1 \left[\frac{\epsilon_2}{\epsilon_2-\epsilon_1} \times \frac{\epsilon_3}{\epsilon_3-\epsilon_1} \times \frac{\epsilon_4}{\epsilon_4-\epsilon_1}\right] - (T_{2\ AS})_2 \left[\frac{\epsilon_1}{\epsilon_2-\epsilon_1} \times \frac{\epsilon_3}{\epsilon_3-\epsilon_2} \times \frac{\epsilon_4}{\epsilon_4-\epsilon_2}\right]$$

$$+ (T_{2\ AS})_3 \left[\frac{\epsilon_1}{\epsilon_3-\epsilon_1} \times \frac{\epsilon_2}{\epsilon_3-\epsilon_2} \times \frac{\epsilon_4}{\epsilon_4-\epsilon_3}\right] - (T_{2\ AS})_4 \left[\frac{\epsilon_1}{\epsilon_4-\epsilon_1} \times \frac{\epsilon_2}{\epsilon_4-\epsilon_2} \times \frac{\epsilon_3}{\epsilon_4-\epsilon_3}\right] \quad (40)$$

Let:

$$\Pi_1 = \frac{\epsilon_2\epsilon_3\epsilon_4}{(\epsilon_2-\epsilon_1)(\epsilon_3-\epsilon_1)(\epsilon_4-\epsilon_1)} \tag{41}$$

$$\Pi_2 = \frac{\epsilon_1\epsilon_3\epsilon_4}{(\epsilon_2-\epsilon_1)(\epsilon_3-\epsilon_2)(\epsilon_4-\epsilon_2)} \tag{42}$$

$$\Pi_3 = \frac{\epsilon_1\epsilon_2\epsilon_4}{(\epsilon_3-\epsilon_1)(\epsilon_3-\epsilon_2)(\epsilon_4-\epsilon_3)} \tag{43}$$

$$\Pi_4 = \frac{\epsilon_1\epsilon_2\epsilon_3}{(\epsilon_4-\epsilon_1)(\epsilon_4-\epsilon_2)(\epsilon_4-\epsilon_3)} \tag{44}$$

Then:

$$T_2 = (T_{2\ AS})_1\ \Pi_1 - (T_{2\ AS})_2\ \Pi_2 + (T_{2\ AS})_3\ \Pi_3 - (T_{2\ AS})_4\ \Pi_4 \tag{45}$$

Also, if $(m_2)_n$ and $(\gamma_2)_n$ are the values of m_2 and γ_2 at $(T_{2\ AS})_n$, then

$$\gamma_2 = (\gamma_2)_1\ \Pi_1 - (\gamma_2)_2\ \Pi_2 + (\gamma_2)_3\ \Pi_3 - (\gamma_2)_4\ \Pi_4 \tag{46}$$

and

$$m_2 = (m_2)_1\ \Pi_1 - (m_2)_2\ \Pi_2 + (m_2)_3\ \Pi_3 - (m_2)_4\ \Pi_4 \tag{47}$$

In order to ensure that sufficient accuracy was obtained using a four-point interpolation, a single temperature was computed using a five-point interpolation. The difference in T_2 computed was 2°F or roughly 0.05% error. Thereafter, the four-point method was used. The absence of any scatter in the points calculated further verifies the accuracy of this method.

Impact Pressures

When a detonation wave collides with a solid wall, the reflected wave must travel back through the burned gases which follow the original detonation wave. This reflection causes another pressure rise behind the

reflected shock wave. Much original work on reflection of detonation waves was done by Morrison[29]. An analysis, similar to the following, was developed by Morrison in unpublished works and was used by Moyle and Churchill[32] in which initial temperature, rather than initial pressure, was varied.

To visualize the flow for the case of a reflected wave, it is easier to consider a moving wave system as opposed to the standing wave representation outlined above. Figure 17 shows the conditions before and after impact of the detonation wave. Primes are attached to all velocities in this analysis to distinguish them from the velocities described by the standing wave reference system.

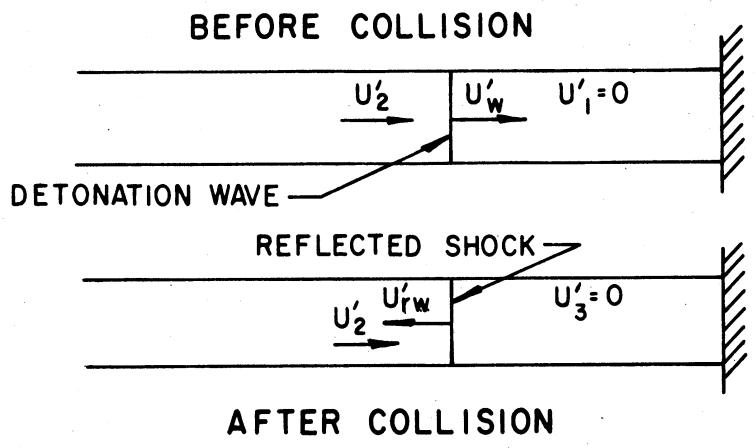

Figure 17. Schematic of Moving Detonation and Reflected Wave Reference System.

If the two reference systems are compared, it is seen that:

$$u'_w = u_1 \tag{48}$$

$$u'_2 - u'_w = u_2 = a_2 \tag{49}$$

$$u'_1 = 0 \tag{50}$$

The momentum equation for the moving reflected wave is:

$$P_3 - P_2 = \rho_2 (u'_{rw} - u'_2)(u'_3 - u'_2) \tag{51}$$

where $\rho_2(u'_{rw} - u'_2)$ is the mass intercepted by the wave and $(u'_3 - u'_2)$ is the velocity change across the wave. When the conditions $u'_3 = 0$ and $\rho_2 = \frac{\gamma_2 P_2}{a_2^2}$ are introduced, equation (51) becomes:

$$\frac{P_3}{P_2} = 1 + \gamma_2 \left(\frac{u'_{rw} - u'_2}{a_2} \right) \left(- \frac{u'_2}{a_2} \right) \tag{52}$$

The quantity $\frac{u'_{rw} - u'_2}{a_2}$ is defined as M'_{rw} and $\frac{u'_2}{a_2}$ is M'_2. Equation (52) becomes:

$$\frac{P_3}{P_2} = 1 - \gamma_2 M'_{rw} M'_2 \tag{53}$$

The pressure ratio across any shock wave is:

$$\frac{P_{upstream}}{P_{downstream}} = \frac{2\gamma M^2}{\gamma+1} - \frac{\gamma-1}{\gamma+1} \tag{54}$$

where M is the Mach number of the wave relative to the gas which the wave is entering. For this case, equation (54) may be written:

$$\frac{P_3}{P_2} = \frac{2\,\gamma_2 M'_{rw}}{\gamma_2 + 1} - \frac{\gamma_2 - 1}{\gamma_2 + 1} \tag{55}$$

Equations (53) and (55) were solved simultaneously for $\frac{P_3}{P_2}$ with the following result:

$$\frac{P_3}{P_2} = \frac{\gamma_2(\gamma_2+1)M_2'^2}{4} + 1 + \sqrt{\left[\frac{\gamma_2(\gamma_2+1)M_2'^2}{4}\right]^2 + (\gamma_2 M_2')^2} \tag{56}$$

where:

$$M_2' = \frac{u_2'}{a_2} = \frac{a_2-u_1}{a_2} = 1 - \frac{u_1}{a_2} \tag{57}$$

$$a_2 = \sqrt{\frac{\gamma_2 RT_2}{m_2}} \tag{58}$$

IV. THE EFFECT OF ERRORS IN PRESSURE SENSITIVE PHYSICAL PROPERTIES ON DETONATION WAVE VELOCITIES

Data is available for the specific heats[18], enthalpies[18], and equilibrium constants[17 from 14] of the six components in the product gas as a function of temperature at low pressure. However, no data were located giving the effect of pressure on these properties or on the compressibility factor and fugacity coefficients at the highest pressure for which computations were made (2000 atm). High pressure data which were available did not go to a high enough temperature. Generalized charts using reduced temperatures and pressures did not in general go high enough. Therefore, all computations were made using idealized values for specific heat and enthalpy (temperature dependent only), fugacity equilibrium constants (temperature dependent only), i.e., fugacity coefficients of unity, and compressibility factors of unity.

In order to determine what errors would be introduced into the computed detonation velocities by using idealized properties in the calculations, it was necessary to find total differentials of many variables in several successive equations, until the error in u_1 resulting from an error in each property was found. This was done for a single computed point: the stoichiometric mixture at 2000 atmospheres final pressure. The development of the general error equations is given in Appendix D. The results for the above mentioned point are presented here in Table II.

TABLE II

THE EFFECT OF PROPERTY ERRORS ON DETONATION VELOCITY

N, Property in Error	$\frac{\Delta u_1/u_1}{\Delta N/N}$	Assumed Max. $\Delta N/N$	$\Delta u_1/u_1$ From Assumed Errors
z_1	0.00917	+ 0.05	+ 0.0005
z_2	0	- 0.10	0
$(H^\circ_{T_1} - H^\circ_0)_{H_2}$	- 0.0698	- 0.01	+ 0.0007
$(H^\circ_{T_1} - H^\circ_0)_{O_2}$	- 0.0355	+ 0.10	- 0.004
$(H^\circ_{T_2} - H^\circ_0)_{H_2}$	0.204	- 0.05	- 0.010
$(H^\circ_{T_2} - H^\circ_0)_{O_2}$	0.0555	- 0.05	- 0.003
$(H^\circ_{T_2} - H_0)_{H_2O}$	1.411	- 0.01	- 0.014
$(H^\circ_{T_2} - H_0)_H$	0.0322	- 0.05	- 0.002
$(H^\circ_{T_2} - H^\circ_0)_O$	0.0177	- 0.05	- 0.0009
$(H^\circ_{T_2} - H^\circ_0)_{OH}$	0.199	- 0.05	- 0.010
$C_{P\ H_2}$	- 0.00436	- 0.05	+ 0.0002
$C_{P\ O_2}$	- 0.00115	- 0.05	+ 0.00006
$C_{P\ H_2O}$	- 0.0301	- 0.05	+ 0.002
$C_{P\ H}$	- 0.000594	- 0.05	+ 0.00003
$C_{P\ O}$	- 0.000333	- 0.05	+ 0.00002
$C_{P\ OH}$	- 0.00412	- 0.05	+ 0.0002
ν_{H_2}	- 0.177	- 0.15	+ 0.027
ν_{O_2}	- 0.0357	- 0.17	+ 0.006
ν_{H_2O}	0.324	- 0.15	- 0.049
ν_H	- 0.0962	- 0.15	+ 0.014
ν_O	- 0.0537	- 0.15	+ 0.008
ν_{OH}	- 0.199	- 0.15	+ 0.030

TABLE II CONT'D

All positive errors	+ 0.089
All negative errors	- 0.093
All errors	- 0.004

In order to determine qualitatively the approximate fractional errors in u_1 resulting from errors in the properties, it was necessary to make some guesses concerning the probable property errors due to the high pressure. These guesses are mainly based upon generalized charts[16,33,34]. z_1 was approximated as a mole average of the compressibility factors of H_2 and O_2 under the initial conditions. Under final conditions, the compressibility factor of H_2 is beyond the range of available reduced charts. The critical properties of H, O, and OH are not known. Therefore, it was assumed that the average compressibility factor of the burned mixture, z_2, would at most be that of O_2 or H_2O, both of which are roughly 1.1 under final conditions. Since the deviation from ideality of the other four components is probably less than that of H_2O and O_2, a maximum error of -10% was assumed to have been made using $z_2 = 1$. Most of the other errors were approximated in this manner. In cases where the desired information fell beyond the range of the charts, the values were estimated by visual extrapolation. Fractional property errors for H, O, and OH, whose critical properties are not known, were assumed as limiting values to be equal to the equivalent values for the other components. These property errors shown in the third column of Table II, when multiplied by the appropriate factor in the second column, yield estimated values for the fractional error in u_1, shown in the fourth column. It is seen that errors in some

properties cause an appreciable error in u_1. The total negative error and the total positive error are very nearly equal in magnitude and thus, if idealized properties are used throughout, there is a natural cancellation of errors such that the net error is very small.

It is noted in Table II that, based on the approximate analysis presented, u_1 is insensitive to small errors in z_2. This occurs because the error in u_1 is proportional to the sum of the errors in T_2 and z_2, and the error in T_2 is equal to the negative of the error in z_2, i.e.,

$$\frac{\Delta T_2}{T_2} = -\frac{\Delta z_2}{z_2} \qquad \text{(for no other errors)} \tag{59}$$

$$\frac{\Delta u_1}{u_1} \alpha \left(\frac{\Delta T_2}{T_2} + \frac{\Delta z_2}{z_2}\right) = \left(\frac{-\Delta z_2}{z_2} + \frac{\Delta z_2}{2_2}\right) = 0 \tag{60}$$

This result merely indicates that for small errors in z_2, the error in u_1 will be small. This is not to say that u_1 is independent of z_2, for certainly, if z_2 is in error, then T_2 will be in error, and the values of the equilibrium constants, enthalpies, and specific heats will be in error. This will in turn cause errors in all of the product mole fractions. The results is obviously an error in u_1. For small errors in z_2, however, this is a second order error effect and the equations presented approach complete accuracy as the error in z_2 becomes smaller. The foregoing discussion on second order error effects applies to all of the properties listed in Table II.

This analysis was made for only one point, where the conditions were probably least ideal. It is reasoned that at lower pressures and for product gases containing less water, errors introduced by using

idealized properties would be less. This was done solely to obtain a qualitative picture of the effect of a major source of error in the computations. It must be borne in mind that for other conditions, the positive and negative errors might not cancel each other so conveniently, and the net error could be a few percent in either direction.

The above discussion qualitatively points out that errors introduced by using idealized properties tend to cancel each other, and thus, the expected error in the computed velocity due to uncertainty in properties is small.

V. RESULTS

Experimental Effect of Initial Pressure on Detonation Velocity

All experimetal runs were made at room temperature, the temperature varying between 70°F and 80°F, depending upon the ambient air temperature at the time. Information presented by Moyle and Churhill[31] indicates that this small variation could be tolerated and did not necessitate building a temperature control. Data were taken at initial pressures of 14.4, 25, 50, 100, 500 and 1,000 lb/sq in. abs. Velocities at each of these pressures were measured for mixtures having nominal mole fractions of hydrogen of 0.4, 0.5, 0.6, 0.667, 0.75, and 0.8. Because of the method of charging, it was difficult to obtain mixtures havigg the exact compositions mentioned above. Only after the measurements were made and the mixtures analyzed were the initial compositions known. In general, the actual composutions were slightly different from the nominal values. It was thus impossible to plot directly the effect of initial pressure on detonation velocity at discrete values of initial composition, since the initial compositions varied slightly for different pressures.

One way to obtain this plot would be to plot detonation velocities versus mole fraction hydrogen at the various initial pressures (which were accurately controlable) and then construct a cross plot to obtain the desired curves. However, with such a method, the identity of the individual experimental points is lost on the final u_1 vs P_1 plot whereon the experimental data are compared to theoretical predictions.

Only the single average cross-plotted points are represented on the final curve so that the illustration of the experimental scatter is lost. Also, the shapes and positions of these cross-plotted "experimental" curves are dependent upon the individual who plots the original curves. Such a procedure does not lead to an accurate comparison of experimental and theoretical relationships. Therefore, the following method was employed.

Detonation velocities were plotted versus mole fraction hydrogen at the various initial pressures. The actual experimental points were then corrected for their deviation from the nominal hydrogen fraction by moving the points parallel to the curves drawn through the original points till the nominal hydrogen fraction was reached. This is illustrated graphically in Figure 18 below. The plot upon which this was actually done is shown in Figure 19.

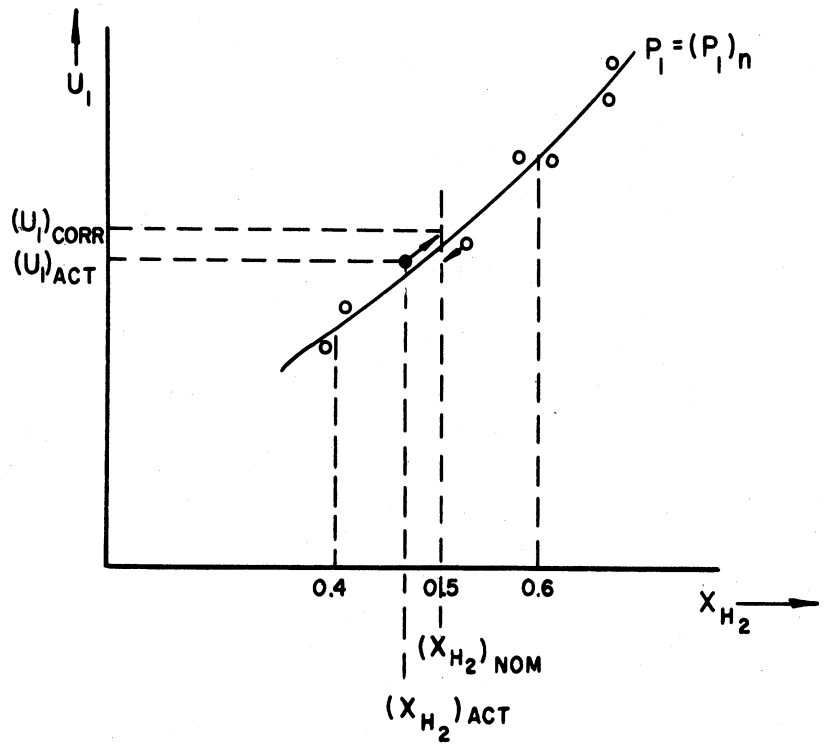

Figure 18. Graphical Illustration of Method of Correcting Points to Nominal Hydrogen Mole Fraction.

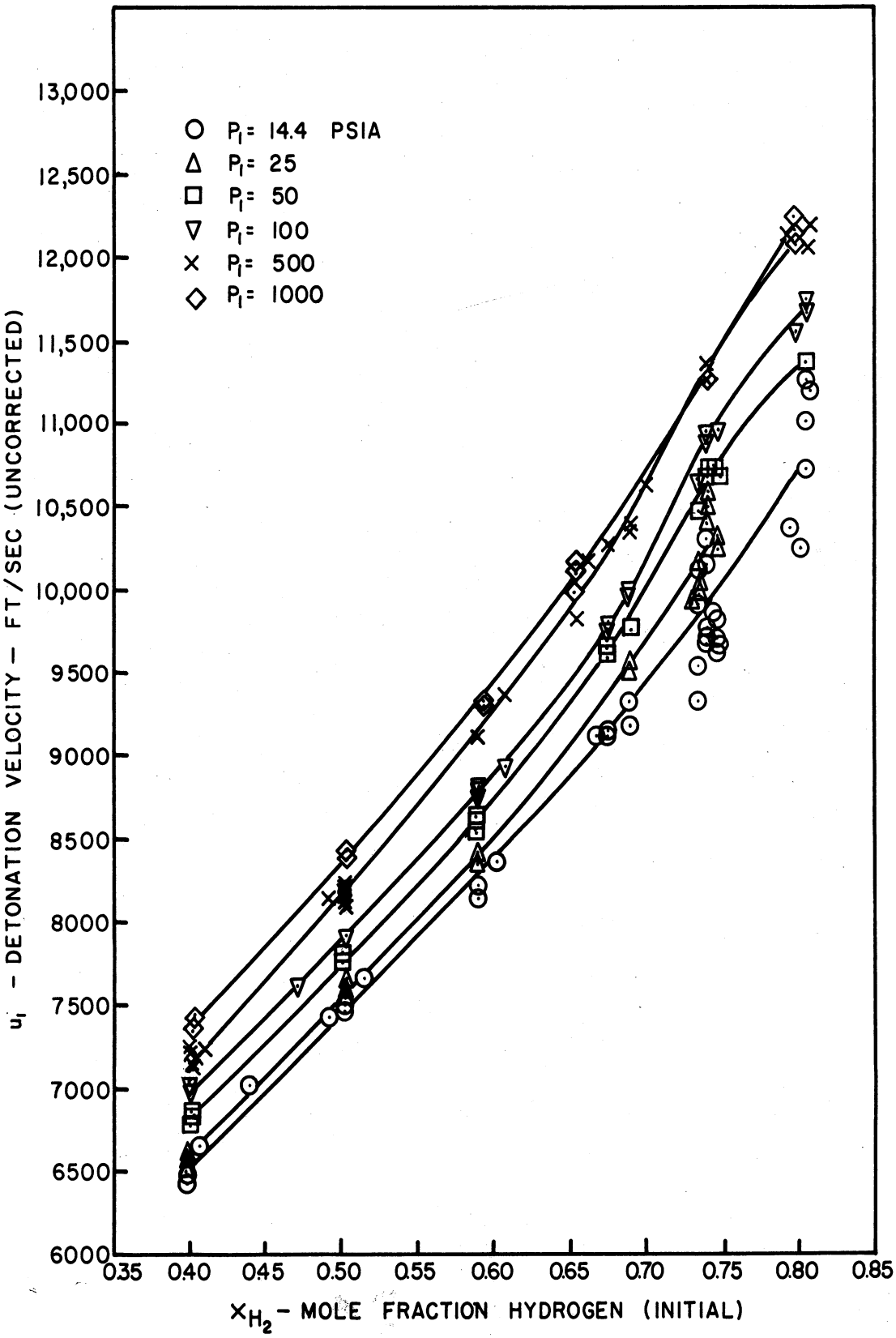

Figure 19. Experimental Effect of Initial Composition on Detonation Velocity at Various Initial Pressures.

Algebraically,

$$s = \frac{u_1 \text{ CORR} - u_1 \text{ ACT}}{x_{H_2 \text{ NOM}} - x_{H_2 \text{ACT}}} \tag{61}$$

or

$$u_{1 \text{ CORR}} = s \left(x_{H_2 \text{ NOM}} - x_{H_2 \text{ ACT}}\right) + u_{1 \text{ ACT}} \tag{62}$$

where s is the slope of the curve at the nominal mole fraction of hydrogen. Then, u_1 could be plotted vs. P_1 at discrete values of x_{H_2}. With this method, the identity of the individual points and the presentation of experimental scatter is preserved, and if $(x_{H_2 \text{ NOM}} - x_{H_2 \text{ ACT}})$ is small and the slope is fairly constant (which it is), the error introduced by moving the points in a straight line to correct them is very small. Also, the slope obtained by various individual plotters is less likely to be in error than the position of the curves, i.e., with this method, the only property of the curve drawn through the experimental points which is used is its slope (whereas with the cross-plot method the absolute position is relied upon to be accurate.).

The theoretical velocities correspond to those which would be measured in an infinite diameter tube. Therefore, in order to compare theoretical and experimental velocities, it is necessary to correct the experimental measurements for tube diameter. This dependence of detonation velocity on tube diameter has previously been obtained. Kistiakowsky and Zinman found that a plot of detonation velocity versus the reciprocal of tube diameter yields a straight line[22]. Thus, the correction for tube wall effects may be made by extrapolating the experimental detonation

velocity vs. reciprocal tube diameter curve to zero reciprocal tube diameter. This was done by Moyle and Churchill[31] for various mixtures of hydrogen and oxygen at one atmosphere using their own data and the data of other investigators. They obtained a relationship equivalent to the following equation from the slopes of these curves (which apparently are independent of mixture composition):

$$(u_1)_\infty = u_1 + \frac{29.7}{\delta} \qquad (63)$$

where u_1 = measured velocity, ft/sec.

$(u_1)_\infty$ = equivalent velocity in an infinite diameter tube, ft/sec.

δ = tube diameter, inches

For a half inch diameter tube, this correction amounts to about 59 ft/sec. In order to make a correction for tube diameter on the data collected in this investigation, it is necessary to assume that the above experimental relationship is independent of pressure as well as composition. This pressure effect in itself would make a good independent research project. A tabulation of actual experimental results along with the corrections mentioned above is given in Table IV in Appendix E.

Theoretical Results

Effect of Initial Pressure on Detonation Velocity

All theoretical points were calculated for an initial temperature of 298.16°K (77°F). This temperature is very nearly the temperature at which the majority of experimental runs were made.

Detonation velocities were predicted for initial mole fractions of hydrogen of 0.4, 0.5, 0.6 0.667, and 0.75; and final pressures of 10,

25, 50, 75, 100, 250, 500, 750, 1000, 1500, and 2000 atmospheres.

Product gas equilibrium compositions for these conditions for product temperatures from 3000 to 5000°K (the output from the IBM-650 digital computer) are given in Table V in Appendix F along with the input conditions. Although this information was obtained as an intermediary in the calculation of detonation velocities, it is general and may be used in any application where the equilibrium compositions of H_2-O_2 mixtures at these conditions is necessary. A sample plot of this data is given in Figure 20. It is seen that at 3000°K, the product (for a stoichiometric mixture) consists mostly of water with very small amounts of the other five components. The concentration of water continuously increases and the concentrations of the other components decrease as the pressure increases. However, at 5000°K, the equilibrium mixture contains much higher concentrations of dissociation products. As the pressure increases, the H and O concentrations decrease, the H_2, O_2, and OH increase to a certain point due to the association of H and O and decrease thereafter due to their association into water. The water concentration continuously increases with pressure. This is the association effect of pressure which is expected to yield an increase in detonation velocity.

As stated in Chapter III, the velocities were predicted for fixed final pressures to avoid an additional successive approximation calculation. These final pressures were selected such that the initial pressures finally resulting from the calculations would bracket the range of experimental data. The predicted detonation velocities are tabulated

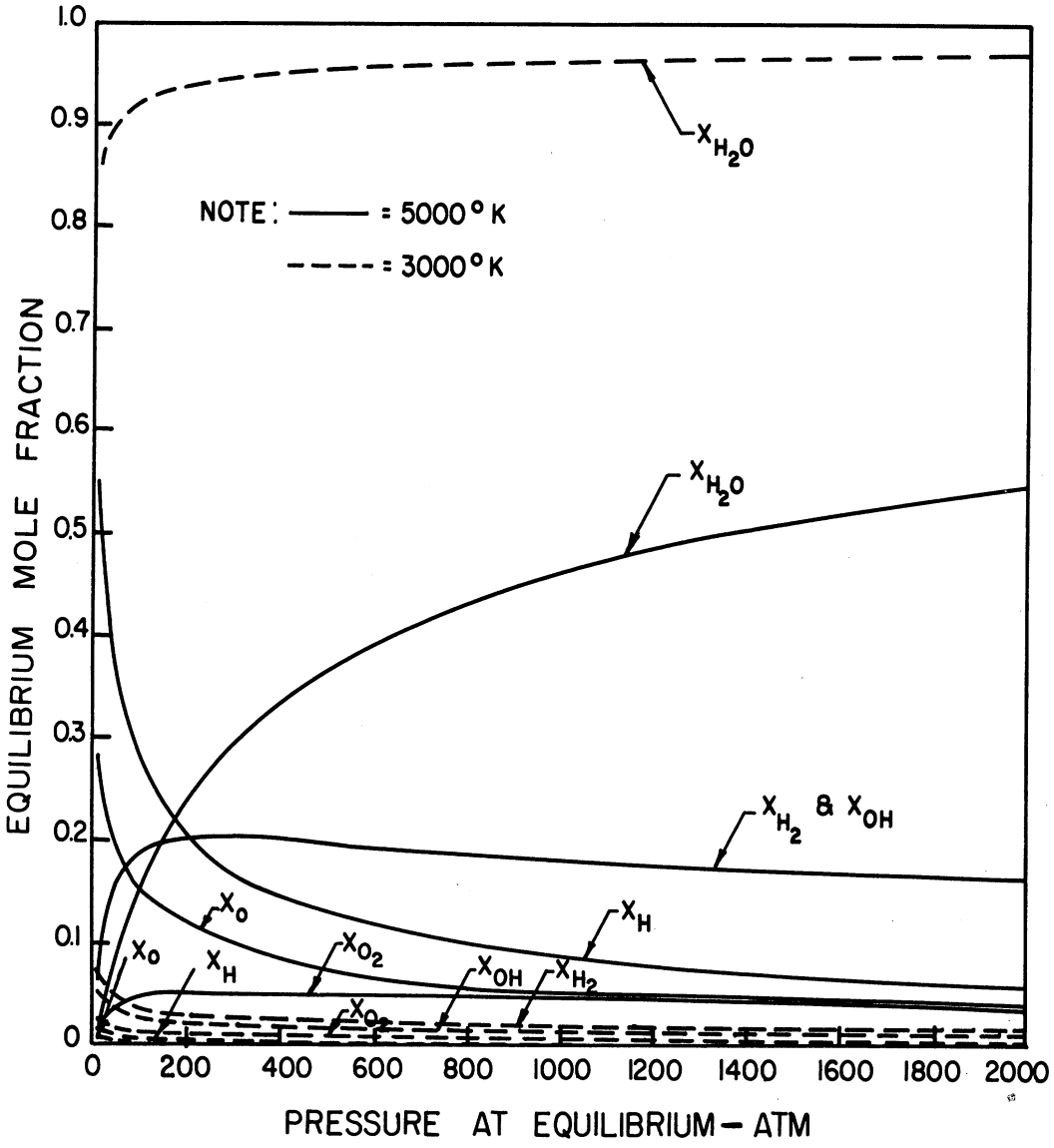

Figure 20. The Effect of Pressure on the Equilibrium Composition of a Stoichiometric Mixture Of Hydrogen and Oxygen at 3000 and 5000°K.

in Table VI in Appendix G.

The experimental and theoretical relationships between detonation velocity and initial pressure at various initial compositions are presented in Figures 21 and 22. Experimental points for 0.75 and 0.8 mole fraction hydrogen at 14.4 and 25 lb/sq in. abs were omitted from the high range curves to avoid the confusion which would result from including these widely scattered points. The scattering of these points is discussed in the next section. The points are included on the low range curves to illustrate their deviation. Experimental points of other investigators are also included on the low range graph. The data of Moyle[30] is not included since data were not taken at the same values of composition as are used in Figure 22. A rough interpolation of his data (up to 2 atm.) seems to indicate fair agreement with data taken in this investigation.

Impact Pressures

Impact pressures were calculated for all of the theoretical points by means of Equation 56. The computed data are given in Table VI in Appendix G and the ratios of impact pressure to initial pressure are plotted in Figure 23 along with ratios of pressure behind the original detonation wave to initial pressure. It should be borne in mind that at the highest initial pressures, it was shown that the calculated velocities were a few percent below the experimental velocities. Therefore, actual impact pressures can be expected to be somewhat higher than those predicted using the calculated velocities. Experimental velocities were not used because of a lack of knowledge of the actual values of γ_2, m_2, and T_2.

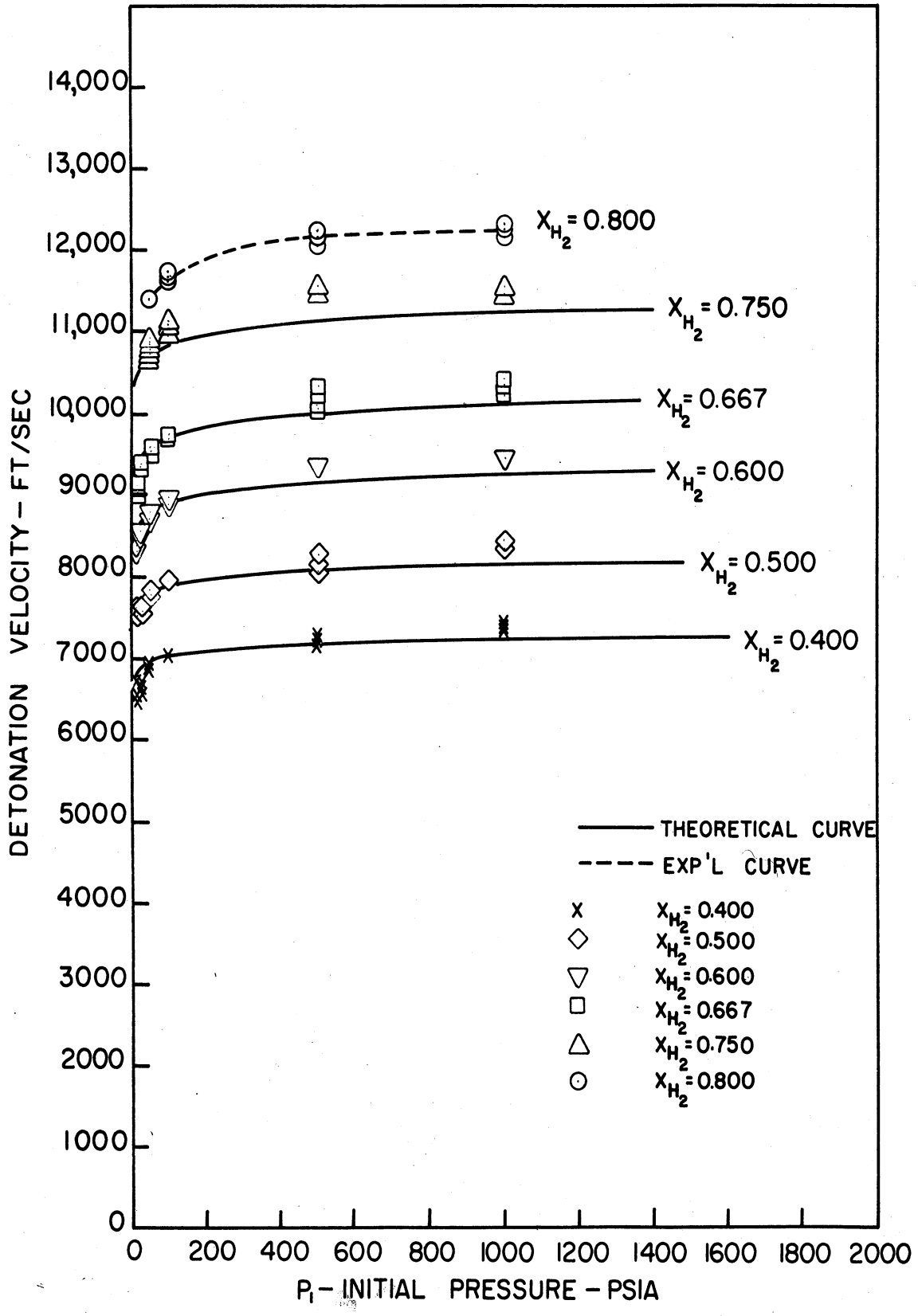

Figure 21. Comparison Between Theoretical and Corrected Experimental Effects of Initial Pressure On Detonation Velocity -- High Range

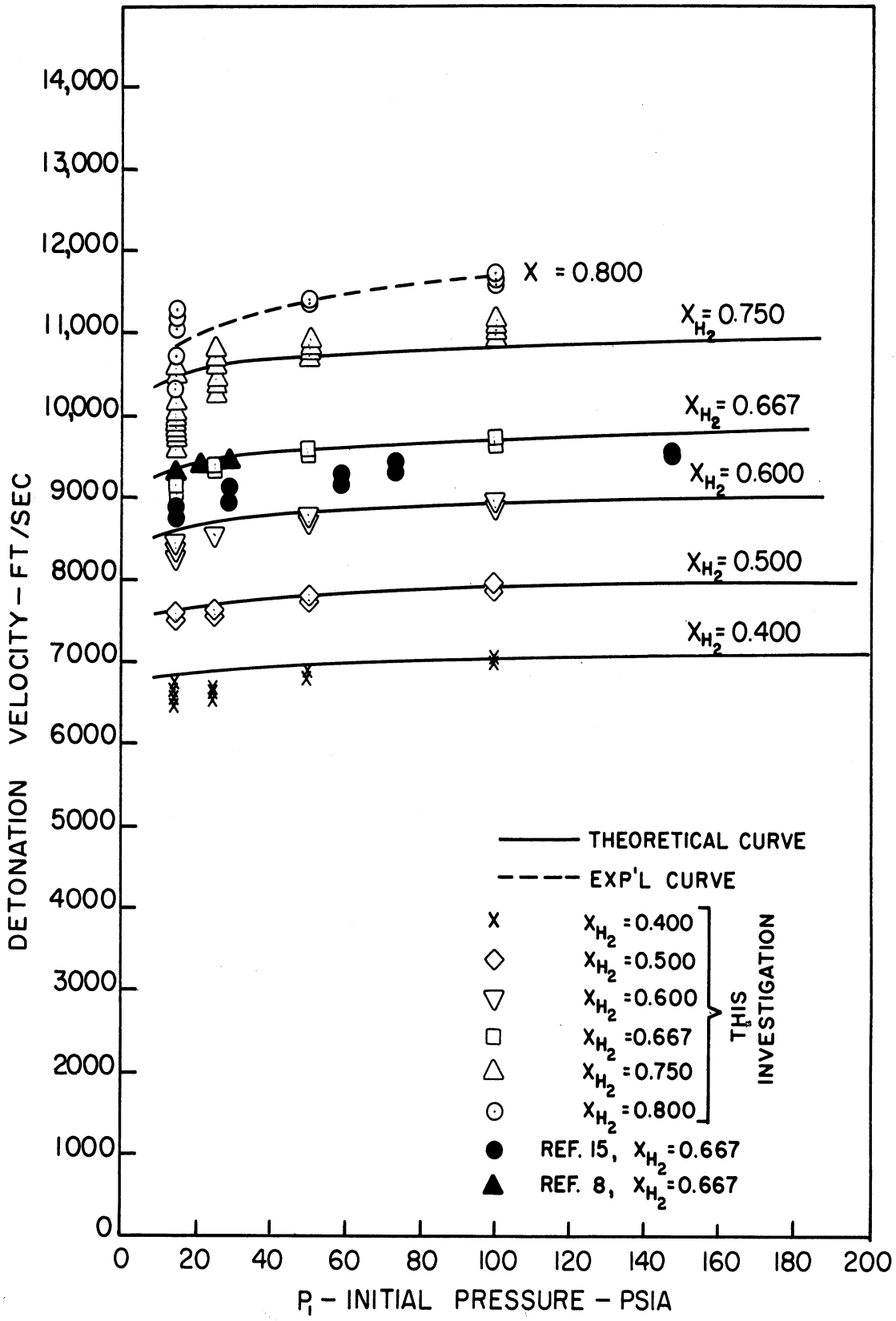

Figure 22. Comparison Between Theoretical and Corrected Experimental Effects of Initial Pressure On Detonation Velocity -- Low Range.

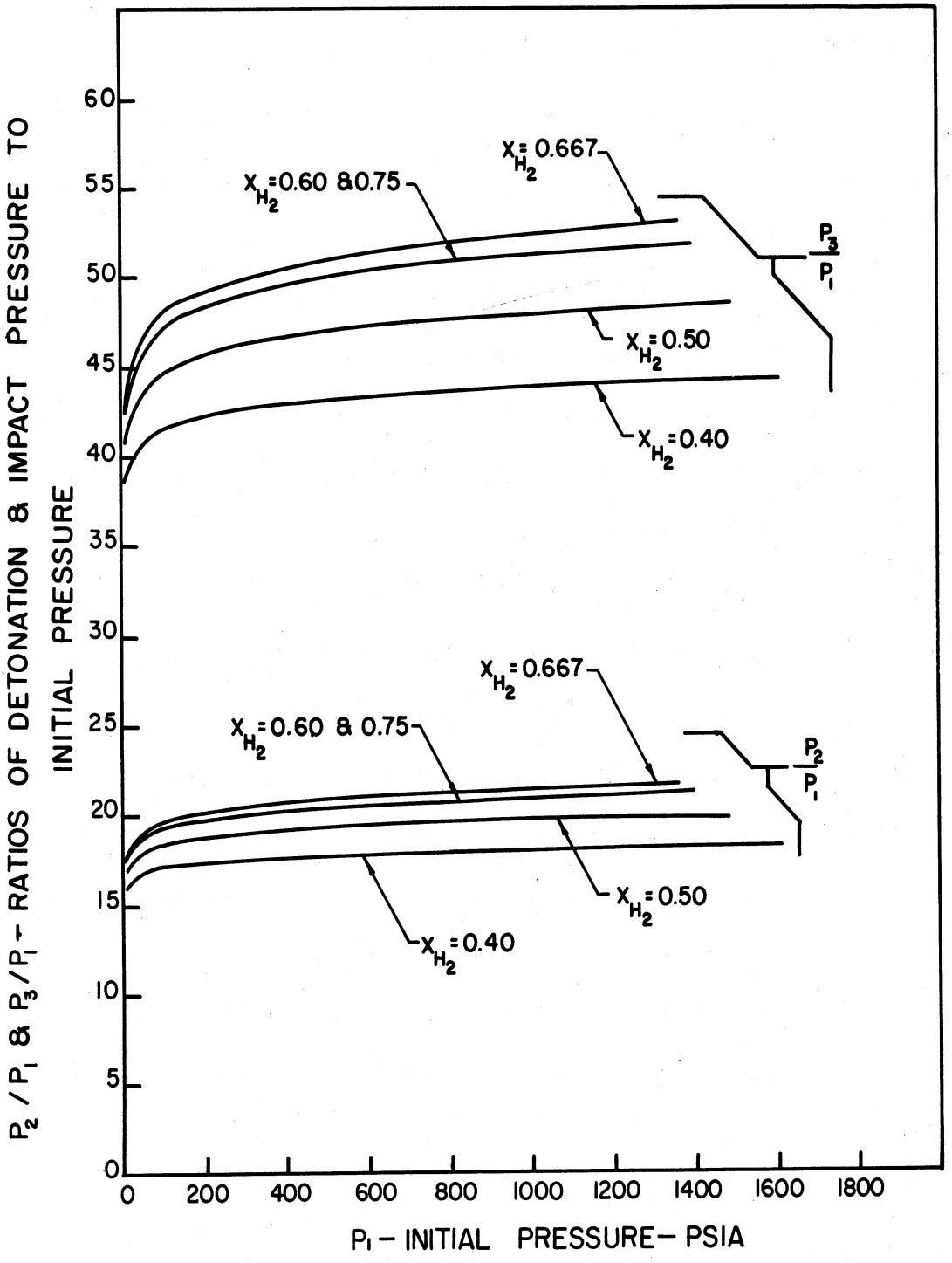

Figure 23. Theoretical Ratios of Detonation and Impact Pressures to Initial Pressure as a Function of Initial Pressure.

Accidental Explosion

It was originally intended to reach initial pressures as high as 10,000 lb/sq in. abs, the hydraulic pump rating. Since there was only a small percentage increase in detonation velocity when the initial pressure was raised from 500 to 1000 lb/sq in. abs, it was planned that data would next be taken at an initial pressure of 4000 lb/sq in. abs, and then at 10,000 lb/sq in. abs. A mixture of 0.8 mole fraction H_2, 0.2 mole fraction O_2 was charged into the pressure tube at 800 lb/sq in. abs. The hydraulic fluid was then pumped into the bottom of the pressure tube with an ultimate goal of 4000 lb/sq in. abs. At 3500 lb/sq in. abs the mixture spontaneously detonated.

The cause of this ignition can only be speculated upon. No valves were being opened or closed during the pressurizing operation, so shock waves at the valve seats are eliminated as a possible cause. The writer can postulate only two possible causes. One possibility is that the mixture was so unstable at this pressure that slight fluctuations in the hydraulic fluid due to pump piston movement created waves strong enough to detonate the mixture. Another possibility is that under the conditions at which the explosion took place, the gas acted as a pyrogallic mixture, i.e., it reacted spontaneously without outside ignition.

Since there was no time for the safety diaphragm on the pressurizing tube to release the pressure created by the detonation, the explosion burst and shattered the pressurizing tube and destroyed all valves, gages, and lines (Figures 24 and 25). It is estimated that

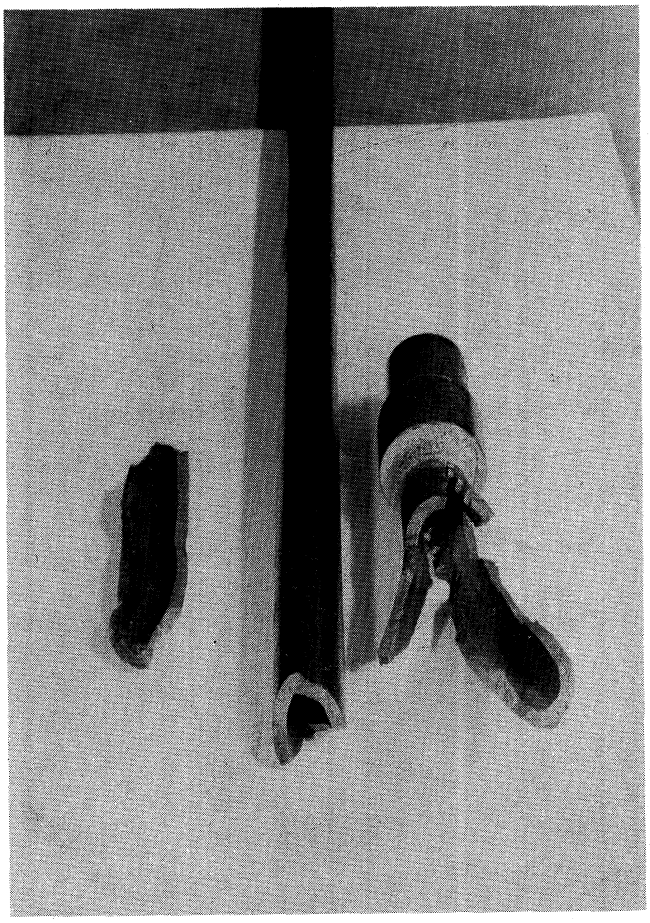

Figure 24. Photograph of Pressurizing Tube After Accidental Explosion.

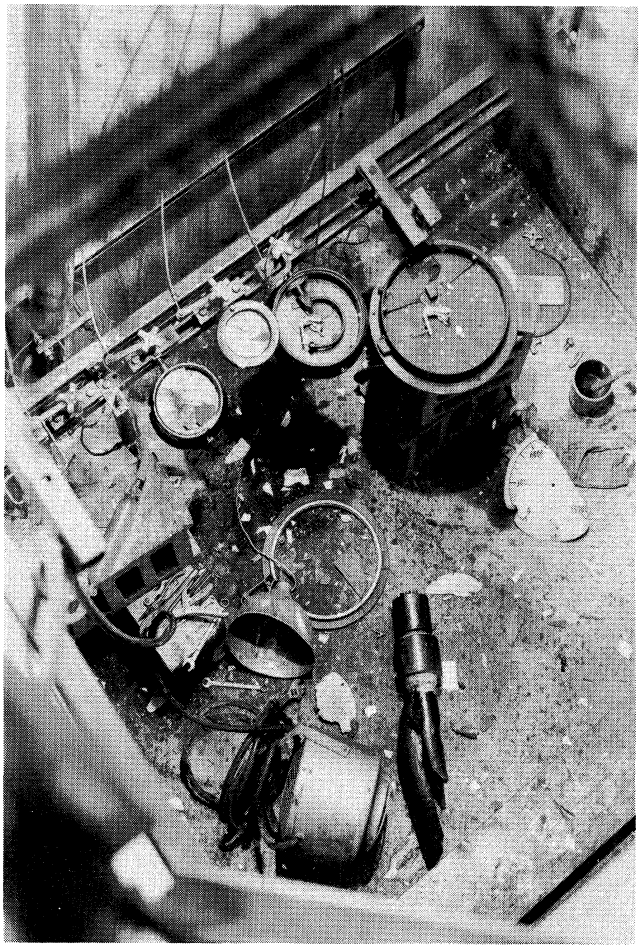

Figure 25. Photograph of Test Pit and Equipment After Accidental Explosion.

the pressure after detonation was at least 70,000 lb/sq in.abs, and none of the equipment auxiliary to the detonation tube itself was designed to hold this pressure. Ordinarily, the detonation tube would have been closed off from the rest of the system and nothing else would have been exposed to detonation pressure. As it happened, the detonation tube was the only piece of equipment not damaged even though it too was exposed to the detonation pressure. Appreciable damage to the test cell occurred: 4 inch thick block facing on the exterior of two walls was detached from the walls, one edge of the roof was pushed up, the door jamb was pushed out of the wall, and the doorknob pulled from the door. However, there were no personal injuries because of precautions taken in building the system, as described in the section on equipment.

Subsequent to the completion of the experimental work, interesting new articles were published concerning the strength of cylindrical vessels under high pressure[13,28] and on the effect of detonations on piping and vessels[35].

VI. DISCUSSION

An inspection of the plot of the original data (Figure 19) and the corrected data (Figures 21 and 22) shows that the experimental scatter is at most 3% and in most cases less than 2% except for the cases of hydrogen rich mixtures at low pressure. No experimental consistency was obtainable with the system used in this investigation for 0.75 and 0.8 mole fraction hydrogen at 14.4 and 25 lb/sq in, abs initial pressure. The data for these conditions scatter widely. One possible explanation is that for the richest mixtures, stable detonation did not consistently develop in the allotted distance between the ignitor wire and the first probe (58 in.). (See Chapter II - Section "Velocity Measuring Equipment" and Table I.) Thus when it did not develop, the measured velocities were much lower than predicted, and individual points differed among themselves depending upon how nearly the wave approached being a stable detonation wave as it passed between the ionization probes. As the initial pressure was increased beyond 50 lb/sq in. abs, the initiation distance apparently decreased enough to allow stable detonation to be achieved before the first probe was reached. Beyond this pressure, reproducibility of data was satisfactory even for the richest mixtures.

The comparison between predicted and corrected experimental detonation velocities is seen in Figures 21 and 22. At low pressures, experimental velocities lie slightly below the predicted curves. These deviations are likely due to imperfections in the model upon which the calculations were based. This model assumes a relative velocity between the wave and the burned gases equal to the speed of sound in the burned gases, and chemical and thermal equilibrium behind the wave. The absence

of equilibrium behind the wave, besides causing an error in the burned gas compositions used, could affect the computations as follows: In developing the theoretical equations, difference equations were written for the mass, momentum, and energy balances. These equations are actually the results of integrating the mass, momentum, and energy one-dimensional differential equations between state 1 and state 2. However, these differential equations also contain terms involving the second derivative with respect to longitudinal position of concentration (corresponding to diffusion in the mass balance), the second derivative of velocity (corresponding to viscosity in the momentum balance), and the second derivative of the temperature (corresponding to thermal conductivity in the energy balance). Integration of these terms results in the presence of first derivatives with respect to longitudinal position of concentration, velocity, and temperature in the difference equations. If the derivatives of each quantity are equal in states 1 and 2 (or specifically, if they are zero in both states) then their net effect is zero. Certainly, there are no concentration, velocity, or temperature gradients in state 1 in front of the wave. If chemical and thermal equilibrium exist at state 2 behind the wave, the gradients are zero there and these terms may be dropped from the equations. However, in the absence of chemical and thermal equilibrium behind the wave there will be a temperature gradient with longitudinal position which will affect the energy balance, and a composition gradient which will affect the mass balance. Each of these effects will induce a velocity gradient which will affect the momentum balance. The inclusion of these terms renders the conservation equations unsolvable in closed form. Thus the assumption of chemical and thermal equilibrium behind the wave is made. As seen from

the results at low pressure, this is not too bad an assumption, although the slight discrepency between experiment and theory might be explained on this basis. The theory also requires that the Chapman-Jouguet plane exist at the point where it is assumed that equilibrium exists. If the Chapman-Jouguet plane does not exist, or if it exists at some other position, this is another possible source of error in the computations. It is assumed that momentum and energy losses to the wall were taken into account by extrapolating the experimental velocities to infinite tube diameter.

At higher pressures, it is noted that the experimental points rise above the theoretical curves. At 1000 lb/sq in. abs, the averages of the various groups of experimental points are 2 - 3% above the predicted curves. These deviations are probably due principally to the use of idealized properties for the theoretical computations. Even though the "error analysis" predicted a much smaller error in detonation velocity, this prediction was based upon very roughly estimated values for the probable property errors. For example, if $\frac{\Delta\nu_{H_2}}{\nu_{H_2}}$ and $\frac{\Delta\nu_{OH}}{\nu_{OH}}$ had been assumed to be -10% instead of -15% (see Table II), the net error in the theoretical detonation velocity would have been -2.3% instead of -0.4%. This increase in velocity error resulting from a decrease in property error occurs because a negative error in these quantities (as well as many others) causes a positive error in velocity. Therefore, when the absolute values of these errors are decreased, the positive component of the net velocity error is decreased, causing a "more negative" net velocity error. Table II shows that u_1 is most sensitive to errors in the enthalpies and fugacity coefficients, and that small errors in the specific heats and compressi-

bility factors have a negligible effect on u_1. The remarks concerning imperfections in the theoretical model also apply to the high pressure conditions, although the effect is probably masked due to the greater effect of non-ideality in the product gases. Furthermore, equilibrium is probably more closely approached at the high pressure because of the shorter mean free path for chemically productive collisions.

VII. CONCLUSIONS

This investigation indicates that the velocities computed from the highly idealized hydrodynamic theory of detonation are in reasonable agreement with experimental detonation velocities throughout an extensive pressure range, 14.4 to 1000 lb/sq in. abs, for hydrogen-oxygen mixtures containing hydrogen mole fractions from 0.4 to 0.8.

At the lower pressures, the disagreement between experimental and predicted detonation velocities is small and might be explained as the result of imperfections in the idealized theoretical model.

Inconsistencies observed in the experimental data at the lowest pressures and richest mixtures were probably due to a peculiarity of the experimental system (insufficient wave development distance) and should not be interpreted as a contradiction of the theory.

At the higher pressures, disagreement is small and can be rationalized in terms of the idealized properties necessarily used in the computations. It is fortuitous that the effects of using idealized properties tend to cancel, leaving a small net error in the predicted velocity in the illustrative calculations for a stoichiometric mixture at 1362 lb/sq in. abs initial pressure. If high pressure values for the properties had been available for use in the computation, a closer agreement between predicted and experimental velocities might have been obtained at the higher pressures. Without these values, discrepancies can only be shown to be reasonable and not necessarily due to defects in the theory.

The detonation velocities are shown to increase at a decreasing rate as the initial pressure increases. The maximum possible theoretical velocity would be attained when there was no dissociation of the product

gases. Under these conditions, no chemical energy is spent in dissociating the products. It is apparent that this state of the product gases would occur if the pressure were infinite, since an increase in pressure causes a decrease in the amount of dissociation. Therefore, a velocity asymptote could be expected on the predicted curves, which the velocity would approach as the pressure increased without bound. This appears to be the case for the predicted curves, based on ideal properties of the product gases.

The experimental curves, need not necessarily behave in the manner outlined above for the predicted curves. As the pressure increases indefinitely the product gases deviate more and more from ideality. At the highest initial pressure for which experimental data were obtained (1000 lb/sq in. abs), velocities in the rich mixtures seem to be approaching some sort of asymptote. However, velocities in the lean mixtures steadily increase as the initial pressure increases. Experimental detonation velocities might increase indefinitely with pressure, or they might even reach a maximum and decrease thereafter, at some point beyond 1000 lb/sq in. abs, depending upon the influence of pressure on the physical properties. The behavior of these curves beyond the experimental range cannot be predicted without an accurate knowledge of the values of the physical properties under actual conditions.

Table III indicates the percentage increase in experimental detonation velocity due to increasing initial pressure from 14.4 to 1000 lb/sq in. abs.

TABLE III

EXPERIMENTAL PERCENT INCREASE IN DETONATION VELOCITY FOR INCREASE IN INITIAL PRESSURE FROM 14.4 PSIA to 1000 PSIA

Mole Fraction Hydrogen	Percent Increase in Detonation Velocity
0.40	12.5
0.50	11.4
0.60	12.8
0.6667	13.5
0.75	15.6
0.80	13.1

An important consideration for design purposes is the pressure realized when a detonation occurs. The ratio of the pressure behind the detonation wave to the initial pressure increases only slightly with increased initial pressure and is highest for the stoichiometric mixture, ranging from 17.7 at P_1=8.29 lb/sq in. abs to 21.6 at P_1=1362 lb/sq in. abs. The ratio of impact pressure (pressure behind the reflected wave) to detonation pressure is fairly independent of initial pressure and composition (slightly under 2.5). Thus, if a detonation occurred in a vessel containing a detonatable mixture of hydrogen and oxygen, the wave could produce, on impact with the vessel walls, a pressure greater than 53 times the initial pressure for initial pressures greater than 1362 lb/sq in. abs. This should be taken into consideration in the design of the vessel.

APPENDIX A

DEVELOPMENT OF THE HYDRODYNAMIC EQUATIONS

APPENDIX A

DEVELOPMENT OF THE HYDRODYNAMIC EQUATIONS

Conservation and state equations may be written between states 1 and 2 as follows (See Figure 13 in text):

$$\rho_1 u_1 = \rho_2 u_2 \tag{A-1}$$

$$P_1 + \rho_1 u_1^2 = P_2 + \rho_2 u_2^2 \tag{A-2}$$

$$h_1 + \frac{u_1^2}{2} = h_2 + \frac{u_2^2}{2} \tag{A-3}$$

$$\rho = Pm/zRT \tag{A-4}$$

Eliminating ρ from (A-1) and (A-2) by means of (A-4):

$$\frac{P_1 m_1}{z_1 R T_1} u_1 = \frac{P_2 m_2}{z_2 R T_2} u_2 \tag{A-5}$$

and

$$P_1 + \frac{P_1 m_1}{z_1 R T_1} u_1^2 = P_2 + \frac{P_2 m_2}{z_2 R T_2} u_2^2 \tag{A-6}$$

From (A-5)

$$\frac{P_1}{P_2} = \frac{\dfrac{m_2 u_2}{z_2 T_2}}{\dfrac{m_1 u_1}{z_1 T_1}} \tag{A-7}$$

From (A-6)

$$\frac{P_1}{P_2} = \frac{1 + \dfrac{m_2 u_2^2}{z_2 R T_2}}{1 + \dfrac{m_1 u_1^2}{z_1 R T_1}} \tag{A-8}$$

Eliminating P_1/P_2 between (A-7) and (A-8) and rearranging:

$$\frac{z_1RT_1 + m_1u_1^2}{m_1u_1} = \frac{z_2RT_2 + m_2u_2^2}{m_2u_2} \qquad \text{(A-9)}$$

Squaring (A-9) and rearranging:

$$m_1^2u_1^4 + \left[2z_1RT_1m_1 - \left(\frac{m_1(z_2RT_2 + m_2u_2^2)}{m_2u_2} \right)^2 \right] u_1^2 + z_1^2R^2T_1^2 = 0 \qquad \text{(A-10)}$$

Solving (A-10) for u_1^2

$$u_1^2 = \frac{-\left[2z_1RT_1m_1 - \left(\frac{m_1^2(z_2RT_2 + m_2u_2^2)^2}{m_2^2u_2^2} \right) \right] \pm \sqrt{\left[2z_1RT_1m_1 - \left(\frac{m_1^2(z_2RT_2 + m_2u_2^2)^2}{m_2^2u_2^2} \right) \right]^2 - 4m_1^2z_1^2R^2T_1^2}}{2m_1^2} \qquad \text{(A-11)}$$

$$\text{(A-11)}$$

Substituting (A-11) into (A-3) and letting $u_2=a_2$ according to the Chapman-Jouguet requirement:

$$h_2=h_1 - \frac{a_2^2}{2} - \frac{\left[2z_1RT_1m_1 - \left(\frac{m_1^2(z_2RT_2 + m_2a_2^2)^2}{m_2^2a_2^2} \right) \right] \pm \sqrt{\left[2z_1RT_1m_1 - \left(\frac{m_1^2(z_2RT_2 + m_2a_2^2)^2}{m_2^2a_2^2} \right) \right]^2 - 4z_1^2R^2T_1^2m_1^2}}{4m_1^2} \qquad \text{(A-12)}$$

This equation could be simplified to a great extent if $4z_1^2R^2T_1^2m_1^2$ were very small compared with $\left[2z_1RT_1m_1 - \frac{m_1^2(z_2RT_2 + m_2a_2^2)^2}{m_2^2a_2^2}\right]^2$. An order of magnitude analysis will be made to show that this is true.

Let

$$A = 2z_1RT_1m_1$$

$$B = \frac{m_1^2(z_2RT_2 + m_2a_2^2)^2}{m_2^2a_2^2}$$

$$C = 4z_1^2R^2T_1^2m_1^2$$

The following assumptions will be made regarding the orders of magnitude of the various quantities. These assumptions are aimed at letting C approach $(A-B)^2$ as close as it probably will.

$$z_1 = \mathcal{O}(1)$$

$$R = 1544 \ \frac{\text{ft lb}}{\text{lb mol}^\circ\text{R}}$$

$$T_1 = 520^\circ\text{R}$$

$$m_1 = \mathcal{O}(10 \ \frac{\text{lb}}{\text{lb mol}})$$

$$z_2 = \mathcal{O}(1)$$

$$m_2 = \mathcal{O}(10 \ \frac{\text{lb}}{\text{lb mol}})$$

$$\gamma_2 = \mathcal{O}(1.2)$$

$$T_2 = \mathcal{O}(5400^\circ\text{R})$$

$$a_2^2 = \frac{\gamma_2RT_2}{m_2}$$

$$A = \mathcal{O}(2 \times 1 \times 1544 \times 520 \times 10) = \mathcal{O}(16 \times 10^6 \frac{\text{ft lb}^2}{(\text{lb mol})^2})$$

$$C = A^2 = \mathcal{O}(256 \times 10^{12} \frac{\text{ft}^2 \text{ lb}^4}{(\text{lb mol})^4})$$

$$B = \frac{m_1^2(z_2RT_2 + \gamma_2RT_2)^2}{\gamma_2RT_2m_2} \approx \frac{m_1^2RT_2(z_2 + \gamma_2)^2}{\gamma_2m_2}$$

$$= \mathcal{O}(\frac{10^2 \times 1544 \times 5400 \times 2.2^2}{1.2 \times 10}) = \mathcal{O}(336 \times 10^6 \frac{\text{ft lb}^2}{(\text{lb mol})^2}$$

$$(A-B)^2 = \mathcal{O}(16 \times 10^6 - 336 \times 10^6)^2 = \mathcal{O}(-3.2 \times 10^8)^2$$

$$= \mathcal{O}(10^{17} \frac{\text{ft}^2 \text{ lb}^4}{(\text{lb mol})^4})$$

The above analysis shows that C is roughly 0.0026 as large as $(A-B)^2$ in the worst case. It was felt that the simplification in Equation (A-12) resulting from neglecting C was more valuable than the small bit of accuracy afforded by including C. Therefore, C was neglected. Equation (A-12) then becomes:

$$h_2 = h_1 - \frac{a_2^2}{2} - 2\left[\frac{2z_1RT_1m_1 - \frac{m_1^2(z_2RT_2 + m_2a_2^2)^2}{m_2^2a_2^2}}{4m_1^2}\right]$$

$$= h_1 - \frac{a_2^2}{2} + \frac{(z_2RT_2 + m_2a_2^2)^2}{2m_2^2a_2^2} - \frac{z_1RT_1}{m_1} \qquad \text{(A-13)}$$

For an ideal gas, $a_2^2 = \frac{\gamma_2RT_2}{m_2}$, which may be derived from the basic relationship $a^2 = dP/d\rho$. The inclusion of a real gas correction rigidly applied throughout the development of the former relationship unnecessarily complicates the final equations. Therefore, a correction is applied only in the equation of state used in arriving at the relation-

ship between a_2 and T_2, i.e., Equation (A-4) is used as the equation of state. The relationship is then:

$$a_2^2 = \frac{\gamma_2 z_2 R T_2}{m_2} \tag{A-14}$$

Substituting (A-14) into (A-13) and rearranging:

$$h_2 - h_1 = R\left[\frac{(1 + 2\gamma_2)}{2\gamma_2}\ \frac{z_2 T_2}{m_2} - \frac{z_1 T_1}{m_1}\right] \tag{A-15}$$

from which

$$T_2 = \left(\frac{\Delta h}{R} + \frac{z_1 T_1}{m_1}\right) \frac{2 m_2 \gamma_2}{(1 + 2\gamma_2) z_2} \tag{A-16}$$

From (A-3)

$$u_1 = \sqrt{2(h_2 - h_1) + \frac{z_2 \gamma_2 R T_2}{m_2}} \tag{A-17}$$

and substituting (A-15) into (A-17) yields:

$$u_1 = \sqrt{2R\left[\frac{z_2 T_2 (1 + \gamma_2)^2}{2 m_2 \gamma_2} - \frac{z_1 T_1}{m_1}\right]} \tag{A-18}$$

Combining (A-8) and (A-18)

$$\frac{P_2}{P_1} = \frac{\dfrac{2}{\left(\dfrac{z_1 T_1}{m_1}\right)}\left[\dfrac{z_2 T_2 (1 + \gamma_2)^2}{2 m_2 \gamma_2}\right] - 1}{1 + \gamma_2} \tag{A-19}$$

Equations (A-16), (A-18), (A-19) were used in the computations.

APPENDIX B

DEVELOPMENT OF THE CHEMICAL EQUILIBRIUM EQUATIONS

APPENDIX B

DEVELOPMENT OF THE CHEMICAL EQUILIBRIUM EQUATIONS

As described in the text, the basic equations are:

$$K_{P1} = \left(\frac{x_{H_2} \, x_{O_2}^{1/2}}{x_{H_2O}} \right)_2 P_2^{1/2} \tag{B-1}$$

$$K_{P2} = \left(\frac{x_{H_2}^{1/2} \, x_{OH}}{x_{H_2O}} \right)_2 P_2^{1/2} \tag{B-2}$$

$$K_{P3} = \left(\frac{x_H}{x_{H_2}^{1/2}} \right)_2 P_2^{1/2} \tag{B-3}$$

$$K_{P4} = \left(\frac{x_O}{x_{O_2}^{1/2}} \right)_2 P_2^{1/2} \tag{B-4}$$

$$2(n_{O_2})_1 = (2n_{O_2} + n_O + n_{H_2O} + n_{OH})_2 \tag{B-5}$$

$$2(n_{H_2})_1 = (2n_{H_2} + n_H + 2n_{H_2O} + n_{OH})_2 \tag{B-6}$$

Dividing (B-5) and (B-6) by $(n_T)_2$

$$\frac{2(n_{O_2})_1}{(n_T)_2} = (2x_{O_2} + x_O + x_{H_2O} + x_{OH})_2 = 2(x_{O_2})_1 \frac{(n_T)_1}{(n_T)_2} \tag{B-7}$$

$$\frac{2(n_{H_2})_1}{(n_T)_2} = (2x_{H_2} + x_H + 2x_{H_2O} + x_{OH})_2 = 2(x_{H_2})_1 \frac{(n_T)_1}{(n_T)_2} \tag{B-8}$$

Dividing (B-7) by (B-8)

$$\frac{(x_{O_2})_1}{(x_{H_2})_1} = \frac{(2x_{O_2} + x_O + x_{H_2O} + x_{OH})_2}{(2x_{H_2} + x_H + 2x_{H_2O} + x_{OH})_2} \qquad \text{(B-9)}$$

Hereafter, the subscript 2 denoting the final mixture will be dropped. Since the sum of the mole fractions of the six components must be unity,

$$x_{O_2} + x_{H_2} + x_O + x_H + x_{H_2O} + x_{OH} = 1 \qquad \text{(B-10)}$$

Rearranging Equations (B-1), (B-2), (B-3), (B-4), and (B-9), respectively, and letting $F = \frac{(x_{O_2})_1}{(x_{H_2})_1}$,

$$x_{O_2} = \frac{K_{P1}^2}{P_2}\left(\frac{x_{H_2O}}{x_{H_2}}\right)^2 \qquad \text{(B-11)}$$

$$x_{OH} = \frac{K_{P2}}{\sqrt{P_2}}\left(\frac{x_{H_2O}}{x_{H_2}^{1/2}}\right) \qquad \text{(B-12)}$$

$$x_H = \frac{K_{P3}}{\sqrt{P_2}}\, x_{H_2}^{1/2} \qquad \text{(B-13)}$$

$$x_O = \frac{K_{P4}}{\sqrt{P_2}}\, x_{O_2}^{1/2} = \frac{K_{P1}K_{P4}}{P_2}\left(\frac{x_{H_2O}}{x_{H_2}}\right) \qquad \text{(B-14)}$$

$$2Fx_{H_2} + Fx_H - 2x_{O_2} - x_O + (2F-1)x_{H_2O} + (F-1)x_{OH} = 0 \qquad \text{(B-15)}$$

Substituting (B-11), (B-12), (B-13) and (B-14) into (B-10) and (B-15) respectively,

$$\frac{K_{P1}^2}{P_2}\left(\frac{x_{H_2O}^2}{x_{H_2}^2}\right) + x_{H_2} + \frac{K_{P1}K_{P4}}{P_2}\left(\frac{x_{H_2O}}{x_{H_2}}\right) + \frac{K_{P3}}{\sqrt{P_2}}\, x_{H_2}^{1/2} + x_{H_2O} + \frac{K_{P2}}{\sqrt{P_2}}\left(\frac{x_{H_2O}}{x_{H_2}^{1/2}}\right) = 1 \qquad \text{(B-16)}$$

$$2Fx_{H_2} + \frac{FK_{P3}}{\sqrt{P_2}} x_{H_2}^{1/2} - \frac{2K_{P1}^2}{P_2}\left(\frac{x_{H_2O}^2}{x_{H_2}^2}\right) - \frac{K_{P1}K_{P4}}{P_2}\left(\frac{x_{H_2O}}{x_{H_2}}\right)$$

$$+ (2F-1)x_{H_2O} + \frac{(F-1)K_{P2}}{\sqrt{P_2}}\left(\frac{x_{H_2O}}{x_{H_2}^{1/2}}\right) = 0 \qquad \text{(B-17)}$$

Rearranging (B-16) and (B-17) respectively,

$$\left[\frac{K_{P1}^2}{P_2 x_{H_2}^2}\right] x_{H_2O}^2 + \left[\frac{K_{P1}K_{P4}}{P_2 x_{H_2}} + \frac{K_{P2}}{\sqrt{P_2}\sqrt{x_{H_2}}} + 1\right] x_{H_2O}$$

$$+ \left[x_{H_2} + \frac{K_{P3}\sqrt{x_{H_2}}}{\sqrt{P_2}} - 1\right] = 0 \qquad \text{(B-18)}$$

$$\left[\frac{2K_{P1}^2}{P_2 x_{H_2}^2}\right] x_{H_2O}^2 + \left[\frac{K_{P1}K_{P4}}{P_2 x_{H_2}} - \frac{(F-1)K_{P2}}{\sqrt{P_2}\sqrt{x_{H_2}}} - (2F-1)\right] x_{H_2O}$$

$$- \left[2Fx_{H_2} + \frac{FK_{P3}}{\sqrt{P_2}}\sqrt{x_{H_2}}\right] = 0 \qquad \text{(B-19)}$$

Solving (B-18) and (B-19), respectively, for x_{H_2O}

$$x_{H_2O} = \frac{-\left[\frac{K_{P1}K_{P4}}{P_2 x_{H_2}} + \frac{K_{P2}}{\sqrt{P_2}\sqrt{x_{H_2}}} + 1\right] \pm \sqrt{\left[\frac{K_{P1}K_{P4}}{P_2 x_{H_2}} + \frac{K_{P2}}{\sqrt{P_2}\sqrt{x_{H_2}}} + 1\right]^2 - \left[\frac{4K_{P1}^2}{P_2 x_{H_2}^2}\right]\left[x_{H_2} + \frac{K_{P3}\sqrt{x_{H_2}}}{\sqrt{P_2}} - 1\right]}}{\frac{2K_{P1}^2}{P_2 x_{H_2}^2}} \qquad \text{(B-20)}$$

$$x_{H_2O} = \frac{-\left[\frac{K_{P1}K_{P4}}{P_2 x_{H_2}} - \frac{(F-1)K_{P2}}{\sqrt{P_2}\sqrt{x_{H_2}}} - (2F-1)\right] \pm \sqrt{\left[\frac{K_{P1}K_{P4}}{P_2 x_{H_2}} - \frac{(F-1)K_{P2}}{\sqrt{P_2}\sqrt{x_{H_2}}} - (2F-1)\right]^2 + \left[\frac{8K_{P1}^2}{P_2 x_{H_2}^2}\right]\left[2Fx_{H_2} + \frac{FK_{P3}\sqrt{x_{H_2}}}{\sqrt{P_2}}\right]}}{\frac{4K_{P1}^2}{P_2 x_{H_2}^2}} \qquad \text{(B-21)}$$

Equations (B-11) through (B-14) then provide the concentrations of the other four components as a function of x_{H_2} and x_{H_2O}.

APPENDIX C

IBM-650 COMPUTER PROGRAM FOR SOLUTION OF CHEMICAL EQUILIBRIUM EQUATIONS

IBM-650 COMPUTER PROGRAM FOR SOLUTION OF CHEMICAL EQUILIBRIUM EQUATIONS

SOAP II SYMBOLIC PROGRAM

Next Instr.	Oper-ation	Data Address	Instr. Address
	BLR	0000	0000
	BLR	1850	1999
	REG	R0051	0060
	BLR	0001	0001
	REG	P0027	0036
	REL	0500	
0000	STD	0003	0006
0006	BMI	0009	0010
0010	SRT	F0002	0017
0017	NZU	0021	0022
0021	STL	0025	0016
0016	SLO	F8002	0028
0028	SRT	F0008	0043
0043	STL	0001	0004
0004	AUP	0007	0011
0011	DVR	0014	0002
0002	STL	0008	0012
0012	RAU	0001	0005
0005	DVR	0008	0020
0020	SLO	F8001	0026
0026	NZE	0030	0034
0030	BMI	0033	0034
0033	ALO	F8001	0039
0039	ALO	F8001	0011
0034	RAL	0025	0029
0029	ALO	0032	0036
0036	SRT	F0008	0042
0042	DIV	0014	0037
0037	ALO	F8003	0019
0019	STL	0025	0031
0031	NZU	0035	0041
0035	RAU	0008	0013
0013	SRT	F0001	0027
0027	MPY	0023	0038
0038	SRD	F0010	0018
0018	SLT	F0002	0024
0024	ALO	0025	0040
0040	RAU	F8002	0003
0041	RAL	0008	0015
0015	SRD	F0002	0018
0022	RAL	F8003	0003

FLOATING DECIMAL POINT SQUARE ROOT SUBROUTINE

MACHINE CODED PROGRAM

Next Instr.	Oper-ation	Data Address	Instr. Address
0500	24	0503	0506
0506	46	0509	0510
0510	30	0002	0517
0517	44	0521	0522
0521	20	0525	0516
0516	16	8002	0528
0528	30	0008	0543
0543	20	0501	0504
0504	10	0507	0511
0511	64	0514	0502
0502	20	0508	0512
0512	60	0501	0505
0505	64	0508	0520
0520	16	8001	0526
0526	45	0530	0534
0530	46	0533	0534
0533	15	8001	0539
0539	15	8001	0511
0534	65	0525	0529
0529	15	0532	0536
0536	30	0008	0542
0542	14	0514	0537
0537	15	8003	0519
0519	20	0525	0531
0531	44	0535	0541
0535	60	0508	0513
0513	30	0001	0527
0527	19	0523	0538
0538	31	0010	0518
0518	35	0002	0524
0524	15	0525	0540
0540	60	8002	0503
0541	65	0508	0515
0515	31	0002	0518
0522	65	8003	0503

SOAP II SYMBOLIC PROGRAM					MACHINE CODED PROGRAM			
Next Instr.	Oper-ation	Data Address	Instr. Address		Next Instr.	Oper-ation	Data Address	Instr. Address
0007	00	F0000	F0001	↑	0507	00	0000	0001
0014	00	F0000	F0002	|	0514	00	0000	0002
0032	50	F0000	F0000	|	0532	50	0000	0000
0023	03	F1622	F7766	|	0523	03	1622	7766
0009	44	F4444	F4444	|	0509	44	4444	4444
0003	00	F0000	F0000	|	0503	00	0000	0000
0025	00	F0000	F0000	|	0525	00	0000	0000
0001	00	F0000	F0000	|	0501	00	0000	0000
0008	00	F0000	F0000	|	0508	00	0000	0000
	REQ	SQRT	0000	↓				
GAMMA	RAU	XH2			0050	60	0003	0007
	LDD		SQRT		0007	69	0010	0500
	STU	SQRTX			0010	21	0014	0017
	RAU	R0005			0017	60	0055	0009
	FMP	R0008			0009	39	0058	0008
	FDV	R0003			0008	34	0053	0103
	FDV	XH2			0103	34	0003	0153
	STU	A			0153	21	0108	0011
	RAU	R0006			0011	60	0056	0061
	FDV	SQRTP			0061	34	0064	0114
	FDV	SQRTX			0114	34	0014	0164
	STU	B			0164	21	0018	0021
	RAU	TWO			0021	60	0024	0079
	FMP	R0005			0079	39	0055	0005
	FMP	R0005			0005	39	0055	0105
	FDV	R0003			0105	34	0053	0203
	FDV	XH2			0203	34	0003	0253
	FDV	XH2			0253	34	0003	0303
	STU	C			0303	21	0158	0111
	RAU	R0007			0111	60	0057	0161
	FMP	SQRTX			0161	39	0014	0214
	FDV	SQRTP			0214	34	0064	0264
	STU	D			0264	21	0068	0071
	RAU	A			0071	60	0108	0013
	FAD	B			0013	32	0018	0045
	FAD	ONE			0045	32	0048	0025
	STU	E			0025	21	0080	0083
	RAU	B			0083	60	0018	0023
	FAD	TWO			0023	32	0024	0101
	FMP	F			0101	39	0004	0104
	STU	G			0104	21	0208	0211
	RAU	E			0211	60	0080	0085
	FSB	G			0085	33	0208	0135
	STU	H			0135	21	0040	0043
	RAU	ONE			0043	60	0048	0353
	FSB	XH2			0353	33	0003	0129
	FSB	D			0129	33	0068	0095
	FMP	C			0095	39	0158	0258
	FMP	TWO			0258	39	0024	0074
	STU	STOR1			0074	21	0078	0081

SQUARE ROOT SUBROUTINE

SOAP II SYMBOLIC PROGRAM

Next Instr.	Oper-ation	Data Address	Instr. Address
	RAU	E	
	FMP	E	
	FAD	STOR1	
	LDD		SQRT
	FSB	E	
	FDV	C	
	STU	XH201	
	RAU	TWO	
	FMP	XH2	
	FAD	D	
	FMP	F	
	FMP	C	
	FMP	FOUR	
	STU	STOR2	
	RAU	H	
	FMP	H	
	FAD	STOR2	
	LDD		SQRT
	FSB	H	
	FDV	C	
	FDV	TWO	
	STU	XH202	
	FSB	XH201	
	STU	DIFF	
	RAU	XH2	
	FSB	ONE	
	NZE		BRCH1
	RAU	DIFF	
	STU	LEFT	
	FMP	RIGHT	
	BMI	BETA	
	LDD	LEFT	
	STD	RIGHT	ALPHA
BRCH1	LDD	DIFF	
	STD	RIGHT	ALPHA
ALPHA	RAU	XH2	
	FSB	DELTA	
	STU	XH2	BETA
BETA	RAU	DELTA	
	SRT	0002	
	STL	EXP	
	RAU	XH2	
	SRT	0002	
	SUP	8003	
	SLO	EXP	
	SLO	ERROR	
	BMI		BRCH2
	RAU	DELTA	
	FDV	TWO	

MACHINE CODED PROGRAM

Next Instr.	Oper-ation	Data Address	Instr. Address
0081	60	0080	0185
0185	39	0080	0130
0130	32	0078	0155
0155	69	0308	0500
0308	33	0080	0107
0107	34	0158	0358
0358	21	0012	0015
0015	60	0024	0179
0179	39	0003	0403
0403	32	0068	0145
0145	39	0004	0154
0154	39	0158	0408
0408	39	0261	0311
0311	21	0016	0019
0019	60	0040	0195
0195	39	0040	0090
0090	32	0016	0093
0093	69	0046	0500
0046	33	0040	0067
0067	34	0158	0458
0458	34	0024	0124
0124	21	0128	0131
0131	33	0012	0039
0039	21	0044	0047
0047	60	0003	0157
0157	33	0048	0075
0075	45	0178	0229
0178	60	0044	0049
0049	21	0204	0207
0207	39	0110	0160
0160	46	0063	0314
0314	69	0204	0257
0257	24	0110	0113
0229	69	0044	0097
0097	24	0110	0113
0113	60	0003	0307
0307	33	0210	0037
0037	21	0003	0063
0063	60	0210	0065
0065	30	0002	0121
0121	20	0125	0228
0228	60	0003	0357
0357	30	0002	0163
0163	11	8003	0171
0171	16	0125	0279
0279	16	0082	0087
0087	46	0140	0041
0140	60	0210	0115
0115	34	0024	0174

SOAP II SYMBOLIC PROGRAM

Next Instr.	Oper-ation	Data Address	Instr. Address
	STU	DELTA	
	FAD	XH2	
	STU	XH2	GAMMA
BRCH2	LDD	XH2	
	STD	P0002	
	LDD	XH201	
	STD	P0003	
	RAU	R0005	
	FMP	R0005	
	FMP	XH201	
	FMP	XH201	
	FDV	R0003	
	FDV	XH2	
	FDV	XH2	
	STU	P0004	
	RAU	R0006	
	FMP	XH201	
	FDV	SQRTP	
	FDV	SQRTX	
	STU	P0005	
	RAU	R0007	
	FMP	SQRTX	
	FDV	SQRTP	
	STU	P0006	
	RAU	R0005	
	FMP	R0008	
	FMP	XH201	
	FDV	R0003	
	FDV	XH2	
	STU	P0007	
	PCH	P0001	0001
0001	RCD	R0001	
	LDD	R0001	
	STD	P0001	
	RAU	R0003	
	LDD		SQRT
	STU	SQRTP	
	RAU	ONE	
	FSB	R0002	
	FDV	R0002	
	STU	F	
	LDD	ONE	
	STD	DELTA	
	STD	XH2	GAMMA
ONE	10	0000	0051
TWO	20	0000	0051
FOUR	40	0000	0051
P0010	00	0000	0080
ERROR	05	0000	0000

MACHINE CODED PROGRAM

Next Instr.	Oper-ation	Data Address	Instr. Address
0174	21	0210	0213
0213	32	0003	0329
0329	21	0003	0050
0041	69	0003	0006
0006	24	0028	0181
0181	69	0012	0165
0165	24	0029	0132
0132	60	0055	0109
0109	39	0055	0205
0205	39	0012	0062
0062	39	0012	0112
0112	34	0053	0453
0453	34	0003	0553
0553	34	0003	0603
0603	21	0030	0133
0133	60	0056	0361
0361	39	0012	0162
0162	34	0064	0364
0364	34	0014	0414
0414	21	0031	0084
0084	60	0057	0411
0411	39	0014	0464
0464	34	0064	0564
0564	21	0032	0235
0235	60	0055	0159
0159	39	0058	0558
0558	39	0012	0212
0212	34	0053	0653
0653	34	0003	0703
0703	21	0033	0086
0086	71	0027	0001
0001	70	0051	0151
0151	69	0051	0254
0254	24	0027	0180
0180	60	0053	0407
0407	69	0260	0500
0260	21	0064	0117
0117	60	0048	0753
0753	33	0052	0379
0379	34	0052	0002
0002	21	0004	0457
0457	69	0048	0201
0201	24	0210	0263
0263	24	0003	0050
0048	10	0000	0051
0024	20	0000	0051
0261	40	0000	0051
0036	00	0000	0080
0082	05	0000	0000

The input and output data cards used formats of eight words each containing ten digits. The last two digits in each word denoted the power of ten associated with the first eight digits in the floating decimal point program used. The input card data were laid out in the following order: Identification number, initial mole fraction hydrogen, pressure, temperature, and the four equilibrium constants in serial order. The output card data were laid out in the following order: Molecular hydrogen, water, molecular oxygen, hydroxyl radical, atomic hydrogen, and atomic oxygen. The results of this program may be found in Appendix F. For further information in IBM-650 and SOAP II conventions, consult Reference (38). This computer work was done by the author at the Statistical Research Laboratory, University of Michigan.

APPENDIX D

DEVELOPMENT OF EQUATIONS FOR DETERMINATION OF THE EFFECT OF ERRORS IN PHYSICAL PROPERTIES ON DETONATION VELOCITY

DEVELOPMENT OF EQUATIONS FOR DETERMINATION OF THE EFFECT OF ERRORS IN PHYSICAL PROPERTIES ON DETONATION VELOCITY

The total differential of $w=f(x, y, z, \ldots)$ is

$$dw = \frac{\partial w}{\partial x} dx + \frac{\partial w}{\partial y} dy + \frac{\partial w}{\partial z} dz + \ldots \qquad \text{(D-1)}$$

If the differentials are replaced by increments, the maximum change in w resulting from small changes in x, y, z, ..., may be obtained from the resulting relationship:

$$\Delta w = \frac{\partial w}{\partial x} \Delta x + \frac{\partial w}{\partial y} \Delta y + \frac{\partial w}{\partial z} \Delta z + \ldots \qquad \text{(D-2)}$$

As Δx, Δy, Δz, ... become smaller, Δw approaches the true change in w. In any event, the Δw obtained from (D-2) is greater than the true Δw. Thus, (D-2) gives conservative errors in w resulting from errors in x, y, z, ... Fractional errors may be obtained by modifying (D-2) to:

$$\frac{\Delta w}{w} = \left(\frac{x}{w} \frac{\partial w}{\partial x}\right)\frac{\Delta x}{x} + \left(\frac{y}{w} \frac{\partial w}{\partial y}\right)\frac{\Delta y}{y} + \left(\frac{z}{w} \frac{\partial w}{\partial z}\right)\frac{\Delta z}{z} + \ldots \qquad \text{(D-3)}$$

If Equation (D-3) is applied to Equation (6) for u_1,

$$u_1 = \sqrt{2R\left[\frac{z_2 T_2 (1+\gamma_2)^2}{2m_2\gamma_2} - \frac{z_1 T_1}{m_1}\right]},$$

partial derivatives being taken with respect to z_2, T_2, γ_2, m_2, and z_1, simplification of the resulting equation yields:

$$\frac{\Delta u_1}{u_1} = \frac{R}{u_1^2}\left[\frac{z_2 T_2 (1+\gamma_2)^2}{2m_2\gamma_2}\left(\frac{\Delta z_2}{z_2} + \frac{\Delta T_2}{T_2} + \frac{\gamma_2 - 1}{\gamma_2 + 1}\frac{\Delta\gamma_2}{\gamma_2}\right) - \frac{1}{m_2}\frac{\Delta m_2}{m_2} - \frac{z_1 T_1}{m_1}\frac{\Delta z_1}{z_1}\right] \qquad \text{(D-4)}$$

Before $\Delta u_1/u_1$ may be evaluated, the effect of property errors on T_2, γ_2 and m_2 must be determined. This series of errors within errors is continued until the equations being dealt with contain nothing but physical

properties which might be pressure sensitive (See Table II). The above statement will become clearer as the procedure is continued. Application of Equation (D-3) to Equation (5) for temperature,

$$T_2 = \left(\frac{\Delta h}{R} + \frac{z_1 T_1}{m_1}\right) \frac{2m_2\gamma_2}{(1+2\gamma_2)z_2} \quad ,$$

results after simplification, in:

$$\frac{\Delta T_2}{T_2} = \frac{2m_2\gamma_2}{(1+2\gamma_2)z_2T_2}\left[\frac{\Delta h}{R}\frac{\Delta(\Delta h)}{\Delta h} + \frac{z_1T_1}{m_1}\frac{\Delta z_1}{z_1}\right] - \frac{\Delta z_2}{z_2} + \frac{\Delta m_2}{m_2} + \frac{1}{(1+2\gamma_2)}\frac{\Delta\gamma_2}{\gamma_2} \qquad \text{(D-5)}$$

Equation (D-3) applied to the definition of Δh,

$$\Delta h = \frac{1}{m_2}\left[\sum_P x_P(H^\circ_{T_2}-H^\circ_0)_P + \sum_P x_P(\Delta H^\circ_f)_P\right] - \frac{1}{m_1}\sum_R x_R(H^\circ_{T_1}-H^\circ_0)_R,$$

results in:

$$\frac{\Delta(\Delta h)}{\Delta h} = \frac{1}{m_2\Delta h}\left[-\sum_P x_P\left((H^\circ_{T_2}-H^\circ_0)_P + (\Delta H^\circ_f)_P\right)\frac{\Delta m_2}{m_2} + \sum_P x_P\left((H^\circ_{T_2}-H^\circ_0)_P + (\Delta H^\circ_f)_P\right)\frac{\Delta x_P}{x_P}\right.$$

$$\left. + \sum_P\left(x_P(H^\circ_{T_2}-H^\circ_0)_P\right)\frac{\Delta(H^\circ_{T_2}-H^\circ_0)_P}{(H^\circ_{T_2}-H^\circ_0)_P} - \sum_R\left(\frac{m_2}{m_1}x_R(H^\circ_{T_1}-H^\circ_0)_R\right)\frac{\Delta(H^\circ_{T_1}-H^\circ_0)_R}{(H^\circ_{T_1}-H^\circ_0)_R}\right] \quad \text{(D-}$$

Equation (D-3) applied to the definition of m_2, $m_2 = \sum_P x_P m_P$, results in:

$$\frac{\Delta m_2}{m_2} = \frac{1}{m_2}\sum_P x_P m_P \frac{\Delta x_P}{x_P} \qquad \text{(D-7)}$$

Equation (D-3) applied to the definition of γ_2, $\gamma_2 = \dfrac{\sum_P x_P(c_P)_P}{\sum_P x_P(c_P)_{P-R}}$

results in:

$$\frac{\Delta\gamma_2}{\gamma_2} = -\sum_P\left[\frac{x_P(c_P)_P R}{(c_P)_2\left((c_P)_2-R\right)}\left(\frac{\Delta x_P}{x_P} + \frac{\Delta(c_P)_P}{(c_P)_P}\right)\right] \qquad \text{(D-8)}$$

Equation (D-3) applied to the equilibrium and mass balance equations yield:

$$\frac{\Delta x_{H_2}}{x_{H_2}} = 2\left(\frac{\Delta x_H}{x_H} - \frac{\Delta K_{P3}}{K_{P3}}\right) \tag{D-9}$$

$$\frac{\Delta x_{O_2}}{x_{O_2}} = 2\left(\frac{\Delta x_O}{x_O} - \frac{\Delta K_{P4}}{K_{P4}}\right) \tag{D-10}$$

$$\frac{\Delta x_{H_2}}{x_{H_2}} = \frac{\Delta x_{H_2O}}{x_{H_2O}} - \frac{1}{2}\frac{\Delta x_{O_2}}{x_{O_2}} + \frac{\Delta K_{P1}}{K_{P1}} \tag{D-11}$$

$$\frac{\Delta x_{H_2}}{x_{H_2}} = 2\left(\frac{\Delta x_{H_2O}}{x_{H_2O}} - \frac{\Delta x_{OH}}{x_{OH}} + \frac{\Delta K_{P2}}{K_{P2}}\right) \tag{D-12}$$

$$x_{H_2}\frac{\Delta x_{H_2}}{x_{H_2}} + x_{O_2}\frac{\Delta x_{O_2}}{x_{O_2}} + x_H\frac{\Delta x_H}{x_H} + x_O\frac{\Delta x_O}{x_O} + x_{OH}\frac{\Delta x_{OH}}{x_{OH}} + x_{H_2O}\frac{\Delta x_{H_2O}}{x_{H_2O}} = 0 \tag{D-13}$$

$$2Fx_{H_2}\frac{\Delta x_{H_2}}{x_{H_2}} + Fx_H\frac{\Delta x_H}{x_H} - 2x_{O_2}\frac{\Delta x_{O_2}}{x_{O_2}} + (2F-1)x_{H_2O}\frac{\Delta x_{H_2O}}{x_{H_2O}}$$

$$- x_O\frac{\Delta x_O}{x_O} + (F-1)x_{OH}\frac{\Delta x_{OH}}{x_{OH}} = 0 \tag{D-14}$$

Equations (D-9) through (D-14) were solved simultaneously for the six fractional errors in mole fraction. The results are:

$$\frac{\Delta x_{H_2}}{x_{H_2}} = -\frac{1}{2D}\left[\left((2F-1)\,x_{H_2O} + (F-1)x_{OH} - 4x_{O_2} - x_O\right)\left(\left\langle\frac{\Delta K_{P1}}{K_{P1}} + \frac{\Delta K_{P4}}{K_{P4}}\right\rangle x_O + 2\frac{\Delta K_{P1}}{K_{P1}}x_{O_2} + \frac{\Delta K_{P2}}{K_{P2}}\,x_{OH} + \frac{\Delta K_{P3}}{K_{P3}}\,x_H\right)\right.$$

$$+\left(x_{H_2O} + x_{OH} + 2x_{O_2} + x_O\right)\left(\left\langle\frac{\Delta K_{P1}}{K_{P1}} + \frac{\Delta K_{P4}}{K_{P4}}\right\rangle x_O + 4\frac{\Delta K_{P1}}{K_{P1}}\,x_{O_2}\right.$$

$$\left.\left. - \frac{\Delta K_{P2}}{K_{P2}}\,(F-1)\,x_{OH} - \frac{\Delta K_{P3}}{K_{P3}}\,Fx_H\right)\right] \qquad \text{(D-15)}$$

$$\frac{\Delta x_{H_2O}}{x_{H_2O}} = \frac{1}{4D}\left[\left(4Fx_{H_2} + Fx_H - (F-1)x_{OH} + 8x_{O_2} + 2x_O\right)\left(\left\langle\frac{\Delta K_{P1}}{K_{P1}} + \frac{\Delta K_{P4}}{K_{P4}}\right\rangle x_O\right.\right.$$

$$\left. + 2\,\frac{\Delta K_{P1}}{K_{P1}}\,x_{O_2} + \frac{\Delta K_{P2}}{K_{P2}}\,x_{OH} + \frac{\Delta K_{P3}}{K_{P3}}\,x_H\right) + \left(2x_{H_2} + x_H - x_{OH} - 4x_{O_2}\right.$$

$$\left.\left. - 2x_O\right)\left(\left\langle\frac{\Delta K_{P1}}{K_{P1}} + \frac{\Delta K_{P4}}{K_{P4}}\right\rangle x_O + 4\,\frac{\Delta K_{P1}}{K_{P1}}\,x_{O_2} - \frac{\Delta K_{P2}}{K_{P2}}\,(F-1)x_{OH} - \frac{\Delta K_{P3}}{K_{P3}}\,Fx_H\right)\right] \qquad \text{(D-16)}$$

$$\frac{\Delta x_H}{x_H} = \frac{\Delta K_{P3}}{K_{P3}} + \frac{1}{2}\,\frac{\Delta x_{H_2}}{x_{H_2}} \qquad \text{(D-17)}$$

$$\frac{\Delta x_{O_2}}{x_{O_2}} = 2\left(\frac{\Delta K_{P1}}{K_{P1}} - \frac{\Delta x_{H_2}}{x_{H_2}} + \frac{\Delta x_{H_2O}}{x_{H_2O}}\right) \qquad \text{(D-18)}$$

$$\frac{\Delta x_{OH}}{x_{OH}} = \frac{\Delta K_{P2}}{K_{P2}} - \frac{1}{2}\frac{\Delta x_{H_2}}{x_{H_2}} + \frac{\Delta x_{H_2O}}{x_{H_2O}} \tag{D-19}$$

$$\frac{\Delta x_{O}}{x_{O}} = \frac{\Delta K_{P1}}{K_{P1}} + \frac{\Delta K_{P4}}{K_{P4}} - \frac{\Delta x_{H_2}}{x_{H_2}} + \frac{\Delta x_{H_2O}}{x_{H_2O}} \tag{D-20}$$

where

$$D = -\frac{1}{4}\left(2x_{H_2} + x_H + 2x_{H_2O} + x_{OH}\right)\left(2Fx_{H_2} + 2(2F+1)\,x_{O_2} - F(F-1)\,x_H + 2Fx_O - F(F-1)x_{OH}\right) \tag{D-21}$$

Equation (D-3) applied to the definitions of the K_P's,

$$\left(K_{P1} = \frac{\nu_{H_2O}}{\nu_{H_2}\nu_{O_2}^{1/2}}K_{f1},\ K_{P2} = \frac{\nu_{H_2O}}{\nu_{H_2}^{1/2}\nu_{OH}}K_{f2},\ K_{P3} = \frac{\nu_{H_2}^{1/2}}{\nu_H}K_{f3},\ \text{and } K_{P4} = \frac{\nu_{O_2}^{1/2}}{\nu_O}K_{f4}\right)$$

yield:

$$\frac{\Delta K_{P1}}{K_{P1}} = \frac{\Delta \nu_{H_2O}}{\nu_{H_2O}} - \frac{\Delta \nu_{H_2}}{\nu_{H_2}} - \frac{1}{2}\frac{\Delta \nu_{O_2}}{\nu_{O_2}} \tag{D-22}$$

$$\frac{\Delta K_{P2}}{K_{P2}} = \frac{\Delta \nu_{H_2O}}{\nu_{H_2O}} - \frac{1}{2}\frac{\Delta \nu_{H_2}}{\nu_{H_2}} - \frac{\Delta \nu_{OH}}{\nu_{OH}} \tag{D-23}$$

$$\frac{\Delta K_{P3}}{K_{P3}} = \frac{1}{2}\frac{\Delta \nu_{H_2}}{\nu_{H_2}} - \frac{\Delta \nu_{H}}{\nu_{H}} \tag{D-24}$$

$$\frac{\Delta K_{P4}}{K_{P4}} = \frac{1}{2}\frac{\Delta \nu_{O_2}}{\nu_{O_2}} - \frac{\Delta \nu_{O}}{\nu_{O}} \tag{D-25}$$

The procedure then was to let all physical property errors (See Table II in text) except one be zero, and work back through the necessary equations until all that remained was $\Delta u_1/u_1$ as a function of the error in the single physical property. It can be seen from the equations that the combined effect of all property errors is merely the summation of the effects of the individual property errors.

APPENDIX E

ORIGINAL AND CORRECTED EXPERIMENTAL DETONATION VELOCITIES

TABLE IV

ORIGINAL AND CORRECTED EXPERIMENTAL DETONATION VELOCITIES

RUN NO.	x_{H_2} ACTUAL	P_1 PSIA	u_1 ACTUAL FT/SEC	x_{H_2} NOMINAL	s FROM FIG.19	u_1 CORRECTED TO NOM x_{H_2} FROM EQ.62 FT/SEC	$(u_1)_\infty$ CORRECTED FOR x_{H_2} & TUBE DIAM, FROM EQ.63
1	0.679	14.3	9130	0.667	10530	9004	9063
2	0.515	14.3	7673	0.500	9320	7533	7592
3	0.808	14.4	11210	0.800	12430	11110	11170
4	0.346	14.4	7006	0.350	———	———	———
5	0.340	14.3	6565	0.350	———	———	———
6	0.602	14.3	8380	0.600	9730	8361	8420
7	0.745	14.3	9875	0.750	13160	9941	10000
8	0.406	14.3	6658	0.400	9180	6603	6662
9	0.492	14.3	7444	0.500	9320	7519	7578
10	0.440	14.2	7046	0.400	9180	6679	6738
11	0.795	14.1	10370	0.800	12430	10430	10490
12	0.471	100	7626	0.500	9240	7894	7953
13	0.608	100	8907	0.600	10600	8822	8881
14	0.801	14.4	10250	0.800	12430	10240	10300
15	0.799	100	11560	0.800	9440	11570	11630
16	0.661	500	10190	0.667	14180	10280	10340
17	0.796	500	12160	0.800	10890	12200	12260
18	0.492	500	8152	0.500	10220	8234	8293
19	0.409	500	7239	0.400	9600	7153	7212
20	0.606	500	9369	0.600	12360	9295	9354
21	0.699	500	10620	0.667	14180	10170	10230
22	0.798	1000	12240	0.800	13590	12270	12330
23	0.675	500	10270	0.667	14180	10160	10220
24	0.675	100	9778	0.667	13150	9673	9732
25	0.675	100	9740	0.667	13150	9635	9694
26	0.675	50	9640	0.667	12660	9539	9598
27	0.675	50	9603	0.667	12660	9502	9561
28	0.675	50	9609	0.667	12660	9508	9567
29	0.675	14.4	9152	0.667	10530	9068	9127
30	0.675	14.4	9119	0.667	10530	9035	9094
31	0.675	14.4	9113	0.667	10530	9029	9088
32	0.805	500	12180	0.800	10890	12130	12190
33	0.805	500	12050	0.800	10890	12000	12060
34	0.805	100	11660	0.800	9440	11610	11670
35	0.805	100	11720	0.800	9440	11670	11730
36	0.805	50	11380	0.800	8700	11340	11400
37	0.805	50	11370	0.800	8700	11330	11390
38	0.805	14.4	11260	0.800	12430	11200	11260
39	0.805	14.4	10720	0.800	12430	10660	10720
40	0.805	14.4	11020	0.800	12430	10960	11020

RUN NO.	x_{H_2} ACTUAL	P_1 PSIA	u_1 ACTUAL FT/SEC	x_{H_2} NOMINAL	s FROM FIG.19	u_1 CORRECTED TO NOM x_{H_2} FROM EQ.62 FT/SEC	$(u_1)_\infty$ CORRECTED FOR x_{H_2} & TUBE DIAM, FROM EQ.63
41	0.503	500	8108	0.500	10220	8077	8136
42	0.503	500	8224	0.500	10220	8193	8252
43	0.503	500	8228	0.500	10220	8197	8256
44	0.503	100	7899	0.500	9240	7871	7930
45	0.503	100	7895	0.500	9240	7867	7926
46	0.503	100	7899	0.500	9240	7871	7930
47	0.503	50	7784	0.500	9540	7755	7814
48	0.503	50	7764	0.500	9540	7735	7794
49	0.503	50	7776	0.500	9540	7747	7806
50	0.503	14.4	7508	0.500	9320	7480	7539
51	0.503	14.4	7496	0.500	9320	7468	7527
52	0.503	14.4	7481	0.500	9320	7453	7512
53	0.503	25	7561	0.500	9440	7533	7592
54	0.503	25	7614	0.500	9440	7586	7645
55	0.503	25	7587	0.500	9440	7559	7618
56	0.590	500	9124	0.600	12360	9248	9307
57	0.590	500	9130	0.600	12360	9254	9313
58	0.590	100	8793	0.600	10600	8899	8958
59	0.590	100	8767	0.600	10600	8873	8932
60	0.590	50	8626	0.600	10780	8734	8793
61	0.590	50	8532	0.600	10780	8640	8699
62	0.590	50	8611	0.600	10780	8719	8778
63	0.590	25	8385	0.600	10690	8492	8551
64	0.590	25	8366	0.600	10690	8473	8532
65	0.590	14.4	8148	0.600	9730	8245	8304
66	0.590	14.4	8148	0.600	9730	8245	8304
67	0.590	25	8380	0.600	10690	8487	8546
68	0.590	100	8746	0.600	10600	8852	8911
69	0.590	14.4	8237	0.600	9730	8334	8393
70	0.740	500	11360	0.750	14010	11500	11560
71	0.740	500	11300	0.750	14010	11440	11500
72	0.740	500	11280	0.750	14010	11420	11480
73	0.740	100	10930	0.750	14750	11080	11140
74	0.740	100	10910	0.750	14750	11060	11120
75	0.740	100	10890	0.750	14750	11040	11000
76	0.740	50	10710	0.750	13810	10850	10910
77	0.740	50	10690	0.750	13810	10830	10890
78	0.740	50	10720	0.750	13810	10860	10920
79	0.740	25	10530	0.750	14040	10670	10730
80	0.740	25	10410	0.750	14040	10550	10610

RUN NO.	x_{H_2} ACTUAL	P_1 PSIA	u_1 ACTUAL FT/SEC	x_{H_2} NOMINAL	s FROM FIG.19	u_1 CORRECTED TO NOM x_{H_2} FROM EQ.62 FT/SEC	$(u_1)_\infty$ CORRECTED FOR x_{H_2} & TUBE DIAM, FROM EQ.63
81	0.740	25	10620	0.750	14040	10760	10820
82	0.740	25	10510	0.750	14040	10650	10710
83	0.740	14.4	10310	0.750	13160	10440	10500
84	0.740	14.4	10160	0.750	13160	10290	10350
85	0.740	14.4	9715	0.750	13160	9847	9906
86	0.740	14.4	9778	0.750	13160	9910	9969
87	0.740	14.4	9677	0.750	13160	9809	9868
88	0.400	500	7219	0.400	9600	7219	7278
89	0.400	500	7232	0.400	9600	7232	7291
90	0.400	500	7243	0.400	9600	7243	7302
91	0.400	100	6974	0.400	8950	6974	7033
92	0.400	100	7003	0.400	8950	7003	7062
93	0.400	100	6983	0.400	8950	6983	7042
94	0.400	50	6818	0.400	8770	6818	6877
95	0.400	50	6848	0.400	8770	6848	6907
96	0.400	50	6794	0.400	8770	6794	6853
97	0.400	25	6637	0.400	9140	6637	6696
98	0.400	25	6579	0.400	9140	6579	6638
99	0.400	25	6539	0.400	9140	6539	6598
100	0.400	14.4	6430	0.400	9180	6430	6489
101	0.400	14.4	6491	0.400	9180	6491	6550
102	0.690	500	10350	0.667	14180	10020	10080
103	0.690	500	10370	0.667	14180	10040	10100
104	0.690	100	9993	0.667	13150	9691	9750
105	0.690	100	9967	0.667	13150	9665	9724
106	0.690	50	9791	0.667	12660	9500	9559
107	0.690	50	9791	0.667	12660	9500	9559
108	0.690	25	9554	0.667	12060	9277	9336
109	0.690	25	9579	0.667	12060	9302	9361
110	0.690	14.4	9334	0.667	10530	9092	9151
111	0.690	14.4	9328	0.667	10530	9086	9145
112	0.690	14.4	9191	0.667	10530	8949	9008
113	0.747	100	10950	0.750	14750	10990	11050
114	0.747	50	10720	0.750	13810	10760	10820
115	0.747	50	10690	0.750	13810	10730	10790
116	0.747	25	10340	0.750	14040	10380	10440
117	0.747	25	10270	0.750	14040	10310	10370
118	0.747	25	10340	0.750	14040	10380	10440
119	0.747	14.4	9830	0.750	13160	9869	9928
120	0.747	14.4	9653	0.750	13160	9692	9751

RUN NO.	x_{H_2} ACTUAL	P_1 PSIA	u_1 ACTUAL FT/SEC	x_{H_2} NOMINAL	s FROM FIG.19	u_1 CORRECTED TO NOM x_{H_2} FROM EQ.62 FT/SEC	$(u_1)_\infty$ CORRECTED FOR x_{H_2},& TUBE DIAM, FROM EQ.63
121	0.747	14.4	9643	0.750	13160	9682	9741
122	0.747	14.4	9709	0.750	13160	9748	9807
123	0.735	100	10670	0.750	14750	10890	10950
124	0.735	50	10480	0.750	13810	10690	10750
125	0.735	50	10490	0.750	13810	10700	10760
126	0.735	25	10200	0.750	14040	10410	10470
127	0.735	25	10070	0.750	14040	10280	10340
128	0.735	25	9970	0.750	14040	10180	10240
129	0.735	25	10050	0.750	14040	10260	10320
130	0.735	14.4	9542	0.750	13160	9739	9798
131	0.735	14.4	9337	0.750	13160	9534	9593
132	0.735	14.4	9921	0.750	13160	10120	10180
133	0.735	14.4	9320	0.750	13160	9517	9576
134	0.735	14.4	10140	0.750	13160	10340	10400
135	0.735	25	10090	0.750	14040	10300	10360
136	0.594	1000	9294	0.600	11420	9363	9422
137	0.594	1000	9311	0.600	11420	9380	9439
138	0.740	1000	11340	0.750	13730	11480	11540
139	0.740	1000	11280	0.750	13730	11420	11480
140	0.503	1000	8403	0.500	9920	8373	8432
141	0.503	1000	8413	0.500	9920	8383	8442
142	0.503	1000	8333	0.500	9920	8303	8362
143	0.503	500	8065	0.500	10220	8034	8093
144	0.503	500	8099	0.500	10220	8068	8127
145	0.503	500	8188	0.500	10220	8157	8216
146	0.503	500	8143	0.500	10220	8112	8171
147	0.654	1000	10160	0.667	14390	10350	10410
148	0.654	1000	9987	0.667	14390	10170	10230
149	0.654	1000	10110	0.667	14390	10300	10360
150	0.654	500	9830	0.667	14180	10010	10070
151	0.654	500	9830	0.667	14180	10010	10070
152	0.798	1000	12170	0.800	13590	12200	12260
153	0.798	1000	12060	0.800	13590	12090	12150
154	0.798	1000	12150	0.800	13590	12180	12240
158	0.402	1000	7353	0.400	9400	7334	7393
159	0.402	1000	7411	0.400	9400	7392	7451
160	0.402	500	7191	0.400	9600	7172	7231
161	0.402	500	7136	0.400	9600	7117	7176
162	0.402	500	7116	0.400	9600	7097	7156

ARITHMETIC AVERAGE DATA

NOMINAL x_{H_2}	P_1, PSIA	AVERAGE $(u_1)_\infty$, FT/SEC
0.400	14.4	6610
	25	6644
	50	6879
	100	7046
	500	7235
	1000	7422
0.500	14.4	7550
	25	7618
	50	7805
	100	7935
	500	8193
	1000	8412
0.600	14.4	8355
	25	8543
	50	8747
	100	8921
	500	9325
	1000	9431
0.667	14.4	9097
	25	9349
	50	9569
	100	9725
	500	10160
	1000	10330
0.750	14.4	9958
	25	10490
	50	10830
	100	11050
	500	11510
	1000	11510
0.800	14.4	10830
	25	
	50	11400
	100	11680
	500	12170
	1000	12250

Note: Data averaged over all experimental points taken at each given initial hydrogen concentration and initial pressure.

APPENDIX F

EQUILIBRIUM COMPOSITIONS IN HYDROGEN-OXYGEN MIXTURES

TABLE V.

EQUILIBRIUM COMPOSITIONS IN HYDROGEN-OXYGEN MIXTURES

Initial x_{H_2} : 0.400

NOTE: XXXXX-Y = .XXXXX x 10^{-Y}
e.g., 90023-2 = 0.90023 x 10^{-2}.

T, °K	P, atm	x_{H_2}	x_{H_2O}	x_{O_2}	x_{OH}	x_H	x_O
3000	10	90023-2	43072-0	45393-0	75941-1	47376-2	25673-1
	25	58439-2	44774-0	46559-0	61967-1	24142-2	16444-1
	50	41927-2	45752-0	47226-0	52862-1	14459-2	11711-1
	75	34472-2	46230-0	47551-0	48096-1	10705-2	95948-2
	100	29984-2	46531-0	47754-0	44953-1	86462-3	83271-2
	250	19181-2	47329-0	48290-0	36155-1	43737-3	52960-2
	500	13654-2	47801-0	48605-0	30603-1	26094-3	37570-2
	750	11185-2	48031-0	48756-0	27742-1	19283-3	30724-2
	1000	97071-3	48182-0	48853-0	25870-1	15557-3	26634-2
	1500	79469-3	48371-0	48977-0	23437-1	11493-3	21774-2
	2000	68940-3	48493-0	49056-0	21847-1	92706-4	18872-2
3200	10	15919-1	39185-0	42744-0	10675-0	11224-1	46869-1
	25	10533-1	41875-0	44596-0	88702-1	57741-2	30278-1
	50	76335-2	43425-0	45658-0	76405-1	34757-2	21663-1
	75	63052-2	44177-0	46173-0	69831-1	25792-2	17788-1
	100	55000-2	44653-0	46499-0	65448-1	20862-2	15459-1
	250	35437-2	45905-0	47349-0	53013-1	10591-2	98659-2
	500	25327-2	46637-0	47840-0	45049-1	63310-3	70123-2
	750	20787-2	46999-0	48084-0	40915-1	46831-3	57401-2
	1000	18061-2	47230-0	48237-0	38200-1	37805-3	49790-2
	1500	14809-2	47522-0	48429-0	34659-1	27950-3	40734-2
	2000	12859-2	47711-0	48555-0	32338-1	22556-3	35323-2
3400	10	25225-1	34080-0	39177-0	13978-0	23515-1	78935-1
	25	17204-1	38021-0	41928-0	11942-0	12283-1	51646-1
	50	12660-1	40311-0	43520-0	10437-0	74501-2	37206-1
	75	10530-1	41432-0	44299-0	96036-1	55481-2	30650-1
	100	92246-2	42138-0	44784-0	90378-1	44968-2	26688-1
	250	60064-2	43998-0	46064-0	73964-1	22949-2	17119-1
	500	43175-2	45084-0	46805-0	63211-1	13758-2	12202-1
	750	35533-2	45619-0	47168-0	57566-1	10191-2	10001-1
	1000	30926-2	45960-0	47399-0	53836-1	82338-3	86824-2
	1500	25411-2	46391-0	47688-0	48949-1	60939-3	71107-2
	2000	22095-2	46669-0	47873-0	45732-1	49212-3	61700-2
3600	10	36217-1	28006-0	34818-0	16818-0	44335-1	12304-0
	25	25863-1	33293-0	38595-0	14963-0	23695-1	81930-1
	50	19470-1	36459-0	40832-0	13354-0	14538-1	59589-1
	75	16359-1	38018-0	41929-0	12404-0	10881-1	49303-1
	100	14419-1	39009-0	42619-0	11741-0	88461-2	43048-1
	250	95288-2	41624-0	44442-0	97464-1	45482-2	27802-1
	500	69038-2	43154-0	45499-0	83941-1	27375-2	19891-1

Initial x_{H_2}: 0.400 (continued)

T, oK	P, atm	x_{H_2}	x_{H_2O}	x_{O_2}	x_{OH}	x_H	x_O
3600	750	57029-2	43906-0	46015-0	76724-1	20315-2	16333-1
	1000	49751-2	44385-0	46343-0	71915-1	16432-2	14195-1
	1500	40995-2	44992-0	46756-0	65571-1	12179-2	11642-1
	2000	35708-2	45379-0	47019-0	61368-1	98438-3	10110-1
3800	10	46550-1	21393-0	29829-0	18763-0	75528-1	17806-0
	25	35539-1	27829-0	34640-0	17667-0	41738-1	12136-0
	50	27646-1	31888-0	37577-0	16230-0	26030-1	89379-1
	75	23566-1	33932-0	39038-0	15273-0	19623-1	74383-1
	100	20948-1	35244-0	39974-0	14571-0	16023-1	65185-1
	250	14132-1	38736-0	42445-0	12332-0	83231-2	42481-1
	500	10349-1	40796-0	43888-0	10731-0	50366-2	30546-1
	750	85921-2	41810-0	44587-0	98557-1	37469-2	25138-1
	1000	75185-2	42457-0	45035-0	92656-1	30354-2	21879-1
	1500	62184-2	43277-0	45600-0	84792-1	22540-2	17976-1
	2000	54291-2	43800-0	45959-0	79539-1	18239-2	15629-1
4000	10	53609-1	14918-0	24448-0	19345-0	11693-0	24236-0
	25	44887-1	21929-0	30141-0	19655-0	67670-1	17019-0
	50	36551-1	26733-0	33780-0	18776-0	43179-1	12740-0
	75	31784-1	29241-0	35630-0	17982-0	32876-1	10683-0
	100	28590-1	30875-0	36822-0	17338-0	27003-1	94056-1
	250	19837-1	35314-0	40022-0	15057-0	14226-1	62017-1
	500	14740-1	37977-0	41917-0	13282-0	86713-2	44879-1
	750	12317-1	39294-0	42847-0	12276-0	64717-2	37048-1
	1000	10821-1	40138-0	43438-0	11585-0	52535-2	32305-1
	1500	89945-2	41210-0	44186-0	10653-0	39106-2	26603-1
	2000	78766-2	41895-0	44662-0	10022-0	31693-2	23162-1
4200	10	55221-1	94819-1	19220-0	18221-0	16542-0	31013-0
	25	52003-1	16251-0	25466-0	20353-0	10152-0	22577-0
	50	44959-1	21457-0	29696-0	20436-0	66750-1	17240-0
	75	40136-1	24319-0	31911-0	20016-0	51495-1	14592-0
	100	36669-1	26231-0	33360-0	19561-0	42626-1	12920-0
	250	26392-1	31571-0	37313-0	17551-0	22872-1	86422-1
	500	19976-1	34854-0	39694-0	15749-0	14070-1	63029-1
	750	16831-1	36499-0	40872-0	14669-0	10545-1	52221-1
	1000	14862-1	37557-0	41629-0	13911-0	85818-2	45642-1
	1500	12428-1	38904-0	42584-0	12866-0	64077-2	37692-1
	2000	10924-1	39765-0	43187-0	12148-0	52024-2	32872-1

Initial x_{H_2}: 0.400 (continued)

T, °K	P, atm	x_{H_2}	x_{H_2O}	x_{O_2}	x_{OH}	x_H	x_O
4400	10	50985-1	54534-1	14454-0	15954-0	21507-0	37534-0
	25	55120-1	11181-0	20794-0	19897-0	14143-0	28473-0
	50	51369-1	16293-0	25419-0	21237-0	96544-1	22260-0
	75	47428-1	19312-0	27930-0	21390-0	75744-1	19052-0
	100	44207-1	21399-0	29603-0	21261-0	63329-1	16986-0
	250	33360-1	27475-0	34278-0	19874-0	34794-1	11560-0
	500	25857-1	31358-0	37161-0	18218-0	21660-1	85112-1
	750	22020-1	33338-0	38611-0	17137-0	16321-1	70836-1
	1000	19568-1	34618-0	39538-0	16348-0	13324-1	62078-1
	1500	16491-1	36261-0	40722-0	15230-0	99872-2	51440-1
	2000	14563-1	37317-0	41479-0	14444-0	81278-2	44961-1
4600	10	43092-1	29033-1	10474-0	12928-0	26054-0	43332-0
	25	53927-1	72038-1	16469-0	18135-0	18434-0	34365-0
	50	54835-1	11765-0	21242-0	20768-0	13144-0	27597-0
	75	52715-1	14708-0	23950-0	21622-0	10523-0	23926-0
	100	50344-1	16833-0	25795-0	21929-0	89056-1	21504-0
	250	40257-1	23370-0	31102-0	21532-0	50366-1	14934-0
	500	32124-1	27765-0	34475-0	20250-0	31814-1	11118-0
	750	27711-1	30055-0	36190-0	19270-0	24125-1	93007-1
	1000	24817-1	31553-0	37300-0	18514-0	19772-1	81773-1
	1500	21107-1	33487-0	38719-0	17395-0	14889-1	68025-1
	2000	18744-1	34740-0	39631-0	16584-0	12151-1	59601-1
4800	10	33911-1	14527-1	73703-1	99586-1	29804-0	48025-0
	25	48885-1	43399-1	12661-0	15671-0	22632-0	39809-0
	50	54664-1	80235-1	17304-0	19374-0	16923-0	32909-0
	75	55049-1	10660-0	20080-0	20944-0	13866-0	28945-0
	100	54100-1	12669-0	22023-0	21743-0	11904-0	26252-0
	250	46380-1	19298-0	27811-0	22624-0	69710-1	18658-0
	500	38343-1	24059-0	31623-0	21935-0	44819-1	14068-0
	750	33600-1	26615-0	33597-0	21165-0	34257-1	11840-0
	1000	30374-1	28307-0	34882-0	20504-0	28206-1	10448-0
	1500	26124-1	30519-0	36540-0	19462-0	21359-1	87309-1
	2000	23355-1	31963-0	37611-0	18670-0	17489-1	76713-1
5000	10	25550-1	70280-2	50639-1	73928-1	32658-0	51627-0
	25	41709-1	24782-1	94506-1	12904-0	26390-0	44606-0
	50	51310-1	51953-1	13723-0	17246-0	20698-0	38008-0
	75	54315-1	73708-1	16433-0	19417-0	17387-0	33960-0
	100	55099-1	91337-1	18390-0	20689-0	15166-0	31112-0
	250	51160-1	15469-0	24474-0	22998-0	92426-1	22700-0
	500	44089-1	20400-0	28655-0	23101-0	60671-1	17368-0
	750	39357-1	23147-0	30866-0	22653-0	46804-1	14718-0
	1000	35974-1	25000-0	32322-0	22162-0	38752-1	13040-0
	1500	31350-1	27453-0	34215-0	21286-0	29538-1	10957-0
	2000	28250-1	29076-0	35448-0	20567-0	24283-1	96587-1

Initial x_{H_2}: 0.500

T °K	P, atm	x_{H_2}	x_{H_2O}	x_{O_2}	x_{OH}	x_H	x_O
3000	10	14979-1	58071-0	29802-0	79373-1	61112-2	20802-1
	25	97067-2	60300-0	30610-0	64754-1	31113-2	13334-1
	50	69520-2	61555-0	31091-0	55230-1	18619-2	95021-2
	75	57101-2	62158-0	31330-0	50246-1	13778-2	77882-2
	100	49632-2	62538-0	31483-0	46959-1	11124-2	67612-2
	250	31680-2	63527-0	31893-0	37761-1	56209-3	43039-2
	500	22517-2	64100-0	32140-0	31958-1	33508-3	30551-2
	750	18430-2	64382-0	32263-0	28968-1	24752-3	24992-2
	1000	15985-2	64559-0	32343-0	27012-1	19964-3	21671-2
	1500	13077-2	64787-0	32446-0	24470-1	14744-3	17722-2
	2000	11339-2	64932-0	32511-0	22809-1	11890-3	15363-2
3200	10	26598-1	52965-0	27972-0	11163-0	14508-1	37915-1
	25	17589-1	56576-0	29195-0	92741-1	74613-2	24498-1
	50	12726-1	58613-0	29929-0	79869-1	44879-2	17539-1
	75	10500-1	59589-0	30294-0	72988-1	33285-2	14408-1
	100	91518-2	60200-0	30523-0	68402-1	26911-2	12525-1
	250	58807-2	61787-0	31150-0	55391-1	13643-2	80022-2
	500	41944-2	62699-0	31525-0	47062-1	81474-3	56924-2
	750	34388-2	63143-0	31713-0	42739-1	60234-3	46616-2
	1000	29857-2	63426-0	31834-0	39899-1	48607-3	40448-2
	1500	24456-2	63782-0	31988-0	36198-1	35919-3	33106-2
	2000	21222-2	64008-0	32088-0	33772-1	28977-3	28715-2
3400	10	42218-1	46120-0	25612-0	14622-0	30422-1	63823-1
	25	28858-1	51510-0	27351-0	12492-0	15908-1	41713-1
	50	21224-1	54592-0	28399-0	10917-0	96463-2	30055-1
	75	17638-1	56075-0	28923-0	10043-0	71801-2	24766-1
	100	15439-1	57006-0	29260-0	94510-1	58176-2	21572-1
	250	10023-1	59419-0	30170-0	77322-1	29647-2	13854-1
	500	71875-2	60797-0	30712-0	66065-1	17752-2	98838-2
	750	59071-2	61467-0	30985-0	60158-1	13140-2	81058-2
	1000	51364-2	61891-0	31160-0	56255-1	10611-2	70397-2
	1500	42149-2	62425-0	31385-0	51142-1	78484-3	57686-2
	2000	36616-2	62763-0	31529-0	47777-1	63351-3	50072-2
3600	10	60411-1	37835-0	22840-0	17593-0	57259-1	99654-1
	25	43453-1	45158-0	25154-0	15658-0	30714-1	66143-1
	50	32769-1	49493-0	26564-0	13974-0	18860-1	48063-1
	75	27533-1	51607-0	27275-0	12979-0	14115-1	39765-1
	100	24257-1	52938-0	27732-0	12284-0	11474-1	34725-1
	250	15991-1	56402-0	28974-0	10194-0	58922-2	22448-1
	500	11557-1	58386-0	29724-0	87777-1	35419-2	16077-1
	750	95313-2	59345-0	30097-0	80217-1	26263-2	13209-1
	1000	83054-2	59952-0	30339-0	75181-1	21231-2	11485-1
	1500	68329-2	60715-0	30648-0	68539-1	15723-2	94255-2
	2000	59452-2	61198-0	30848-0	64140-1	12702-2	81893-2

Initial x_{H_2} : 0.500 (continued)

T, °K	P, atm	x_{H_2}	x_{H_2O}	x_{O_2}	x_{OH}	x_H	x_O
3800	10	77025-1	28776-0	19711-0	19620-0	97155-1	14475-0
	25	59607-1	37718-0	22620-0	18489-0	54054-1	98070-1
	50	46614-1	43344-0	24421-0	16989-0	33801-1	72054-1
	75	39790-1	46155-0	25336-0	15988-0	25498-1	59923-1
	100	35386-1	47948-0	25929-0	15253-0	20824-1	52499-1
	250	23848-1	52661-0	27547-0	12906-0	10812-1	34223-1
	500	17426-1	55384-0	28533-0	11228-0	65353-2	24629-1
	750	14442-1	56706-0	29029-0	10310-0	48579-2	20284-1
	1000	12622-1	57539-0	29348-0	96914-1	39329-2	17662-1
	1500	10421-1	58587-0	29759-0	88674-1	29178-2	14522-1
	2000	90873-2	59253-0	30022-0	83171-1	23597-2	12632-1
4000	10	87706-1	19939-0	16319-0	20216-0	14956-0	19800-0
	25	74880-1	29636-0	19782-0	20566-0	87401-1	13788-0
	50	61564-1	36323-0	21982-0	19658-0	56038-1	10277-0
	75	53725-1	39808-0	23112-0	18830-0	42743-1	86043-1
	100	48408-1	42071-0	23849-0	18156-0	35137-1	75694-1
	250	33643-1	48155-0	25875-0	15766-0	18526-1	49866-1
	500	24962-1	51736-0	27124-0	13905-0	11284-1	36102-1
	750	20830-1	53489-0	27758-0	12849-0	84165-2	29819-1
	1000	18278-1	54596-0	28170-0	12125-0	68278-2	26015-1
	1500	15164-1	55990-0	28695-0	11147-0	50778-2	21438-1
	2000	13261-1	56872-0	29037-0	10486-0	41122-2	18676-1
4200	10	89169-1	12580-0	12976-0	19025-0	21020-0	25482-0
	25	85924-1	21847-0	16857-0	21285-0	13050-0	18369-0
	50	75332-1	29073-0	19420-0	21392-0	86403-1	13941-0
	75	67659-1	33064-0	20757-0	20960-0	66859-1	11768-0
	100	62017-1	35728-0	21635-0	20487-0	55435-1	10405-0
	250	44886-1	43129-0	24074-0	18385-0	29827-1	69418-1
	500	33985-1	47617-0	25595-0	16495-0	18352-1	50612-1
	750	28612-1	49837-0	26371-0	15363-0	13749-1	41947-1
	1000	25241-1	51249-0	26875-0	14567-0	11183-1	36672-1
	1500	21072-1	53034-0	27527-0	13470-0	83435-2	30304-1
	2000	18497-1	54163-0	27949-0	12717-0	67695-2	26445-1
4400	10	81471-1	71926-1	98469-1	16647-0	27187-0	30980-0
	25	90130-1	14943-0	13891-0	20796-0	18085-0	23272-0
	50	85442-1	21988-0	16734-0	22223-0	12451-0	18061-0
	75	79552-1	26186-0	18253-0	22395-0	98096-1	15402-0
	100	74520-1	29097-0	19261-0	22266-0	82223-1	13702-0
	250	56819-1	37572-0	22098-0	20825-0	45408-1	92819-1
	500	44164-1	42945-0	23892-0	19091-0	28308-1	68246-1
	750	37614-1	45654-0	24816-0	17956-0	21330-1	56790-1
	1000	33411-1	47393-0	25421-0	17128-0	17410-1	49777-1
	1500	28122-1	49602-0	26203-0	15954-0	13042-1	41263-1
	2000	24805-1	51010-0	26714-0	15129-0	10608-1	36082-1

Initial x_{H_2} : 0.500 (continued)

T, °K	P, atm	x_{H_2}	x_{H_2O}	x_{O_2}	x_{OH}	x_H	x_O
4600	10	68288-1	38112-1	71869-1	13481-0	32798-0	35894-0
	25	87193-1	95665-1	11110-0	18939-0	23440-0	28225-0
	50	90285-1	15787-0	14109-0	21718-0	16866-0	22491-0
	75	87674-1	19850-0	15770-0	22627-0	13570-0	19415-0
	100	84278-1	22802-0	16890-0	22958-0	11522-0	17401-0
	250	68438-1	31931-0	20092-0	22564-0	65669-1	12003-0
	500	54937-1	38060-0	22149-0	21226-0	41604-1	89113-1
	750	47463-1	41231-0	23216-0	20200-0	31574-1	74493-1
	1000	42520-1	43290-0	23917-0	19405-0	25881-1	65479-1
	1500	36149-1	45928-0	24830-0	18231-0	19484-1	54475-1
	2000	32078-1	47623-0	25428-0	17379-0	15896-1	47741-1
4800	10	53474-1	19016-1	50787-1	10381-0	37426-0	39866-0
	25	78317-1	57330-1	86083-1	16356-0	28646-0	32825-0
	50	89096-1	10705-0	11595-0	20247-0	21605-0	26939-0
	75	90697-1	14311-0	13332-0	21905-0	17798-0	23585-0
	100	89802-1	17080-0	14528-0	22753-0	15337-0	21322-0
	250	78533-1	26313-0	18033-0	23706-0	90711-1	15024-0
	500	65543-1	32977-0	20332-0	22996-0	58597-1	11281-0
	750	57621-1	36544-0	21538-0	22191-0	44860-1	94797-1
	1000	52159-1	38896-0	22333-0	21500-0	36963-1	83597-1
	1500	44896-1	41948-0	23373-0	20406-0	28000-1	69829-1
	2000	40133-1	43928-0	24057-0	19573-0	22927-1	61352-1
5000	10	40174-1	91849-2	34981-1	77048-1	40952-0	42910-0
	25	66358-1	32608-1	64642-1	13461-0	33287-0	36891-0
	50	82866-1	68954-1	92681-1	18012-0	26303-0	31235-0
	75	88647-1	98423-1	11000-0	20296-0	22213-0	27785-0
	100	90630-1	12251-0	12229-0	21637-0	19451-0	25370-0
	250	86115-1	21023-0	15955-0	24091-0	11991-0	18328-0
	500	75178-1	27927-0	18471-0	24219-0	79225-1	13944-0
	750	67456-1	31779-0	19804-0	23755-0	61275-1	11789-0
	1000	61817-1	34371-0	20690-0	23243-0	50799-1	10436-0
	1500	53994-1	37788-0	21853-0	22326-0	38764-1	87569-1
	2000	48690-1	40034-0	22623-0	21571-0	31879-1	77160-1

Initial x_{H_2} : 0.600

T, °K	P, atm	x_{H_2}	x_{H_2O}	x_{O_2}	x_{OH}	x_H	x_O
3000	10	29410-1	74742-0	12807-0	72907-1	85631-2	13636-1
	25	19244-1	77851-0	12981-0	59375-1	43809-2	86829-2
	50	13833-1	79558-0	13118-0	50605-1	26264-2	61722-2
	75	11374-1	80363-0	13197-0	46027-1	19445-2	50548-2
	100	98911-2	80862-0	13253-0	43011-1	15704-2	43867-2
	250	63142-2	82132-0	13420-0	34581-1	79355-3	27919-2
	500	44843-2	82844-0	13535-0	29267-1	47288-3	19826-2
	750	36681-2	83186-0	13597-0	26531-1	34920-3	16225-2
	1000	31800-2	83401-0	13639-0	24740-1	28158-3	14073-2
	1500	25996-2	83669-0	13694-0	22414-1	20787-3	11514-2
	2000	22528-2	83838-0	13731-0	20894-1	16759-3	99845-3
3200	10	51091-1	67684-0	12380-0	10293-0	20107-1	25224-1
	25	34511-1	72814-0	12562-0	85212-1	10451-1	16070-1
	50	25210-1	75668-0	12710-0	73260-1	63165-2	11430-1
	75	20876-1	77016-0	12802-0	66903-1	46932-2	93659-2
	100	18229-1	77851-0	12867-0	62677-1	37980-2	81319-2
	250	11749-1	79971-0	13073-0	50719-1	19285-2	51840-2
	500	83833-2	81150-0	13220-0	43085-1	11518-2	36862-2
	750	68710-2	81711-0	13302-0	39126-1	85143-3	30191-2
	1000	59635-2	82062-0	13358-0	36528-1	68694-3	26201-2
	1500	48814-2	82500-0	13433-0	33141-1	50746-3	21453-2
	2000	42336-2	82774-0	13483-0	30921-1	40927-3	18614-2
3400	10	78300-1	58246-0	11876-0	13560-0	41430-1	43460-1
	25	55466-1	65853-0	12101-0	11520-0	22053-1	27746-1
	50	41545-1	70221-0	12263-0	10037-0	13496-1	19750-1
	75	34792-1	72311-0	12361-0	92214-1	10084-1	16190-1
	100	30584-1	73613-0	12433-0	86709-1	81882-2	14062-1
	250	20027-1	76931-0	12668-0	70824-1	41907-2	89771-2
	500	14400-1	78775-0	12847-0	60478-1	25126-2	63924-2
	750	11842-1	79653-0	12947-0	55059-1	18604-2	52398-2
	1000	10297-1	80197-0	13019-0	51484-1	15024-2	45504-2
	1500	84481-2	80878-0	13114-0	46802-1	11111-2	37288-2
	2000	73364-2	81302-0	13179-0	43723-1	89672-3	32373-2
3600	10	10688-0	47005-0	11262-0	16432-0	76162-1	69976-1
	25	80792-1	57089-0	11629-0	14517-0	41880-1	44973-1
	50	62698-1	63189-0	11828-0	12898-0	26088-1	32072-1
	75	53372-1	66178-0	11936-0	11954-0	19653-1	26305-1
	100	47387-1	68061-0	12011-0	11299-0	16037-1	22853-1
	250	31781-1	72920-0	12261-0	93494-1	83063-2	14603-1
	500	23192-1	75649-0	12457-0	80394-1	50106-2	10408-1
	750	19120-1	76946-0	12573-0	73434-1	37197-2	85376-2
	1000	16679-1	77755-0	12654-0	68807-1	30087-2	74177-2
	1500	13733-1	78759-0	12767-0	62711-1	22292-2	60835-2
	2000	11950-1	79382-0	12846-0	58682-1	18008-2	52846-2

Initial x_{H_2} : 0.600 (continued)

T, °K	P, atm	x_{H_2}	x_{H_2O}	x_{O_2}	x_{OH}	x_H	x_O
3800	10	12959-0	35115-0	10369-0	18458-0	12602-0	10498-0
	25	10637-0	47010-0	11034-0	17250-0	72211-1	68494-1
	50	86411-1	54748-0	11338-0	15761-0	46020-1	49096-1
	75	75161-1	58680-0	11477-0	14789-0	35044-1	40332-1
	100	67623-1	61202-0	11568-0	14083-0	28787-1	35066-1
	250	46868-1	67852-0	11840-0	11862-0	15157-1	22437-1
	500	34698-1	71663-0	12049-0	10296-0	92217-2	16005-1
	750	28903-1	73490-0	12174-0	94453-1	68721-2	13135-1
	1000	25327-1	74631-0	12263-0	88741-1	55711-2	11417-1
	1500	20964-1	76049-0	12390-0	81151-1	41385-2	93702-2
	2000	18300-1	76932-0	12479-0	76095-1	33486-2	81440-2
4000	10	14084-0	23922-0	91092-1	19139-0	18953-0	14794-0
	25	12784-0	36360-0	10217-0	19311-0	11420-0	99087-1
	50	10989-0	45282-0	10723-0	18343-0	74867-1	71779-1
	75	98186-1	50041-0	10935-0	17509-0	57783-1	59184-1
	100	89830-1	53170-0	11061-0	16844-0	47865-1	51551-1
	250	64953-1	61692-0	11393-0	14536-0	25742-1	33089-1
	500	49197-1	66737-0	11620-0	12776-0	15841-1	23629-1
	750	41409-1	69190-0	11753-0	11789-0	11867-1	19403-1
	1000	36512-1	70733-0	11849-0	11115-0	96501-2	16872-1
	1500	30448-1	72656-0	11986-0	10208-0	71951-2	13855-1
	2000	26698-1	73862-0	12083-0	95975-1	58349-2	12048-1
4200	10	13777-0	14880-0	76046-1	18103-0	26129-0	19508-0
	25	14053-0	26390-0	91959-1	20105-0	16689-0	13567-0
	50	12908-0	35721-0	99847-1	20079-0	11310-0	99965-1
	75	11906-0	41014-0	10315-0	19600-0	88689-1	82961-1
	1100	11111-0	44604-0	10506-0	19109-0	74199-1	72508-1
	250	84538-1	54795-0	10955-0	17020-0	40934-1	46827-1
	500	65866-1	61091-0	11216-0	15201-0	25549-1	33504-1
	750	56174-1	64216-0	11359-0	14128-0	19265-1	27530-1
	1000	49931-1	66201-0	11460-0	13379-0	15729-1	23947-1
	1500	42043-1	68695-0	11602-0	12353-0	11785-1	19674-1
	2000	37079-1	70266-0	11705-0	11652-0	95847-2	17114-1
4400	10	12250-0	84218-1	59716-1	15895-0	33337-0	24126-0
	25	14216-0	17812-0	79338-1	19738-0	22713-0	17587-0
	50	14091-0	26644-0	90346-1	20970-0	15990-0	13271-0
	75	13483-0	32051-0	95181-1	21055-0	12771-0	11122-0
	100	12877-0	35864-0	98001-1	20878-0	10809-0	97735-1
	250	10399-0	47270-0	10442-0	19366-0	61432-1	63806-1
	500	83797-1	54711-0	10771-0	17657-0	38993-1	45822-1
	750	72617-1	58508-0	10935-0	16562-0	29638-1	37698-1
	1000	65186-1	60952-0	11046-0	15771-0	24318-1	32812-1
	1500	55552-1	64057-0	11199-0	14659-0	18330-1	26976-1
	2000	49355-1	66031-0	11307-0	13884-0	14963-1	23474-1

Initial x_{H_2} : 0.60C (continued)

T, °K	P, atm	x_{H_2}	x_{H_2O}	x_{O_2}	x_{OH}	x_H	x_O
4600	10	10082-0	44321-1	44588-1	12902-0	39853-0	28272-0
	25	13355-0	11280-0	65837-1	18044-0	29009-0	21728-0
	50	14384-0	18890-0	79582-1	20588-0	21289-0	16892-0
	75	14338-0	23982-0	86069-1	21377-0	17354-0	14343-0
	100	14050-0	27743-0	89963-1	21634-0	14878-0	12699-0
	250	12131-0	39723-0	98966-1	21084-0	87432-1	84241-1
	500	10154-0	48054-0	10336-0	19713-0	56561-1	60874-1
	750	89619-1	52446-0	10536-0	18699-0	43386-1	50184-1
	1000	81371-1	55320-0	10665-0	17926-0	35803-1	43724-1
	1500	70331-1	59021-0	10833-0	16797-0	27177-1	35982-1
	2000	63031-1	61402-0	10948-0	15985-0	22281-1	31326-1
4800	10	78123-1	22027-1	31926-1	99483-1	45237-0	31608-0
	25	11746-0	67070-1	52375-1	15624-0	35083-0	25604-0
	50	13804-0	12677-0	67742-1	19263-0	26892-0	20590-0
	75	14384-0	17096-0	75641-1	20778-0	22413-0	17765-0
	100	14500-0	20540-0	80583-1	21533-0	19490-0	15880-0
	250	13483-0	32362-0	92552-1	22252-0	11886-0	10763-0
	500	11777-0	41229-0	98428-1	21448-0	78549-1	78487-1
	750	10610-0	46085-0	10102-0	20623-0	60874-1	64922-1
	1000	97599-1	49328-0	10258-0	19932-0	50562-1	56658-1
	1500	85729-1	53573-0	10455-0	18859-0	38692-1	46703-1
	2000	77608-1	56344-0	10584-0	18054-0	31882-1	40694-1
5000	10	58352-1	10616-1	22150-1	73890-1	49355-0	34144-0
	25	98120-1	37944-1	40033-1	12881-0	40477-0	29032-0
	50	12566-0	81006-1	55621-1	17183-0	32391-0	24198-0
	75	13711-0	11648-0	64409-1	19314-0	27625-0	21261-0
	100	14243-0	14586-0	70189-1	20549-0	24384-0	19221-0
	250	14346-0	25576-0	85091-0	22708-0	15477-0	13385-0
	500	13126-0	34561-0	92789-1	22682-0	10469-0	98832-1
	750	12096-0	39705-0	96155-1	22164-0	82054-1	82147-1
	1000	11285-0	43217-0	98159-1	21631-0	68635-1	71879-1
	1500	10091-0	47909-0	10058-0	20704-0	52994-1	59407-1
	2000	92378-1	51022-0	10208-0	19958-0	43910-1	51831-1

Initial x_{H_2}: 0.6667

T, °K	P, atm	x_{H_2}	x_{H_2O}	x_{O_2}	x_{OH}	x_H	x_O
3000	10	74268-1	83037-0	24788-1	50971-1	13608-1	59994-2
	25	56720-1	87472-0	18864-1	38859-1	75211-2	33101-2
	50	45930-1	90050-0	15244-1	31434-1	47857-2	21041-2
	75	40509-1	91306-0	13432-1	27711-1	36697-2	16126-2
	100	37026-1	92101-0	12269-1	25320-1	30384-2	13347-2
	250	27706-1	94180-0	91651-2	18930-1	16623-2	72960-3
	500	22185-1	95382-0	73306-2	15150-1	10518-2	46139-3
	750	19464-1	95966-0	64274-2	13287-1	80438-3	35276-3
	1000	17731-1	96336-0	58536-2	12102-1	66490-3	29154-3
	1500	15542-1	96799-0	51279-2	10605-1	50827-3	22280-3
	2000	14151-1	97093-0	46676-2	96544-2	42002-3	18409-3
3200	10	10618-0	73937-0	34207-1	77997-1	28986-1	13259-1
	25	82973-1	80597-0	26625-1	60829-1	16206-1	73982-2
	50	68028-1	84526-0	21782-1	49819-1	10376-1	47316-2
	75	60351-1	86456-0	19302-1	44172-1	79796-2	36368-2
	100	55362-1	87680-0	17695-1	40507-1	66187-2	30156-2
	250	41809-1	90900-0	13338-1	30562-1	36378-2	16559-2
	500	33648-1	92768-0	10724-1	24585-1	23076-2	10499-2
	750	29593-1	93680-0	94259-2	21615-1	17670-2	80368-3
	1000	27000-1	94256-0	85967-2	19717-1	14617-2	66469-3
	1500	23711-1	94981-0	75462-2	17312-1	11184-2	50847-3
	2000	21614-1	95438-0	68770-2	15778-1	92477-3	42037-3
3400	10	13960-0	62643-0	43215-1	10921-0	55321-1	26216-1
	25	11279-0	71801-0	34793-1	88085-1	31448-1	14878-1
	50	94139-1	77352-0	28980-1	73445-1	20316-1	96011-2
	75	84210-1	80112-0	25899-1	65668-1	15689-1	74108-2
	100	77644-1	81875-0	23865-1	60529-1	13046-1	61608-2
	250	59398-1	86549-0	18227-1	46267-1	72168-2	34052-2
	500	48147-1	89284-0	14761-1	37486-1	45945-2	21668-2
	750	42487-1	90624-0	13019-1	33071-1	35239-2	16616-2
	1000	38847-1	91473-0	11900-1	30233-1	29182-2	13757-2
	1500	34204-1	92542-0	10474-1	26614-1	22358-2	10538-2
	2000	31231-1	93219-0	95605-2	24297-1	18502-2	87193-3
3600	10	16931-0	49885-0	50545-1	13855-0	95861-1	46880-1
	25	14334-0	61375-0	42699-1	11717-0	55785-1	27251-1
	50	12263-0	68641-0	36482-1	10018-0	36486-1	17812-1
	75	11095-0	72328-0	32990-1	90613-1	28336-1	13829-1
	100	10302-0	74706-0	30619-1	84117-1	23646-1	11538-1
	250	80198-1	81091-0	23812-1	65449-1	13195-1	64354-2
	500	65634-1	84879-0	19476-1	53547-1	84406-2	41154-2
	750	58179-1	86745-0	17259-1	47459-1	64885-2	31632-2
	1000	53344-1	87932-0	15821-1	43511-1	53806-2	26228-2
	1500	47132-1	89431-0	13976-1	38439-1	41295-2	20128-2
	2000	43128-1	90383-0	12786-1	35171-1	34210-2	16673-2

Initial x_{H_2} : 0.6667 (continued)

T, °K	P, atm	x_{H_2}	x_{H_2O}	x_{O_2}	x_{OH}	x_H	x_O
3800	10	18845-0	36886-0	54103-1	16079-0	15197-0	75835-1
	25	16996-0	49945-0	48782-1	14499-0	91275-1	45543-1
	50	15031-0	58737-0	43133-1	12821-0	60695-1	30282-1
	75	13808-0	63334-0	39617-1	11777-0	47500-1	23696-1
	100	12939-0	63430-0	37125-1	11036-0	39822-1	19865-1
	250	10307-0	74575-0	29571-1	87908-1	22478-1	11213-1
	500	85419-1	79555-0	24500-1	72844-1	14469-1	72171-2
	750	76162-1	82032-0	21844-1	64949-1	11156-1	55642-2
	1000	70086-1	83615-0	20101-1	59767-1	92675-2	46224-2
	1500	62203-1	85623-0	17839-1	53043-1	71287-2	35555-2
	2000	57078-1	86902-0	16368-1	48671-1	59138-2	29495-2
4000	10	19278-0	24941-0	52845-1	17055-0	22174-0	11268-0
	25	18874-0	38268-0	51919-1	16727-0	13876-0	70636-1
	50	17429-0	48072-0	48040-1	15462-0	94289-1	48045-1
	75	16330-0	53420-0	45051-1	14493-0	74521-1	37989-1
	100	15488-0	56995-0	42754-1	13751-0	62850-1	32050-1
	250	12711-0	67044-0	35138-1	11293-0	36011-1	18376-1
	500	10703-0	73293-0	29610-1	95130-1	23366-1	11928-1
	750	96155-1	76445-0	26608-1	85472-1	18083-1	92322-2
	1000	88895-1	78473-0	24604-1	79027-1	15057-1	76884-2
	1500	79346-1	81059-0	21968-1	70548-1	11615-1	59317-2
	2000	73065-1	82715-0	20232-1	64969-1	96527-2	49299-2
4200	10	18098-0	15433-0	47400-1	16381-0	29947-0	15401-0
	25	19576-0	27575-0	51739-1	17800-0	19698-0	10177-0
	50	19074-0	37602-0	50668-1	17387-0	13749-0	71211-1
	75	18316-0	43386-0	48771-1	16716-0	11000-0	57045-1
	100	17634-0	47360-0	47023-1	16105-0	93476-1	48509-1
	250	15014-0	58939-0	40184-1	13738-0	54551-1	28361-1
	500	12894-0	66403-0	34581-1	11810-0	35747-1	18604-1
	750	11690-0	70235-0	31377-1	10711-0	27791-1	14469-1
	1000	10867-0	72722-0	29192-1	99614-1	23206-1	12087-1
	1500	97678-1	75918-0	26253-1	89563-1	17963-1	93586-2
	2000	90330-1	77978-0	24290-1	82845-1	14960-1	77959-2
4400	10	15678-0	87052-1	38948-1	14523-0	37715-0	19484-0
	25	19006-0	18516-0	47961-1	17744-0	26263-0	13674-0
	50	19753-0	27865-0	50284-1	18522-0	18932-0	99006-1
	75	19545-0	33660-0	49960-1	18365-0	15376-0	80578-1
	100	19165-0	37787-0	49114-1	18031-0	13186-0	69189-1
	250	17072-0	50395-0	44034-1	16114-0	78710-1	41434-1
	500	15020-0	58917-0	38878-1	14202-0	52204-1	27529-1
	750	13770-0	63393-0	35704-1	13031-0	40813-1	21541-1
	1000	12890-0	66334-0	33458-1	12205-0	34196-1	18059-1
	1500	11683-0	70148-0	30365-1	11070-0	26582-1	14047-1
	2000	10860-0	72627-0	28249-1	10294-0	22195-1	11733-1

Initial x_{H_2} : 0.6667 (continued)

T, °K	P, atm	x_{H_2}	x_{H_2O}	x_{O_2}	x_{OH}	x_H	x_O
4600	10	12699-0	45717-1	29904-1	11858-0	44727-0	23154-0
	25	17352-0	11683-0	41838-1	16396-0	33066-0	17321-0
	50	19391-0	19657-0	47424-1	18453-0	24717-0	13040-0
	75	19863-0	25043-0	48904-1	18966-0	20426-0	10812-0
	100	19897-0	29052-0	49192-1	19038-0	17704-0	93907-1
	250	18687-0	42031-0	46694-1	17975-0	10851-0	57864-1
	500	16911-0	51322-0	42501-1	16314-0	72995-1	39036-1
	750	15707-0	56342-0	39582-1	15173-0	57440-1	30759-1
	1000	14822-0	59685-0	37416-1	14330-0	48320-1	25899-1
	1500	13566-0	64074-0	34316-1	13129-0	37745-1	20251-1
	2000	12687-0	66955-0	32132-1	12286-0	31611-1	16971-1
4800	10	97525-1	22694-1	21747-1	91738-1	50543-0	26087-0
	25	14973-0	69293-1	34402-1	14297-0	39610-0	20751-0
	50	18094-0	13145-0	42391-1	17446-0	30789-0	16288-0
	75	19268-0	17776-0	45576-1	18667-0	25941-0	13790-0
	100	19775-0	21407-0	47060-1	19216-0	22760-0	12135-0
	250	19747-0	34033-0	47714-1	19336-0	14384-0	77282-1
	500	18471-0	43722-0	45005-1	18162-0	98371-1	53072-1
	750	17420-0	49140-0	42609-1	17162-0	78000-1	42164-1
	1000	16592-0	52812-0	40685-1	16366-0	65927-1	35681-1
	1500	15361-0	57700-0	37776-1	15174-0	51794-1	28073-1
	2000	14467-0	60950-0	35643-1	14304-0	43530-1	23615-1
5000	10	72495-1	10931-1	15215-1	68258-1	55012-0	28299-0
	25	12357-0	39140-1	26856-1	11840-0	45425-0	23779-0
	50	16151-0	83782-1	36016-1	15675-0	36722-0	19472-0
	75	17922-0	12074-0	40501-1	17510-0	31584-0	16859-0
	100	18887-0	15147-0	43045-1	18531-0	28079-0	15052-0
	250	20191-0	26764-0	47034-1	20029-0	18362-0	99512-1
	500	19607-0	36435-0	46222-1	19566-0	12794-0	69756-1
	750	18815-0	42067-0	44608-1	18829-0	10233-0	55952-1
	1000	18113-0	45962-0	43093-1	18158-0	86955-1	47626-1
	1500	16998-0	51237-0	40589-1	17066-0	68759-1	37740-1
	2000	16126-0	54796-0	38367-1	16223-0	58016-1	31888-1

Initial x_{H_2} : 0.750

T, °K	P, atm	x_{H_2}	x_{H_2O}	x_{O_2}	x_{OH}	x_H	x_O
3000	10	32255-0	62879-0	75357-3	18521-1	28358-1	10460-2
	25	32608-0	64323-0	30863-3	11917-1	18033-1	42339-3
	50	32803-0	65028-0	15585-3	84939-2	12790-1	21274-3
	75	32896-0	65329-0	10427-3	69575-2	10458-1	14208-3
	100	32949-0	65535-0	78446-4	60396-2	90637-2	10673-3
	250	33087-0	65909-0	31473-4	38335-2	57444-2	42755-4
	500	33150-0	66228-0	15829-4	27212-2	40658-2	21440-4
	750	33225-0	66388-0	10556-4	22247-2	33234-2	14296-4
	1000	33203-0	66164-0	78738-5	19208-2	28772-2	10693-4
	1500	33192-0	66260-0	52679-5	15709-2	23489-2	71410-5
	2000	33318-0	66061-0	38978-5	13538-2	20380-2	53196-5
3200	10	31824-0	58969-0	24222-2	35931-1	50182-1	35282-2
	25	32263-0	61920-0	10393-2	23699-1	31956-1	14617-2
	50	32529-0	63365-0	53536-3	17079-1	22689-1	74181-3
	75	32658-0	63997-0	36120-3	14056-1	18562-1	49750-3
	100	32738-0	64360-0	27264-3	12227-1	16095-1	37432-3
	250	32941-0	65241-0	11068-3	78147-2	10211-1	15084-3
	500	33047-0	65679-0	55728-4	55540-2	72318-2	75684-4
	750	33102-0	65825-0	37193-4	45411-2	59098-2	50484-4
	1000	33134-0	65986-0	27978-4	39404-2	51204-2	37919-4
	1500	33181-0	66135-0	18683-4	32223-2	41838-2	25301-4
	2000	33183-0	66180-0	14030-4	27925-2	36233-2	18988-4
3400	10	31476-0	52543-0	59806-2	61008-1	83066-1	97528-2
	25	31959-0	57829-0	28109-2	42145-1	52937-1	42287-2
	50	32258-0	60508-0	15103-2	31037-1	37607-1	21918-2
	75	32412-0	61682-0	10364-2	25772-1	30779-1	14825-2
	100	32511-0	62375-0	79001-3	22535-1	26696-1	11209-2
	250	32774-0	63997-0	32734-3	14564-1	16952-1	45634-3
	500	32921-0	64791-0	16626-3	10403-1	12014-1	22997-3
	750	32990-0	65150-0	11160-3	85322-2	98196-2	15384-3
	1000	33036-0	65369-0	84032-4	74088-2	85099-2	11561-3
	1500	33088-0	65613-0	56263-4	60670-2	69538-2	77236-4
	2000	33130-0	65719-0	42226-4	52593-2	60260-2	57947-4
3600	10	31062-0	43624-0	11484-1	89453-1	12984-0	22346-1
	25	31731-0	51683-0	61785-2	66316-1	82998-1	10366-1
	50	32053-0	56073-0	35639-2	50620-1	58985-1	55671-2
	75	32212-2	58057-0	25219-2	42688-1	48280-1	38237-2
	100	32317-0	59241-0	19566-2	37661-1	41880-1	29168-2
	250	32607-0	62045-0	84325-3	24835-1	26606-1	12110-2
	500	32786-0	63432-0	43591-3	17905-1	18865-1	61569-3
	750	32873-0	64043-0	29466-3	14740-1	15423-1	41331-3
	1000	32928-0	64402-0	22273-3	12826-1	13368-1	31120-3
	1500	32992-0	64830-0	14989-3	10532-1	10926-1	20844-3
	2000	33037-0	65066-0	11293-3	91480-2	94685-2	15669-3

Initial x_{H_2} : 0.750 (continued)

T, °K	P, atm	x_{H_2}	x_{H_2O}	x_{O_2}	x_{OH}	x_H	x_O
3800	10	30083-0	33242-0	17244-1	11469-0	19200-0	42813-1
	25	31415-0	43620-0	10891-1	93140-1	12409-0	21519-1
	50	31891-0	49888-0	69120-2	74759-1	88410-1	12122-1
	75	32077-0	52870-0	51153-2	64501-1	72397-1	85146-2
	100	32188-0	54696-0	40781-2	57691-1	62805-1	65839-2
	250	32482-0	59132-0	18721-2	39266-1	39902-1	28213-2
	500	32668-0	61382-0	99723-3	28740-1	28296-1	14560-2
	750	32764-0	62375-0	68248-3	23811-1	23138-1	98349-3
	1000	32825-0	62964-0	51961-3	20796-1	20056-1	74319-3
	1500	32903-0	63658-0	35241-3	17147-1	16395-1	49973-3
	2000	32954-0	64066-0	26688-3	14933-1	14210-1	37662-3
4000	10	28080-0	22939-0	21071-1	12998-0	26761-0	71149-1
	25	30696-0	34352-0	15817-1	11774-0	17696-0	38987-1
	50	31635-0	42155-0	11213-1	10064-0	12703-0	23211-1
	75	31947-0	46127-0	87761-2	89474-1	10423-0	16767-1
	100	32105-0	48649-0	72496-2	81523-1	90488-1	13197-1
	250	32434-0	55053-0	36386-2	58049-1	57523-1	59133-2
	500	32609-0	58451-0	20289-2	43465-1	40784-1	31223-2
	750	32700-0	59974-0	14161-2	36362-1	33347-1	21299-2
	1000	32761-0	60884-0	10905-2	31939-1	28906-1	16186-2
	1500	32839-0	61962-0	74937-3	26508-1	23630-1	10956-2
	2000	32891-0	62604-0	57192-3	23176-1	20480-1	82886-3
4200	10	24868-0	14381-0	21801-1	13023-0	35103-1	10445-0
	25	29171-0	25237-0	19517-1	13345-0	24045-1	62503-0
	50	30956-0	33776-0	15521-1	12259-0	17515-1	39413-1
	75	31573-0	38469-0	12903-1	11289-0	14443-0	29342-1
	100	31878-0	41575-0	11088-1	10515-0	12568-0	23556-1
	250	32404-0	49928-0	61904-2	79214-1	80141-1	11132-1
	500	32595-0	54638-0	36634-2	61117-1	56835-1	60551-2
	750	32680-0	56810-0	26267-2	51817-1	46466-1	41864-2
	1000	32734-0	58125-0	20554-2	45877-1	40274-1	32071-2
	1500	32806-0	59697-0	14391-2	38429-1	32920-1	21911-2
	2000	32853-0	60639-0	11104-2	33781-1	28530-1	16669-2
4400	10	20789-0	81773-1	19546-1	11847-0	43429-0	13803-0
	25	26704-0	17170-0	20891-1	13881-0	31130-0	90248-1
	50	29621-0	25469-0	18680-1	13825-0	23183-0	60344-1
	75	30737-0	30446-0	16527-1	13246-0	19282-0	46345-1
	100	31314-0	33897-0	14804-1	12654-0	16855-0	37986-1
	250	32324-0	43828-0	92903-2	10185-0	10831-0	19032-1
	500	32622-0	49864-0	59038-2	81562-1	76936-1	10728-1
	750	32718-0	52762-0	43806-2	70360-1	62910-1	75452-2
	1000	32769-0	54549-0	35010-2	62950-1	54524-1	58415-2
	1500	32830-0	56719-0	25140-2	53393-1	44560-1	40417-2
	2000	32870-0	58034-0	19691-2	47283-1	38613-1	30978-2

Initial x_{H_2} : 0.750 (continued)

T, °K	P, atm	x_{H_2}	x_{H_2O}	x_{O_2}	x_{OH}	x_H	x_O
4600	10	16487-0	43148-1	15803-1	98222-1	50964-0	16832-0
	25	23444-0	10928-0	20055-1	13195-0	38435-0	11992-0
	50	27513-0	18189-0	20169-1	14334-0	29442-0	85037-1
	75	29249-0	22984-0	18996-1	14344-0	24786-0	67384-1
	100	30203-0	26484-0	17741-1	14086-0	21813-0	56395-1
	250	32018-0	37329-0	12545-1	12196-0	14204-0	29992-1
	500	32579-0	44484-0	86037-2	10188-0	10131-0	17563-1
	750	32739-0	48077-0	66342-2	89680-1	82926-1	12593-1
	1000	32811-0	50345-0	54323-2	81240-1	71895-1	98683-2
	1500	32880-0	53153-0	40199-2	69958-1	58763-1	69313-2
	2000	32915-0	54883-0	32076-2	62525-1	50917-1	53620-2
4800	10	12514-0	21476-1	11827-1	76635-1	57254-0	19238-0
	25	19729-0	65186-1	17537-1	11717-0	45465-0	14816-0
	50	24710-0	12267-0	19796-1	13932-0	35980-0	11131-0
	75	27075-0	16485-0	19849-1	14603-0	30751-0	91005-1
	100	28462-0	19746-0	19330-1	14775-0	27305-0	77775-1
	250	31363-0	30724-0	15416-1	13851-0	18128-0	43927-1
	500	32382-0	38648-0	11441-1	12125-0	13025-0	26759-1
	750	32687-0	42830-0	91931-2	10920-0	10685-0	19585-1
	1000	32822-0	45542-0	77320-2	10035-0	92723-1	15555-1
	1500	32937-0	48979-0	59205-2	87966-1	75840-1	11114-1
	2000	32985-0	51141-0	48270-2	79485-1	65728-1	86905-2
5000	10	92451-0	10358-1	84006-2	57277-1	62124-0	21028-0
	25	16027-0	36950-1	14229-1	98149-1	51732-0	17308-0
	50	21490-0	78645-1	17926-1	12756-0	42359-0	13737-0
	75	24367-0	11280-0	19122-1	14029-0	36828-0	11584-0
	100	26161-0	14092-0	19417-1	14648-0	33047-0	10110-0
	250	30282-0	24467-0	17476-1	14951-0	22486-0	60658-1
	500	31939-0	32716-0	14045-1	13765-0	16330-0	38451-1
	750	32484-0	37309-0	11772-1	12709-0	13446-0	28743-1
	1000	32735-0	40376-0	10181-1	11865-0	11690-0	23149-1
	1500	32955-0	44365-0	82862-2	10610-0	95767-1	16845-1
	2000	33045-0	46935-0	67505-2	97072-1	83050-1	13329-1

APPENDIX G

THEORETICAL DETONATION VELOCITIES, PRESSURES, AND TEMPERATURES

TABLE VI.

THEORETICAL DETONATION VELOCITIES,
PRESSURES, AND TEMPERATURES
(Based on Idealized Properties)

POINT NO.	x_{H_2}	P_1 PSIA	u_1 FT/SEC	P_2 PSIA	P_3 PSIA	T_2 °K
1	0.4000	9.186	6801	147.0	355.5	3172
2		22.36	6890	367.4	890.3	3274
3		43.89	6953	734.8	1783	3349
4		65.15	6988	1102	2675	3392
5		86.19	7014	1470	3568	3423
6		210.8	7092	3674	8934	3518
7		414.8	7146	7348	17890	3586
8		617.1	7176	11020	26830	3624
9		817.9	7196	14700	35800	3650
10		1217	7224	22040	53730	3686
11		1616	7242	29390	71630	3710
12	0.5000	8.714	7573	147.0	356.5	3383
13		21.12	7688	367.4	892.8	3516
14		41.29	7775	734.8	1789	3619
15		61.11	7825	1102	2683	3681
16		80.73	7860	1470	3581	3724
17		196.2	7967	3674	8969	3861
18		384.7	8045	7348	17960	3963
19		570.7	8087	11020	26940	4021
20		755.1	8118	14700	35950	4063
21		1121	8160	22040	53950	4120
22		1483	8189	29390	71950	4160
23	0.6000	8.405	8498	147.0	357.3	3525
24		20.30	8643	367.4	894.8	3685
25		39.56	8752	734.8	1793	3811
26		58.43	8817	1102	2691	3887
27		77.12	8862	1470	3590	3941
28		186.7	8999	3674	8990	4116
29		364.7	9103	7348	18000	4253
30		539.9	9160	11020	27030	4332
31		713.2	9202	14700	36050	4389
32		1056	9258	22040	54110	4469
33		1395	9297	29390	72200	4526

POINT NO.	x_{H_2}	P_1 PSIA	u_1 FT/SEC	P_2 PSIA	P_3 PSIA	T_2 °K
34	0.6667	8.292	9247	147.0	357.4	3568
35		19.99	9409	367.4	895.3	3736
36		38.93	9534	734.8	1793	3870
37		57.48	9607	1102	2692	3951
38		75.82	9654	1470	3592	4008
39		183.2	9816	3674	8997	4200
40		357.4	9933	7348	18020	4349
41		528.0	10004	11020	27060	4439
42		697.2	10051	14700	36090	4503
43		1031	10118	22040	54150	4594
44		1362	10164	29390	72260	4659
45	0.7500	8.351	10362	147.0	357.1	3506
46		20.17	10536	367.4	894.7	3661
47		39.34	10666	734.8	1792	3782
48		58.11	10743	1102	2691	3855
49		76.69	10798	1470	3589	3907
50		186.0	10959	3674	8987	4072
51		364.0	11072	7348	18000	4197
52		538.6	11143	11020	27010	4269
53		712.1	11190	14700	36030	4320
54		1056	11252	22040	54080	4390
55		1397	11293	29390	72130	4438

BIBLIOGRAPHY

1. Becker, R., Z. Physik, 8, 321 (1922).

2. Berets, D. J., Greene, E. F., and Kistiakowsky, G. B., J. Am. Chem. Soc., 72, 1080 (1950).

3. Berthelot, M. and Vieille, P., Compt. rend., 93, 18 (1881).

4. Bridgman, "The Physics of High Pressure," Macmillan, New York, 1931.

5. Brinkley Jr., S. R. and Kirkwood, J. G., "Third Symposium on Combustion and Flame and Explosion Phenomena," Williams and Wilkins Co., Baltimore, 1949, p. 586.

6. Chapman, D. L., Phil. Mag., 47, 90 (1899).

7. Cook, M. A., Filler, A. S., and Robinson, D., "Calculation of Products of Detonation Using IBM Machines," Technical Report XXI, Institute for the Study of Rate Processes, University of Utah, Salt Lake City, October 16, 1953.

8. Dixon, H. B., Phil. Trans. Roy. Soc., A184, 97 (1893); A200, 315 (1903).

9. Doering, W. and Burkhardt, G., "Contributions to the Theory of Detonation," Translation from German prepared by Brown University, Technical Report No. F-TS-1227-IA, Wright-Patterson Air Force Base, Dayton, Ohio, May 1949.

10. Wolfson, B. T. and Dunn, R. G., "Generalized Charts of Detonation Parameters for Gaseous Mixtures," Chem. & Eng. Data Ser. 1, 77 (1956).

11. Edse, R., "Calculation of Detonation Velocities in Gases," WADC Technical Report 54-416, Wright-Patterson Air Force Base, Ohio, March 1956.

12. Evans, M. W., Given, F. I., and Richeson Jr., W. E., "Effects of Attenuating Materials on Detonation Induction Distances in Gases," J. Appl. Phy., 26, 1111, (1955).

13. Faupel, J. H. and Harris, D. B., Ind. and Eng. Chem., 49, 1979, (1957).

14. Hirschfelder, J. O., McClure, F. T., Curtis, C. F., and Osborne, D. W., "Thermodynamic Properties of Propellant Gases," NDRC Report No. A-48 (OSRD No. 547), Abs. Bib. Sci. and Ind. Reps., 2, 743, (1946).

15. Hoelzer, C. A. and Stobaugh, W. K., "Influence of Initial Pressure on Detonation Parameters in Combustible Gases," Thesis, Air University Command, USAF Inst. Tech, Wright-Patterson Air Force Base, Ohio, March, 1954.

16. Hougen, O. A. and Watson, K. M., "Chemical Process Principles, Part II, John Wiley & Sons, Inc., New York, 1949.

17. Huff, V. N. and Calvert, C. S., "Charts for the Computation of Equilibrium Compositions of Chemical Reactions in the Carbon-Hydrogen-Oxygen-Nitrogen System at Temperatures from 2000° to 5000°K," NACA Technical Note 1653, Washington, D. C., July 1948.

18. Huff, V. N., Gordon, S., and Morrell, V. E., "General Method and Thermodynamic Tables for Computation of Equilibrium Composition and Temperature of Chemical Reactions," NACA Report 1037, Washington, D. C., 1951.

19. Hugoniot, H., Journal de l' ecole polytechnique, 58, 1, (1889).

20. Jost, W. and Croft, H. O., "Explosion and Combustion Processes in Gases," McGraw-Hill Book Co., Inc., 1946.

21. Jouguet, E., J. Mathematique, Ser. 6, 1, 347 (1905); Ser. 6, 2, 6 (1906).

22. Kistiakowsky, G. B. and Zinman, W. G., "The Attainment of Thermodynamic Equilibrium in Detonation Waves," Second ONR Symposium on Detonation, Washington, D. C., Feb., 9-11, 1955, p. 80.

23. Laffitte, P., Ann phys. Ser. 10, 4, 623 (1925).

24. Dumanois, P. and Laffitte, P., Compt. rend, 183, 284 (1926).

25. Lewis, B. and Friauf, J. B., J. Am. Chem. Soc., 52, 3905 (1930).

26. Lewis, B. and VonElbe, G., "Combustion, Flames and Explosions of Gases," Academic Press Inc., New York, 1951.

27. Mallard, E. and Le Chatelier, H. L., Compt. rend., 93, 145 (1881).

28. Manning, W. R. D., Ind. and Eng. Chem., 49, 1969 (1957.)

29. Morrison, R. B., "A Shock Tube Investigation of Detonative Combustion," University of Michigan Press, Ann Arbor, Michigan, 1955.

30. Moyle, M. P., "The Effect of Temperature on the Detonation Characteristics of Hydrogen-Oxygen Mixtures," Ph.D. Thesis, University of Michigan, Ann Arbor, Dec., 1956.

31. Moyle, M. P. and Churchill, S. W., "Experimental Detonation Velocities in Hydrogen-Oxygen Mixtures," (Paper presented at Am. Chem. Soc. Meeting, Miami, Florida, April, 1957).

32. Moyle, M. P. and Churchill, S. W., "Impact Pressures Developed in Hydrogen-Oxygen Detonations," (Paper presented at Am. Inst. of Chem. Eng. Meeting at Chicago, Illinois, December 8-11, 1957).

33. Nelson, L. C. and Obert, E. A., "Generalized PVT Properties of Gases" (with bibliography of data), Trans. Am. Soc. Mech. Eng., 76, 1057 (1954).

34. Perry, J. H., "Chemical Engineers' Handbook," McGraw-Hill Book Co. Inc., New York, 1950.

35. Randall, P. N., Bland, J., Dudley, W. M., and Jacobs, R. B., Chem. Eng. Prog., 53, 574, (1957).

36. Rankine, W. J. M., "On the Thermodynamic Theory of Waves of Finite Longitudinal Disturbance," Trans. Roy. Soc. London, 160, 277 (1870).

37. Scorah, R. L., J. Chem. Phys., 3, 425 (1935).

38. "Summary of IBM Type 650 Computer and Symbolic Optional Assembly Program (II) for the IBM-650 Data Processing System," Statistical Research Laboratory, University of Michigan, Ann Arbor, 1956.

39. Weir Jr., A. and Morrison, R. B., "Equilibruim Temperature and Composition Behind a Detonation Wave," Ind. and Eng. Chem., 46, 1056, (1954).

40. Worthing, A. G. and Geffner, J., "Treatment of Experimental Data," John Wiley and Sons Inc., New York, 1946.

41. Zeldovich, Y. B., "Theory of Combustion and Detonation of Gases," Translation from Russian Prepared by Brown University, Technical Report No. F-TS-1226-IA, Wright-Patterson Air Force Base, Dayton, Ohio, May, 1949.